Lake Rotoiti fieldwork and modelling to support considerations of Ohau Channel diversion from Lake Rotoiti

CBER Contract Report 91

Prepared for Environment Bay of Plenty

By David P. Hamilton, Chris McBride, and Toradji Uraoka

Centre for Biodiversity and Ecology Research
The University of Waikato
Private Bag 3105
Hamilton, 3240
New Zealand

March 2005

THE UNIVERSITY OF WAIKATO
Te Whare Wānanga o Waikato

CBER
University of Waikato
Centre for Biodiversity and Ecology Research

Table of Contents

List of Tables

List of Figures

Executive Summary

A detailed assessment of the water quality effects of the Ohau Channel inflow to Lake Rotoiti was carried out using field and computer modelling analyses. The modelling assessment evaluates the effects on Lake Rotoiti of partial (50%) or complete (100%) diversion of the Ohau Channel. A comprehensive bathymetric survey of Lake Rotoiti and the eastern end of Lake Rotorua was also carried out to provide information for the application of a three-dimensional model run by NIWA, so that different diversion wall positions and designs might be tested prior to possible implementation. Field measurements based on temperature, conductivity and chlorophyll fluorescence carried out from February to May 2004 captured instances when the Ohau Channel entered Lake Rotoiti as a buoyant overflow. These data and historical records suggest that approximately 20% of the buoyant surface inflow enters the main basin of Lake Rotoiti, while the remainder is short-circuited through the Kaituna arm to the outflow. In other instances, particularly just prior to winter turnover, there was a readily identifiable underflow that inserted in the metalimnion region and took approximately 10 hours to travel from the inflow entrance to the Narrows location in the lake. Despite entrainment with lake water, this inflow was recognisable by higher levels of conductivity and chlorophyll fluorescence than the adjacent water in Lake Rotoiti. The depth of insertion of the inflow may be highly dynamic as a result of relatively wide diurnal variations in temperature (up to 5^{o}C) in the Ohau Channel, and a constricted, highly irregular bathymetry in the western end of Lake Rotoiti, which enhances internal waves that propagate through the basin with a period of approximately 24-hours. These features ensure that there will be a wide range of insertion depths of the Ohau Channel and that there may be rapid switches between overflow and interflow conditions throughout summer. Estimates of the depth of inflow intrusion based on simulations with the hydrodynamic-ecological model DYRESM-CAEDYM indicate that underflow conditions dominate in winter, surface overflows dominate in spring, and interflows become dominant later in summer. Model simulations may, however, underestimate the variability of intrusion depths due to internal wave action in Lake Rotoiti and the wide range of temperatures in the Ohau Channel, both of which are only partly accounted for

in the one-dimensional model simulations. A 2-year period was used to calibrate the DYRESM-CAEDYM model output to temperature and biogeochemical measurements at the Crater station in Lake Rotoiti. The model reproduced the observed dominance of cyanobacteria under stratified summer conditions and other phytoplankton, particularly diatoms, in the well mixed conditions of winter, as well as the variations in temperature and oxygen through the water column. The seasonal release of nutrients into the hypolimnion was also captured, though there is scope for improvement in the timing of nutrient release events, particularly as knowledge is developed about nutrient fluxes from the lake bed. Simulations with the calibrated model were used to examine the water quality effects of different flow regimes (100, 50 and 0% of current flow in the Ohau Channel). The duration of the simulations was extended to 4.5 years by duplicating daily meteorological, inflow and outflow data from the period 2002-3. There was little change in simulated temperature, dissolved oxygen, nutrients or diatom biomass between the three flow scenarios. Cyanobacterial biomass, however, decreased progressively in comparisons between the low-flow (0%) and 100% Ohau inflow cases; the maximum summer level was 4% lower in the 0% flow case in the first summer (2001-2) but was 68% lower by the fourth summer (2004-5). These results suggest a likely reduction in the frequency and intensity of cyanobacterial blooms in Lake Rotoiti with a complete diversion of the Ohau Channel, but the results also appeared to be sensitive to the proportion of the total phytoplankton biomass that was contributed by cyanobacteria in the Ohau Channel. Ongoing monitoring of the Channel should be used to better refine the variability of phytoplankton biomass and species composition, and may assist in understanding an apparent transition towards greater proportional representation and biomass of cyanobacteria in the Lake Rotorua commencing in summer 2002-3.

Acknowledgments

We are grateful to Environment Bay of Plenty for provision of data to support the water quality modelling. John McIntosh in particular is thanked for his responsiveness and knowledge in handling our many requests for data. Dr Bob Spigel from NIWA in Christchurch put in many hours to modify DYRESM to encompass effects of geothermal heating, and he was able to carry out many iterations of model coding as we applied the DYRESM model on Lake Rotoiti. We thank many people who assisted us in the field, including Bryan Coxhead and other boat operators from Sea Quest, harbour master Andrew Lang and co-workers, Matt Bloxham (Environment Bay of Plenty) and co-workers and Nina Von Westernhagen (University of Waikato) whose research will continue to elucidate the mechanisms influencing water quality in Lake Rotoiti. David Burger (University of Waikato) assisted with data collation and analysis and Alex Ring and several others from the University of Waikato provided field and technical support for the project. The development and completion of this project was supported with useful discussions with, in particular, Dr Scott Stephens and Max Gibbs (NIWA, Hamilton), as well as members of the Technical Advisory Group for the Rotorua lakes.

1. Introduction

1.1 General Introduction

The fate of water entering Lake Rotoiti from Lake Rotorua via the Ohau Channel may have important implications for water quality in Lake Rotoiti. Lake Rotorua water is enriched in nutrients and organic matter, and this enrichment has the potential to add significantly to the nutrient load of Lake Rotoiti, depending on the path of the inflow. If the Ohau Channel inflow plume entering Lake Rotoiti is warmer than water where it enters the lake, it will be buoyant and will "overflow" to become part of the upper water column (epilimnion) in the lake. Under these circumstances nutrient inputs from Lake Rotorua may be largely diverted down the Kaituna River, with very little contribution to the eastern basin of Rotoiti. If the inflow from the Ohau Channel is cooler than Lake Rotoiti, it will initially "underflow" and may become either an interflow, whereby it intrudes horizontally at some intermediate depth, or be maintained as an underflow at the bottom of the water column in Lake Rotoiti. The underflow or interflow cases can be expected to produce little if any direct outflow of Ohau Channel water down the Kaituna River.

This report is part of a joint NIWA/University of Waikato programme to investigate a partial or complete diversion of the Ohau Channel towards the Kaituna River. This University of Waikato component of the report consists of three main components: bathymetric surveys, fieldwork measurements and modelling of lakes Rotorua and Rotoiti.

From the point of view of water quality assessments of the Ohau Channel diversion, the main focus of this report is on the modelling component and use of various scenarios relating to different diversion options. The model results presented here utilise a one-dimensional model of vertical stratification in Lake Rotoiti to determine the influence of the diversion on temperature and water quality properties. The diversion options considered involve 100%, 50% and the 'current case' of 0% diversion. The one-dimensional hydrodynamic model DYRESM is used to quantify the Ohau Channel plume

effects on vertical transport and stratification in Lake Rotoiti, and the ecological model CAEDYM is used to quantify the ecological effects. Field data relating to the volume, temperature and composition of the Ohau Channel inflow are used together with coupled DYRESM-CAEDYM modelling, to more precisely define the impacts of the Ohau Channel on concentrations and distributions of dissolved oxygen, chlorophyll and nutrients in Lake Rotoiti. Relatively long-term simulations (>1 year) are possible with this one-dimensional approach, in contrast to the three-dimensional modelling undertaken by NIWA, which is used to simulate short-term (c. 1-4 week) events, and to examine specific design criteria for the implementation of a diversion.

Updated bathymetric data were required as part of this project, as an input to the three-dimensional hydrodynamic model of Lake Rotoiti and for any engineering works to be undertaken in relation to a diversion of the Ohau Channel. The most recent bathymetric surveys of Lakes Rotorua and Lake Rotoiti were in 1966 and 1976, respectively, and a very detailed survey has been undertaken in the eastern end of Lake Rotorua and the western end of Lake Rotoiti by the University of Waikato for this purpose. In this report we present graphical illustrations of the bathymetry and append more complete information on the survey as part of a report by Dirk Immenga and Brad Scaife from the Coastal Marine Group of the University of Waikato.

In order to determine the potential benefits for water quality of Lake Rotoiti of diverting the Ohau Channel down the Kaituna River, an understanding is required of the conditions under which each of the different inflow scenarios is likely to occur. The complex multi-basin shape of Lake Rotoiti, and the horizontal variability associated with the Ohau Channel plume insertion mean that there are likely to be significant horizontal variations in lake water properties in the lake. This will weaken the accuracy of simulation models such as DYRESM-CAEDYM that are reliant on the dominance of vertical stratification in hindering redistribution and mixing of water, solutes and particulates in the lake. On the other hand, when it is established *a priori* the relative fraction of Ohau Channel water that enters the surface layer of Lake Rotoiti, as opposed to the region at or below the thermocline, then it is possible to partially compensate for this shortcoming by directing

some of the Ohau Channel water to the Kaituna outlet, effectively negating this volume as a model input.

1.2 Background on Lake Rotoiti

Until recently Lake Rotoiti was considered to be mesotrophic and in a relatively stable state with respect to temporal changes in water quality (Burns et al., 1997). In the summer of 2002-3, however, there were major blooms of cyanobacteria characterised by very dense aggregations of *Anabaena planktonica* in many of the lake's embayments. These blooms gradually subsided with the progression of winter in 2003, but the summer of 2003-4 was again characterised by cyanobacterial blooms, though these were less prolific, which may have been a result of a cooler, windier summer in 2003-4. There is now sufficient data to suggest a step-like change in summertime chlorophyll *a* concentrations and Secchi disk readings in Lake Rotoiti, commencing in 2002-3. Interestingly, however, there has not been a clearly discernible pattern in deoxygenation rates in bottom waters of Lake Rotoiti in the past 24 years (Hamilton et al., in press). However, about 20 tonnes of phosphorus (measured as DRP) and 50 tonnes of nitrogen (mostly as ammonium) are added to the bottom waters of Lake Rotoiti during the period of stratification, presumably mostly as inputs from the bottom sediments (Hamilton et al., 2003).

Diversion of the Ohau Channel has been considered in previous studies (Vincent et al., 1986; Gibbs, 1992). One of the outcomes of those studies was that there was unlikely to be a significant benefit with the diversion because of inputs of dissolved oxygen from the underflow plume, which would act to reduce rates of biogenic consumption of oxygen in the hypolimnion. The benefits of gains in oxygen, however, need to be carefully evaluated against the disadvantages associated with inputs of oxygen-consuming detritus and cyanobacterial cells arising from the Ohau plume.

1.3 Field data collection

The predictive capabilities of ecological simulation models depend a great deal on the accuracy and availability of data for input to the model. Because ecological models are

highly reliant on calibration, unlike many models of physical processes, hindcast and calibration to an existing data set are required. In this study the approach was to run DYRESM-CAEDYM over a 2-year period, with calibration of several ecological parameters until reasonable confidence in the simulation output was developed through comparisons with measured data. In addition, a detailed field study was used to examine the dynamics of the Ohau Channel plume, and to develop a good understanding of spatial variability of water quality properties through Lake Rotoiti. This field study was carried out from Fenruary to May 2004 and a subset of these data has also been used by NIWA in assessing the performance of their three-dimensional model simulations.

1.4 Overview of models

DYRESM is a one-dimensional model that simulates the vertical variation of temperature and density in lakes, using boundary conditions of inflow volume and temperature, outflow volume and climate (Figure 1). It is ideally applied to lakes where there are strong vertical gradients of density and weak horizontal gradients. Lakes Rotorua and Rotoiti are not ideal cases for application of DYRESM because of sediment resuspension in Lake Rotorua (effectively a two-dimensional, horizontally varying process) and short-circuiting of the Ohau Channel inflow to the Kaituna Outlet in Lake Rotoiti. However, an awareness of these issues and directly addressing the case of short-circuiting to the Kaituna River by removing this component of the inflow from the model can at least partially compensate for this shortcoming.

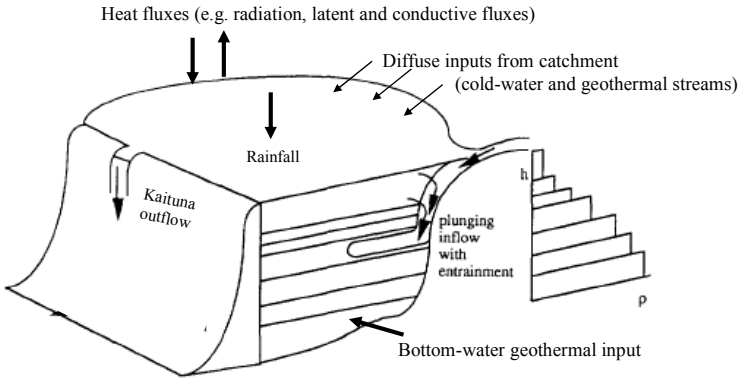

Figure 1. *Schematic of the DYRESM one-dimensional model as it relates to Lake Rotoiti. Right-hand side shows conceptualisation of vertical density (ρ) distribution with elevation above bottom (h).*

2.1 Computational Aquatic Ecosystem Dynamics Model (CAEDYM)

CAEDYM (Figure 2) is an aquatic ecological model that has been designed to be readily linked to hydrodynamic models. The model is based on the 'N-P-Z' (nutrients-phytoplankton-zooplankton) trophic cascade, but also includes comprehensive budgets for carbon, dissolved oxygen, inorganic particulates, and nutrients. CAEDYM has developed the N-P-Z concept in tandem with simulating biogeochemical processes, while also retaining a capacity to resolve at a species or group-specific level (e.g. at the level of phytoplankton or zooplankton species). In the present application to Lake Rotoiti, zooplankton are not simulated explicitly, but phytoplankton have been broadly separated into buoyant species, typifying cyanobacteria, and non-buoyant species, typifying diatoms.

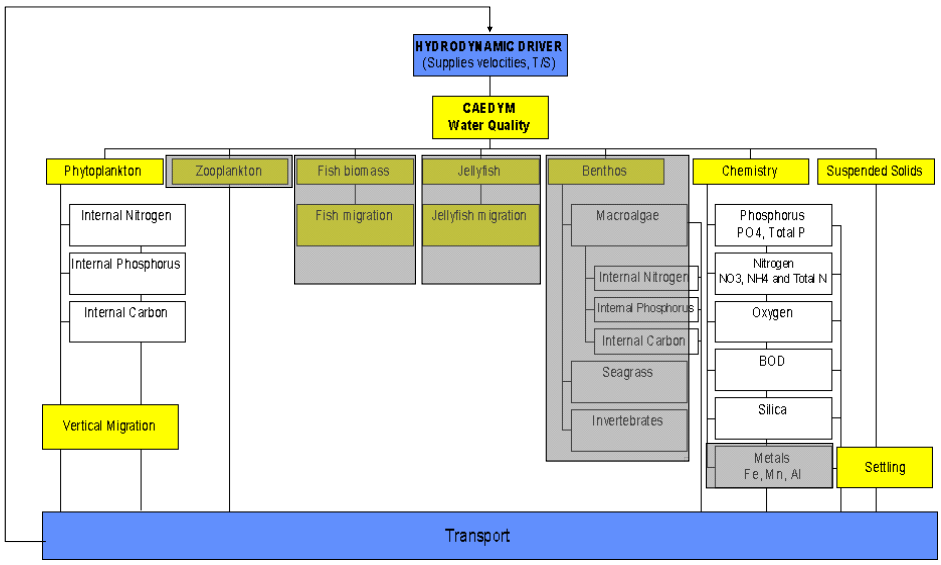

Figure 2. *Schematic of variables included in the CAEDYM model. Shaded areas are components of the model that were not activated in the present application.*

1.5 Model input data

Figure 3 shows the inflows and the outflow included in the application of DYRESM-CAEDYM to Lake Rotoiti. In addition to the specification of daily discharge required for each inflow by DYRESM, properties of the inflows are required as an input to the CAEDYM model. These properties include concentrations of dissolved oxygen, chlorophyll *a* divided into buoyant and non-buoyant groups, nutrients (NO_3-N, NH_4-N, total nitrogen (TN), DRP and total phosphorus (TP)), biochemical oxygen demand specified in carbon equivalents using a stoichiometric conversion of 32/12, and suspended solids, as well as pH. Further details of the inflow data are given in section 2.3. The outflow used in the application to Lake Rotoiti is represented solely by the Kaituna River, for which only daily discharges are specified, as outflow properties are determined as part of the DYRESM-CAEDYM model simulation output.

Another forcing data input to the model is daily meteorological data. These data include shortwave radiation, cloud cover (which is converted to longwave radiation using simulated surface water temperature as part of the calculation), air temperature, vapour pressure (converted from relative humidity and air temperature), wind speed and rainfall. It should be noted that these inputs are daily total values (precipitation) or daily mean values (remaining variables). There is potential for some error in daily averaged inputs. For example, energy inputs from wind speed are non-linear (see application of DYRESM to Lake Rotorua by Rutherford et al. (1996)), but new versions of DYRESM partially compensate for this non-linearity by allowing some adjustment of physical parameters that were fixed in earlier versions of the model.

Other input data to the model are fixed and are therefore read in at the outset of the model runs. The relevant files include lake hyposography (water depth vs area), physical parameters for DYRESM, ecological parameters for CAEDYM, and an initial depth profile of temperature and water quality properties (see input variables specified above for the inflows). An input file specifying the geothermal heat flux to the bottom waters of the lake is also used on this study, though this is not part of the mainstream DYRESM model.

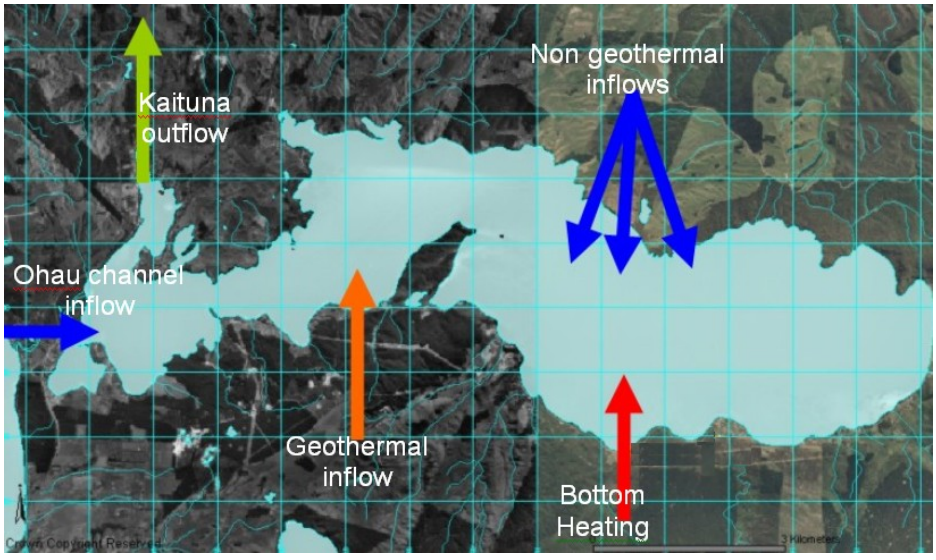

Figure 3. *Schematic of inflows and outflows for Lake Rotoiti. Note that the model is one-dimensional and therefore does not truly represent the horizontal location of the inflows and outflows. The bottom of the lake has a conductive geothermal heating component.*

2. Data collection

2.1 Bio-Fish data

The Bio-Fish is an instrument that takes underwater readings of temperature, conductivity, dissolved oxygen, chlorophyll fluorescence and photosynthetically active radiation at a frequency of 4Hz as it is towed in an operator-controlled vertically undulating mode from a boat (Fig. 4). A pressure transducer on the instrument and a GPS unit on the boat allow for precise location of the position of the Bio-Fish at the time that each reading is taken. Only a small selection of the data collected from the Bio-Fish is presented here; more information is contained in the CD appended to this report. The data presented below are used to illustrate some of the dominant features of Lake Rotorua Lake Rotoiti and the Ohau Channel insertion.

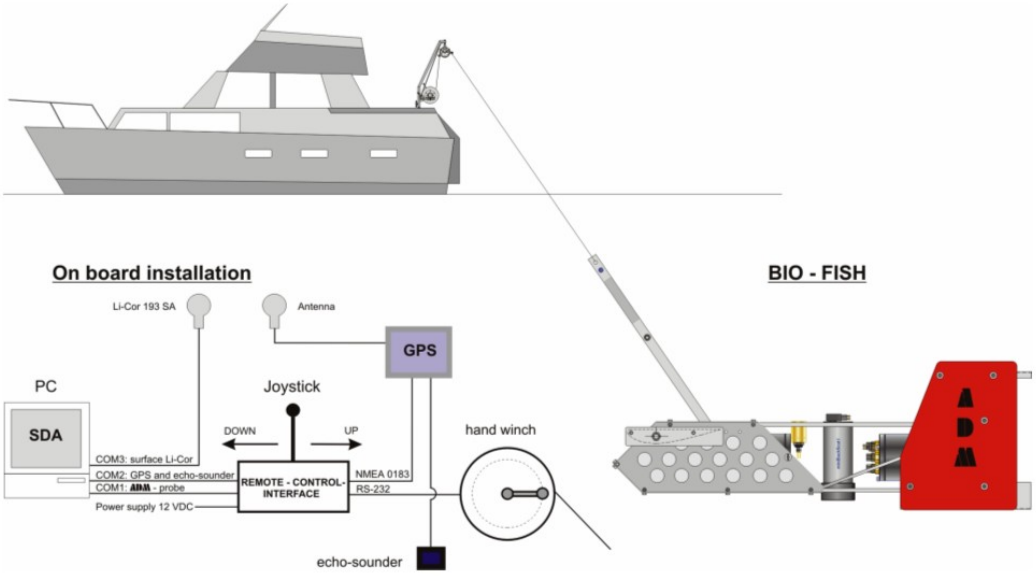

Figure 4. *Illustration of Bio-Fish set-up. The size of the boat has been scaled around 10-fold smaller compared with the Bio-Fish and on-board installation.*

The coordinates of the Bio-Fish transect for Lake Rotoiti are shown in Figure 5, with additional areas that progress from near the Kaituna outlet into Okawa Bay. The distances shown in Figure 6 represent progression of this transect from near the Kaituna River outflow (0 km), advancing to the shallow entrance of Okawa Bay (2.5 km) and then back out of the bay (3.5 km) before proceeding to the eastern end of the lake. Figure

6 also illustrates whereabouts measurements are taken in order to interpolate data and create a colour contour map for the Bio-Fish transect.

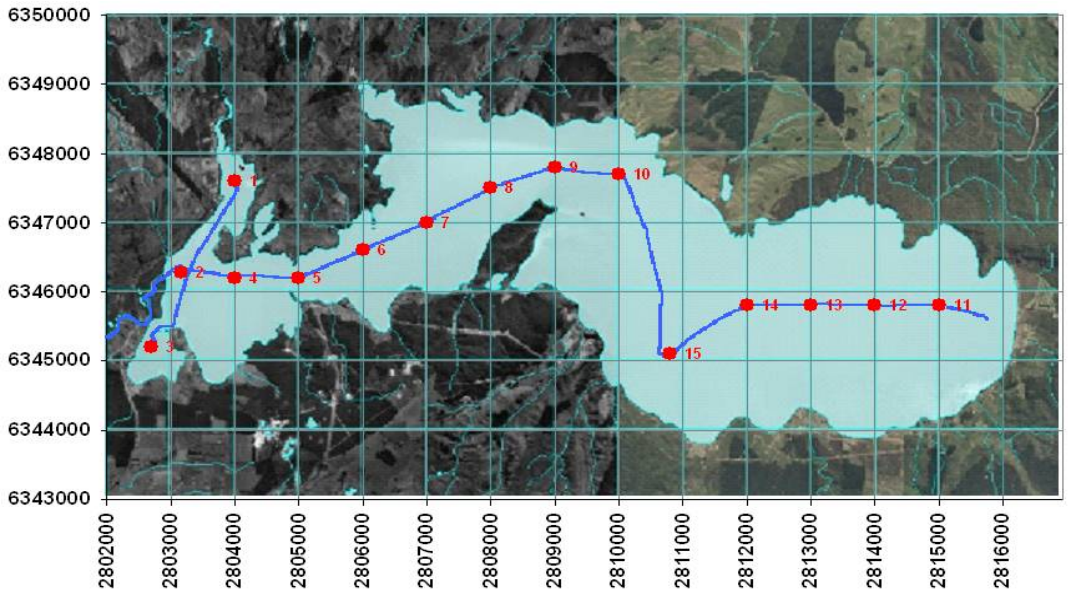

Figure 5. *UTM coordinates (North and East in metres) for Lake Rotoiti, showing the position of the main GPS waypoints (red dots) and the actual path followed by the boat (blue line) in the Bio-Fish transect.*

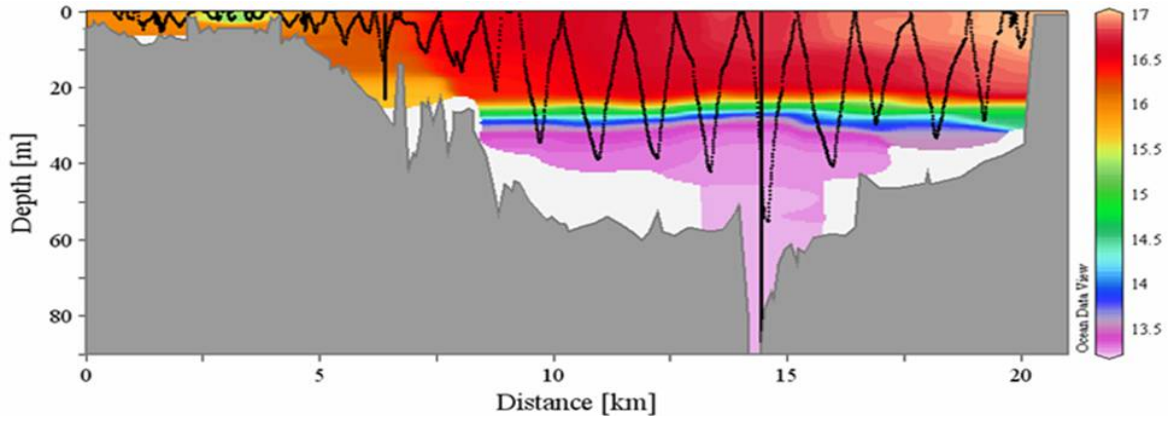

Figure 6. *Cross section of Lake Rotoiti showing the undulating path of the Bio-Fish from near the Kaituna River outflow (0 km), advancing into the shallow entrance of Okawa Bay (2.5 km) and then back out (3.5 km), and proceeding to the eastern end of the lake (22 km) on 7 April 2004. Dark vertical lines show conductivity-temperature-depth vertical profile points. Colours illustrate values of dissolved oxygen [mg L^{-1}].*

Comparisons are made in Figure 7 of four different variables: temperature, conductivity, dissolved oxygen and chlorophyll fluorescence, for a Bio-Fish transect on 7 April 2004. A prominent feature of this transect is a marked thermocline at a depth of 30m (Figure 7a), producing strong vertical gradients in conductivity, dissolved oxygen and chlorophyll fluorescence. There are also horizontal gradients in water properties between Okawa Bay and the deeper basins of Lake Rotoiti, indicating reduced horizontal mixing and transport of water through the connecting channel. With low flushing rates and higher light intensities in the water column of Okawa Bay compared with the main lake basin, it follows that levels of chlorophyll fluorescence are strongly elevated in the bay (Figure 7), without any consideration of variations in nutrient levels. Chlorophyll fluorescence is also elevated in the Kaituna arm of Lake Rotoiti.

Figure 8 shows BioFish data from a run from the western end of Lake Rotorua (Ngongotaha) through the Ohau Channel (very shallow region) and extending to the western basin of Lake Rotoiti for two days; 31 March and 19 April 2004. Conductivity of Lake Rotorua is approximately 35 $\mu S\ cm^{-1}$ higher in Lake Rotorua than in Lake Rotoiti; this difference has little effect impact on the water density and, as conductivity behaves relatively conservatively, it may therefore be used as a tracer for the path of water from Lake Rotorua to Lake Rotoiti. On 31 March there is an apparent dilution and plunging of the Ohau Channel water as it enters Lake Rotoiti. It may be surmised in Fig. 8a, based on a horizontal intrusion of constant conductivity from the western bed of Lake Rotoiti c. 30m depth, that this case represents an interflow, with the temperature of Ohau Channel water at some intermediate level that equates to that in a region of the thermocline in Rotoiti. Figure 7b is more likely to represent a surface intrusion, with conductivity in the surface layer of the western basin of Lake Rotoiti in the range 190-200 $\mu S\ cm^{-1}$ and considerably greater than near the centre of the lake. Strict categorisation of surface intrusions and interflow cases is complicated, however, because there is high diurnal variability in temperature and, therefore, in insertion depths. However, the case of Lake Rotoiti on 7 April 2004 (Figure 7) is also indicative of a surface intrusion of Ohau Channel water into Lake Rotoiti, with elevated chlorophyll fluorescence and conductivity in the Kaituna arm of the lake.

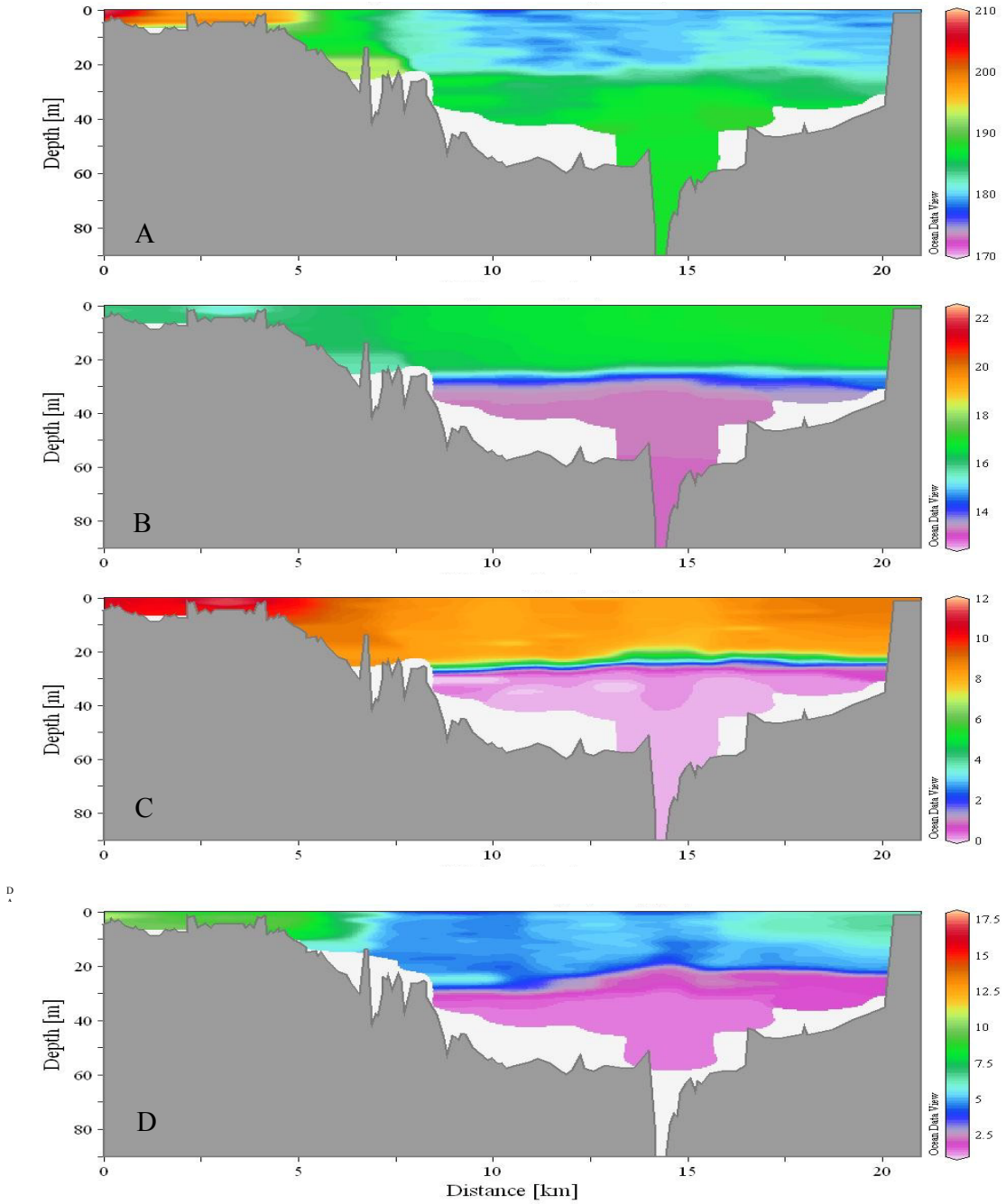

Figure 7. *Bio-fish transect of Lake Rotoiti from near the Kaituna River outflow (0 km), advancing into the shallow entrance of Okawa Bay (2.5 km) and then back out (3.5 km) and proceeding to the eastern end of the lake (22 km) on 7 April 2004. Variables include (a) conductivity [μS cm^{-1}], (b) temperature [^{o}C], dissolved oxygen [mg L^{-1}] and fluorescence in units approximating to chlorophyll* a *in μg L^{-1}.*

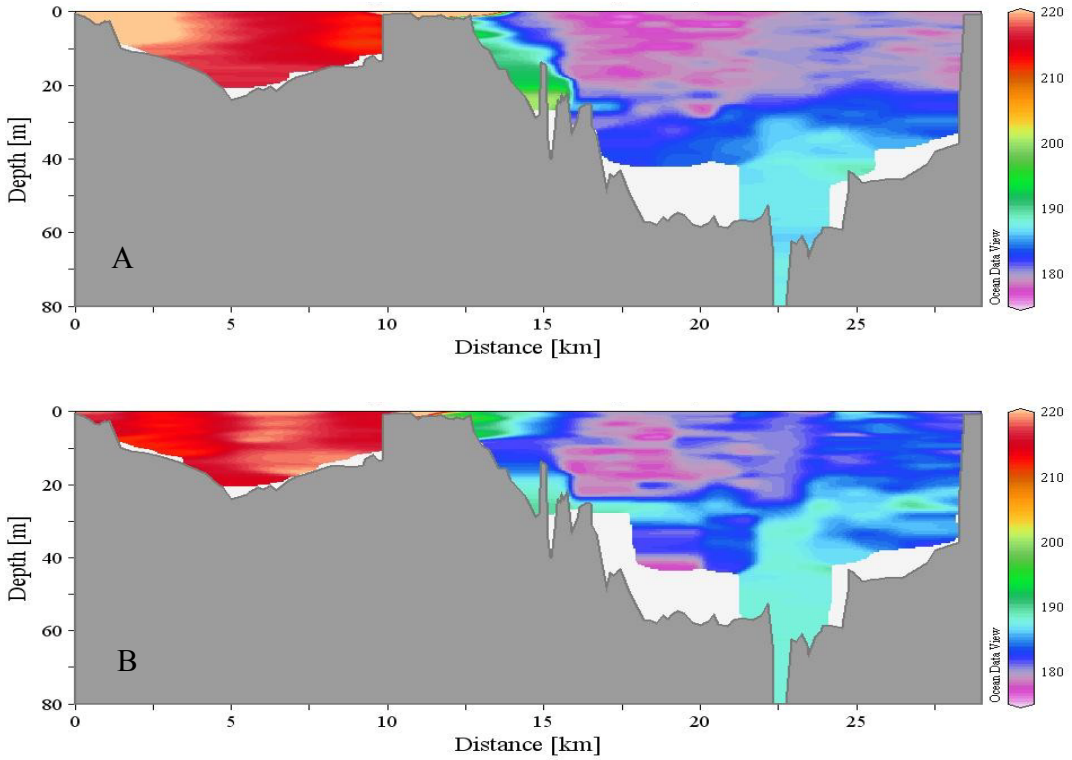

Figure 8. *Conductivity [μS cm^{-1}] in a transect across Lake Rotorua from Ngongotaha to the Ohau Channel (0-10 km), through the Ohau Channel (10-12 km) and as far as the eastern end of Lake Rotoiti (12-30 km). Transects are for (a) 31 March and (b) 19 April, 2004.*

On 17 May 2004, an attempt was made to track the path of the Ohau Channel plume into Lake Rotoiti. This transect examined the region from the Ohau Channel entrance to approximately 2.5 km into the lake, as shown in Figure 9. Properties of the Ohau Channel inflow are substantially different from those of the surface waters of Lake Rotoiti and make it easily distinguished as an intrusion along the sloping bottom of the lake (Figure 10). However, there is some dilution associated with the entrainment of water from the lake into the plume. The initial stages of the horizontal intrusion of the plume in the thermocline region are also demonstrated in Figure 10, which occurs as the plume temperature begins to approximate lake temperature for the corresponding depth.

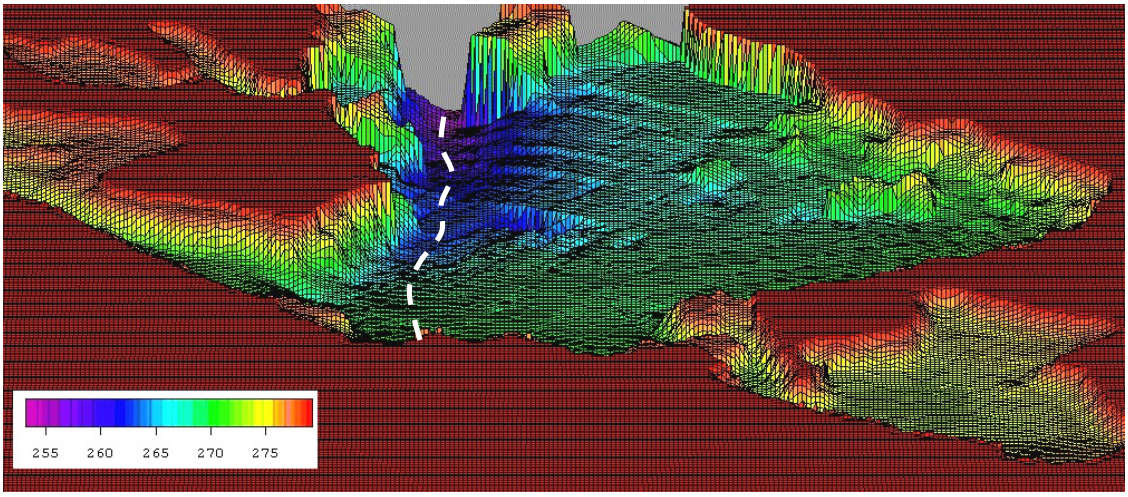

Figure 9. *Plunging Ohau Channel plume (white dashed line) as it proceeds towards the main basin of Lake Rotoiti. The distance of this line is approximately 2.5 km and is the path followed in the Bio-Fish transect of Figure 10. Colours represent elevation (masl) with shoreline and land areas assigned a value of 279.20m.*

It is now evident that there is a range of intrusion depths of the Ohau Channel plume into Lake Rotoiti. The intrusion depths are influenced by the temperature of the plume relative to the lake water temperature, the extent of entrainment of lake water into the plume, and by the stratification that exists in Lake Rotoiti. The intrusion depth will strongly influence whether water from Lake Rotorua is likely to have an effect on Lake Rotoiti water quality. There is evidence to indicate that when there is a surface intrusion, most of the effects are localised to the western basin (Fig. 7) and that the outflow from the Kaituna River will act to draw water from the Ohau Channel towards the Kaituna arm region of the lake. By contrast, intrusions of the plume into the stratified region just below the surface mixed layer (i.e. the metalimnion) can be expected to propagate eastwards through the western basin and into the main basin of Lake Rotoiti. In sections that follow a more detailed analysis of the Ohau Channel insertion depths is made using temperature data, a re-examination of historical data, and model simulations.

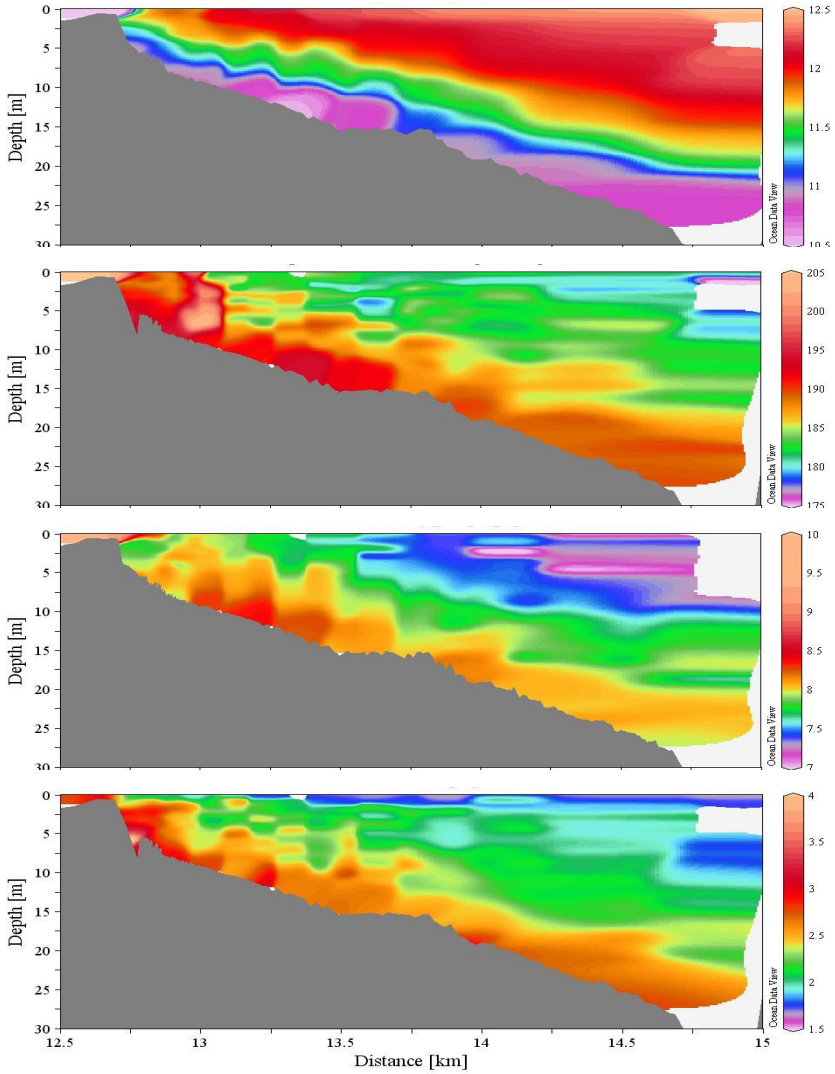

Figure 10. *Properties of Lake Rotoiti in the region of the Ohau Channel and eastward towards the main basin of the lake on 17 May 2004. Variables include (a) temperature [^{o}C], (b) conductivity [$\mu S\ cm^{-1}$], (c) dissolved oxygen [$mg\ L^{-1}$] and (d) fluorescence in units approximating to chlorophyll a in $\mu g\ L^{-1}$.*

2.2 Bathymetry

A hydrographic survey of lakes Rotorua and Rotoiti was undertaken as part of this project, primarily to provide input data for the three-dimensional modelling undertaken by NIWA, but also to support engineering design considerations related to possible implementation of groynes near the Ohau Channel outlet of Lake Rotorua or a diversion

of the channel in Lake Rotoiti. The existing bathymetric data from 1966 in Lake Rotorua and 1971 in Lake Rotoiti was considered inadequate for these purposes. Appendix 1 should be consulted for details of the bathymetric study. In addition the attached CD provides the raw bathymetric data. In this report we present graphical images of the data that are additional to the existing study, and discuss these briefly in the context of the Ohau Channel diversion and water quality in Lake Rotoiti. Figure 9 shows the western end of Lake Rotoiti, including part of the Kaituna arm, as well as Okawa Bay. A narrow, shallow channel connects Okawa Bay to the body of the lake; the maximum cross-sectional depth of this channel is less than 2m in some places. This channel can be expected to impose a major restriction on flushing of Okawa Bay and is the main reason why the bay has different characteristics to those of the main body of the lake at corresponding depths (refer to Figure 7). The Kaituna arm is also mostly shallow, with the cross-sectional depth around 5m through much of the arm. There is a steep drop-off or shelf near where the Ohau Channel enters Lake Rototi, with the water depth changing from around 0.5m to greater than 5m in just a few metres along the lake bed.

Lake Rotoiti as a whole has a highly irregular bathymetry (Figure 11). A relatively deep extant river channel is readily distinguished along the east-west axis of the lake. One could envisage the path of an underflow from the Ohau Channel extending eastward along this river channel and either lifting off the bed at some intermediate depth when it attained neutral buoyancy, or proceeding into the deeper region of the main basin where there is a small, deep hole extending to a depth of 125m. The east-west dissolved oxygen transect of Lake Rotoiti given in Fig. 7c can be used in conjunction with the bathymetry (Figure 11), to provide a conceptualisation of the region of bottom sediments that would be subject to anoxia. There is a large area of the bottom sediments in a depth band from approximately 30 to 50m, i.e., mostly just below the thermocline and therefore in the zone of anoxia. From a depth of 30 to 40m, the water volume increases by 42% (Ellery, 2004), suggesting that relatively small changes in the depth of the thermocline or anoxic zone will have large impacts on the area of bottom sediments and the volume of water that is anoxic.

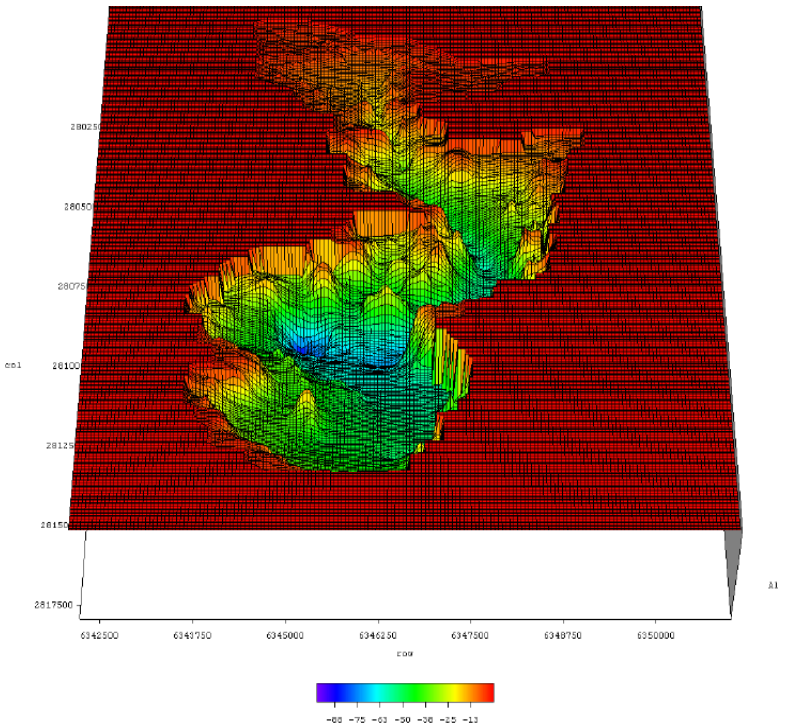

Figure 11. *Bathymetry of Lake Rotoiti viewed from the eastern end of the lake. The 'col' and 'row' axis labels refer to UTM longitude and latitude values [m], respectively. Vertical elevations are given with respect to an assigned value of 279.20 m for the lake shoreline, with elevations exceeding this value coloured red.*

Figure 12 shows the bathymetry of Lake Rotorua in the north-east end of the lake, including a region where the Ohau Channel exits the lake. The maximum depth shown is close to that in the central lake basin; just over 20m (excluding a deep hole around 45m in the Sulphur Point region of the lake). The central feature of Figure 12, however, is the relatively shallow (c. 1m) shelf which extends approximately 500m offshore at its maximum. The shelf region falls off sharply into a well defined central basin, with an associated transition from mostly coarse, erosional sediments to finer depositional material (Hendy, pers. comm.).

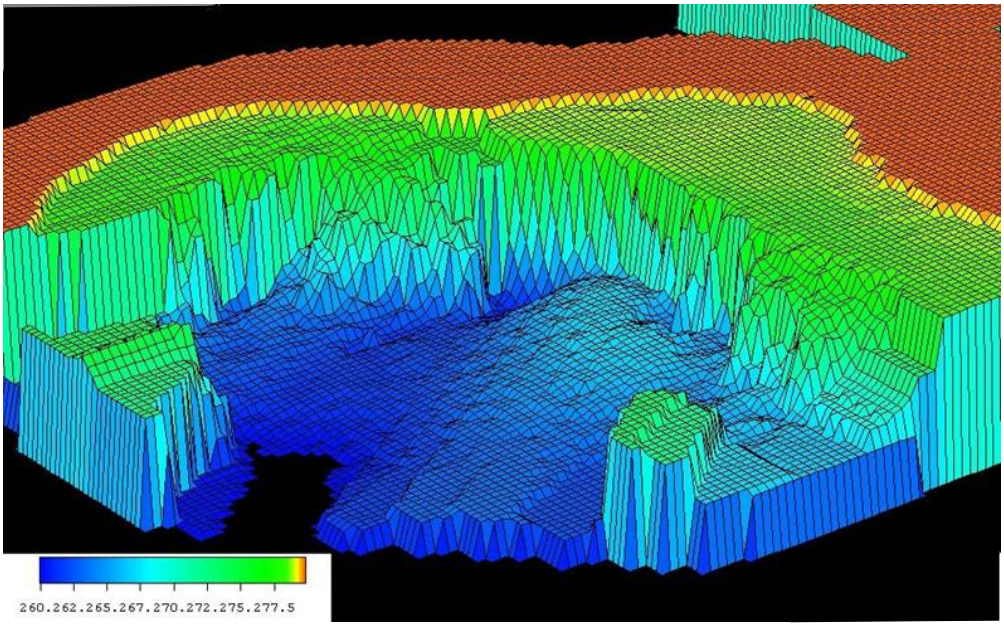

Figure 12. *Bathymetry of the north-east region of Lake Rotorua. The values in the left-hand corner refer to depths in metres, with the shoreline assigned a value of 279.80 m (coloured red). The maximum horizontal distance of the shelf (c. 1m depth) is approximately 500m. The Ohau Channel exit is not clearly delineated but is in the top right-hand corner of the figure.*

2.3 Temperature recordings for Ohau Channel and Lake Rotoiti

Detailed temperature measurements were required in the Ohau Channel and in Lake Rotoiti, in order to understand the likely depth of insertion of the Ohau Channel into the lake. Temperature was measured using autonomous Tidbit® loggers, with readings taken at 15-minute intervals from each sensor from the locations shown in Figure 13. The Ohau Channel sensor was placed at around 1m depth while the Narrows chain consisted of measurements at depths of 0.5, 2.5, 5, 7.5, 10, 12.5, 15, 17.5, 20 and 25m, and the Crater chain had measurements at depths of 0.5, 5, 10, 15, 17.5, 20, 22.5, 25, 27.5, 30, 32.5 and thereafter at 5-m intervals from 35 to 95m.

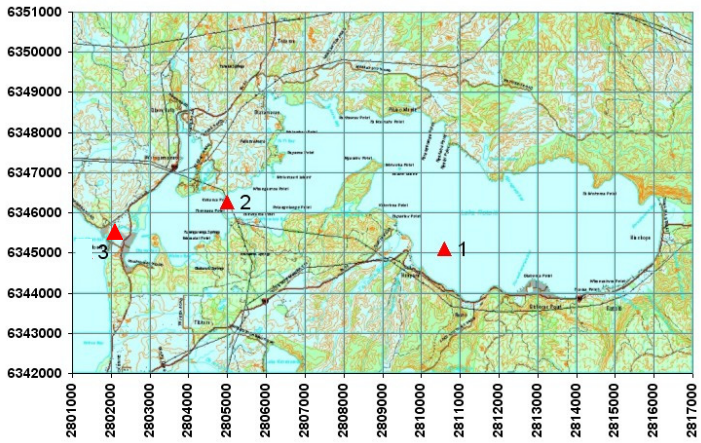

Figure 13. *UTM coordinates (north and east in metres) for Lake Rotoiti, showing the position of the thermistors. (1) The Crater chain (95m depth), (2) The Narrows chain (25m depth) and (3) the Ohau Channel logger at 1m depth.*

Because of the extensive nature of the temperature record, not all of the data are presented here and the subset of data presented is designed to pick out distinctive features. The reader is referred to the attached CD for the complete temperature data sequence (February to May) collected during the project.

Temperature in the Ohau Channel was quite variable between days but also varied by up to 5^{o}C within individual days (Figure 14). These variations are far greater than observed in the surface waters of Lake Rotorua (Burger, pers. com.) and support the hypothesis that there may be rapid heating or cooling across the shallow shelf of Lake Rotorua (Gibbs et al., 2004) as well as through the 2.5 km reach of the Ohau Channel itself. This suggests that even within individual days the depth of insertion of the Ohau Channel may be quite variable. Figure 15 provides a detailed examination of surface water temperature across a transect on 17 May 2004, from just inside the Ohau Channel, proceeding across

the shallow sand bar, across the 'drop-off' and then approximately 150m into the western basin. The blue line shows the bottom depth and the red line shows surface water temperature. The water temperature increases sharply around 55m distance in association with the Ohau Channel water plunging and the surface water being displaced by water from Lake Rotoiti. The region from 55 to 130m is still an active zone of mixing, however, between Ohau Channel water and Lake Rotoiti water, which is reflected in the high variability of surface water temperatures in this region. By 130m, the temperature is almost constant which suggests that the Ohau Channel plume has descended below the immediate surface waters. From the perspective of maintaining the distinctive characteristics of the Ohau Channel inflow to Lake Rotoiti, it would be useful, should a diversion proceed, to have the Ohau Channel water confined initially to the shallower entrance region prior to the 'drop-off' before progression into the Kaituna arm region of the lake.

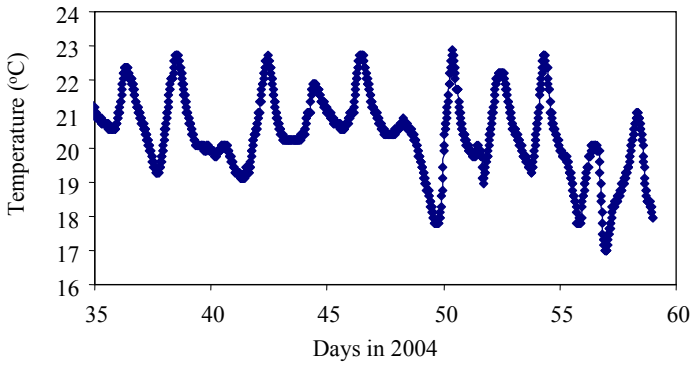

Figure 14. *Temperature in the Ohau Channel from 4 to 27 February 2004. Each point represents a measurement separated in time by 15 minutes.*

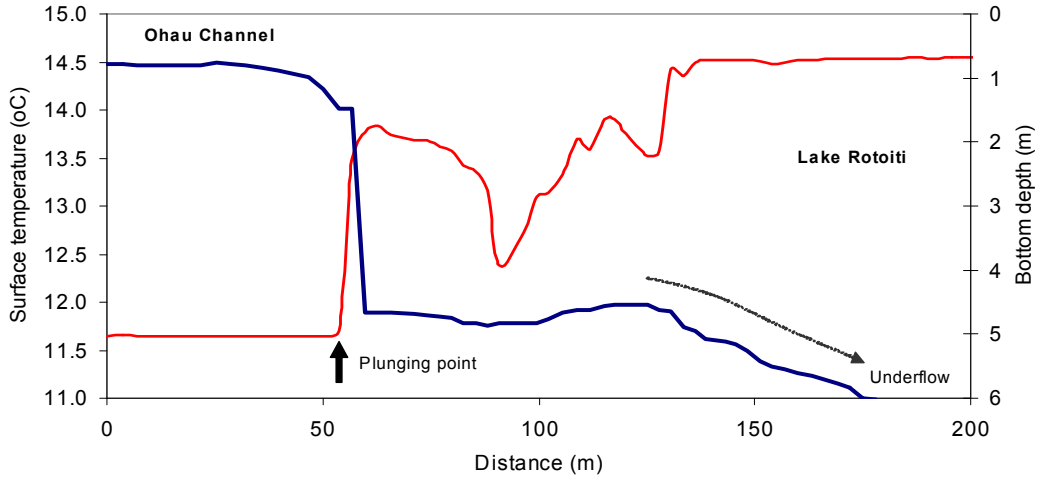

Figure 15. *Water depth (blue line) and surface water temperature (red line) from just inside the Ohau Channel (0m), across the sand bar to the 'drop off' at 55m and towards the main western basin of Lake Rotoiti at 1230 hrs on 17 May 2004. The likely underflow path of the Ohau Channel plume along the lake bottom is denoted by an arrow.*

A factor that also complicates the analysis of Ohau Channel insertion depths is the variation in thermal structure in Lake Rotoiti. The seasonal monomictic (single winter mixing period each year) is invariant, but temperatures can be highly variable at certain locations in the lake within shorter periods of time. An example of this variability is provided in Figure 16, which shows depth-time contours of temperature at the Narrows and Crater stations. The central location of the Crater station and the relatively constant nature of its temperature record suggest that it may be close to a fulcrum point for internal waves. By contrast these waves create seiching and large oscillations in temperature at the Narrows. The internal waves, with periods close to 24 hours, are probably energised by diurnal oscillations in wind and are reinforced in the confined boundaries of the Narrows, creating very large oscillations. Regions of constant temperature in the Narrows may vary by 15m depth or more in the course of a single day (Figure 16). The internal waves also interact with the highly irregular bathymetry in the Narrows region, most likely creating a great deal of turbulence and mixing in this region. Evidence of the mixing dynamics is provided by Bio-Fish transects on some of the

sample days, which showed a marked increase in the vertical extent of the metalimnion in the Narrows region compared with elsewhere in the lake.

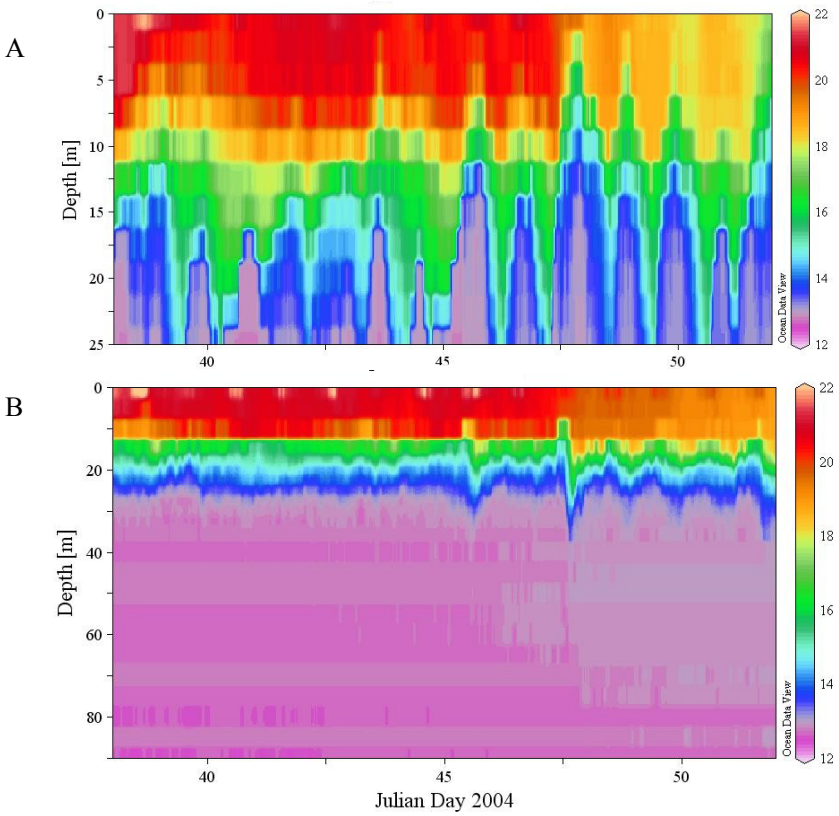

***Figure 16**. Data from thermistor chains at (a) the Narrows and (b) the Crater (note different depth scales). The numbers corresponding to Julian Day 2004 equate to 7 to 21 February. Note that no inter-sensor correction has been applied; temperatures may be in error by up to 0.2^{o}C from individual sensors and this is likely to have produced the subtle banding of colours (i.e. small temperature variations) in the hypolimnion in (b).*

In summary, the Ohau Channel temperature varies in tandem with the daily cycle of heating and cooling. The heating-cooling cycle is accentuated as water is transported across the shallow shelf region of Lake Rotorua and through the Ohau Channel. The Ohau Channel plume inserts into a highly dynamic hydrodynamic environment in Lake Rotoiti, with internal waves likely to also influence the depth of insertion in the case of

an interflow, and also acting to mix and disperse interflows. The turbulence generated by the internal waves and the highly irregular bathymetry in Lake Rotoiti, mean that the Ohau plume may be spread over a substantial depth range within the course of a day as a result of mixing and turbulence, as well as depth oscillations in the temperature structure. Most models are likely to underestimate the will range of variation of inflow insertion depths under these circumstances.

2.4 DYRESM-CAEDYM input data

Meteorological data used for input to Lake Rotoiti were taken from Rotorua Airport meteorological station as discussed above. Plots of the data, formatted as daily values and with units adjusted for input to DYRESM-CAEDYM, are given in Figure 17.

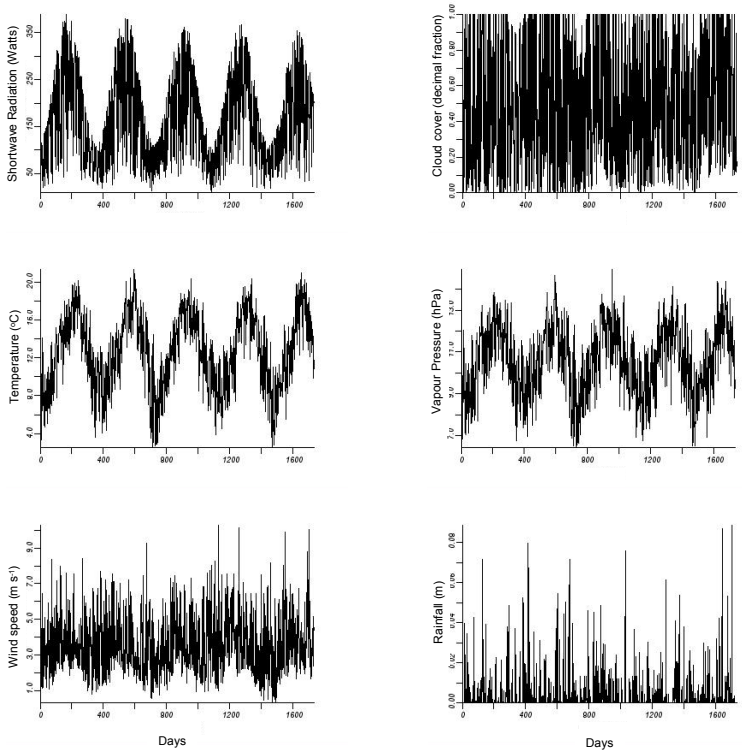

Figure 17*. Meteorological data from Rotorua Airport and formatted as input for DYRESM-CAEDYM model runs. The 'days' axis commences on 1 July 1999 and extends to 1 April 2004.*

To provide the required inflow volumes to Lake Rotoiti, it was necessary to create a water balance as follows:

$$\frac{\Delta V}{\Delta t} = Ohau\ Channel - Kaituna + Rainfall - Evaporation + Residual$$

where ΔV is the change in lake volume with change in time, Δt. The change in lake volume was derived from water level gaugings and corresponding changes in storage volume (Table 1). The residual term includes the groundwater flow, the storm run off as well the base flow from all inflows other than the Ohau Channel. This term was used to 'close' the water balance. The inflow and outflow components of the water balance are shown in Figures 18 and 19 respectively.

Table 1. Storage table for Lake Rotoiti which was used for DYRESM model input and for specification of changes in lake volume with water level changes. Note that elevation extends only to 93.5m and does not include the very small volume and area (< 1%) associated with the Crater deep hole. Volume 1 is cumulative with elevation and volume 2 represents values between the elevation contour.

Elevation (m)	Volume 1 (m^3)	Volume 2 (m^3)	Area (m^2)
93.5	1042300000	295070000	31750000
83.5	747230000	252990000	27048000
73.5	494240000	213880000	22811000
63.5	280360000	155620000	18670000
53.5	124740000	89225000	11438000
43.5	35515000	25948100	3964100
33.5	9566900	4814100	1351900
28.5	4752800	2228600	615620
23.5	2524200	1850860	250130
13.5	673340	626747	106740
3.5	46593	46593	19013
0	0	0	0

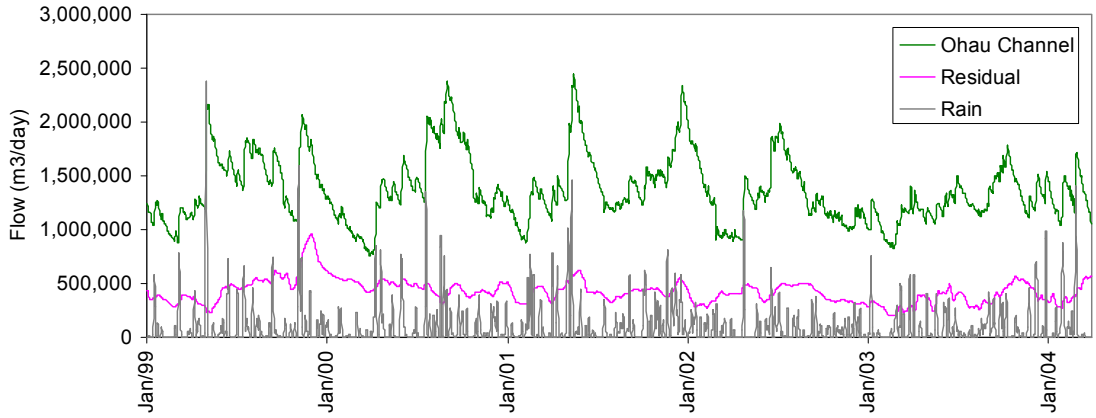

Figure 18. *Inflows included in the water balance*

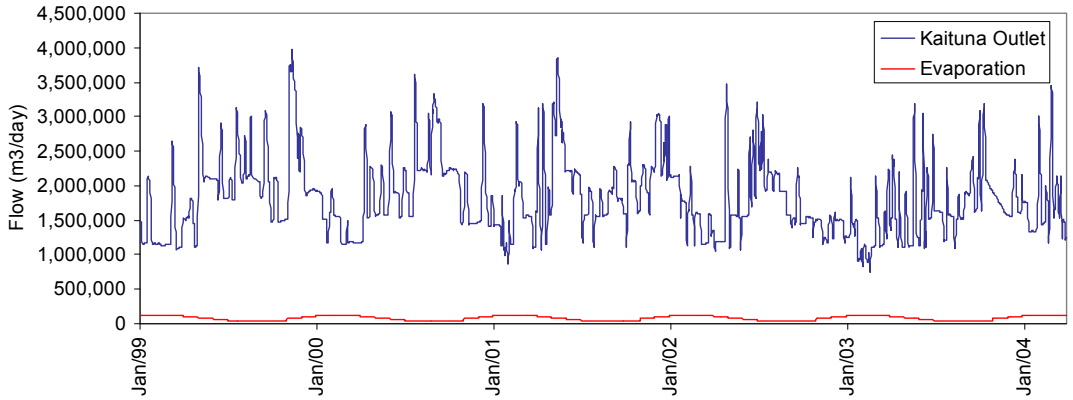

Figure 19. *Outflows included in the water balance*

The mean flows of the various components for the period 1 January 1999 to 28 February 2004 are: Ohau Channel 15.84 m^3 s^{-1}, Kaituna outflow 21.09 m^3 s^{-1}, rainfall 1.30 m^3 s^{-1}, evaporation 0.96 m^3 s^{-1} and the residual term 4.93 m^3 s^{-1}. The residual term was split into two different sources of water, with 70% corresponding to coldwater springs and storm runoff around the lake, entering at a temperature corresponding to a mean air temperature for the preceding 7 days, and the remaining 30% entering as surface hotwater springs at temperature 30°C.

The water temperature assigned for the Ohau Channel in the model input required careful analysis. A correlation indicated that daily mean air temperature measured at Rotorua Airport (elevation 10m) explained 80% of daily average water temperatures of the Ohau Channel, which were derived from the 15-minute thermistor readings (Figure 20). While this correlation provided a reasonable match for the period of February to May 2004, the predicted values tended to underestimate water temperature in the Ohau Channel for the longer duration used for DYRESM-CAEDYM simulations, in which data commenced from 1 January 1999 and in which most water temperature data were likely to be collected as grab samples from the Ohau Channel in the early morning. To rectify this, water temperature predicted from the correlation with air temperature was simply increased by 1^{o}C. The final estimated temperatures are compared against measurements in Figure 21 for the period 1 January 1999 to 28 February 2004.

The monthly pattern of overflow and interflow/underflow events in the Ohau Channel has been documented by Vincent et al. (1986) for a period in 1981-82 (Figure 22). This estimate was based on the relative temperature difference between the Ohau Channel and the vertical profile of lake water temperature.

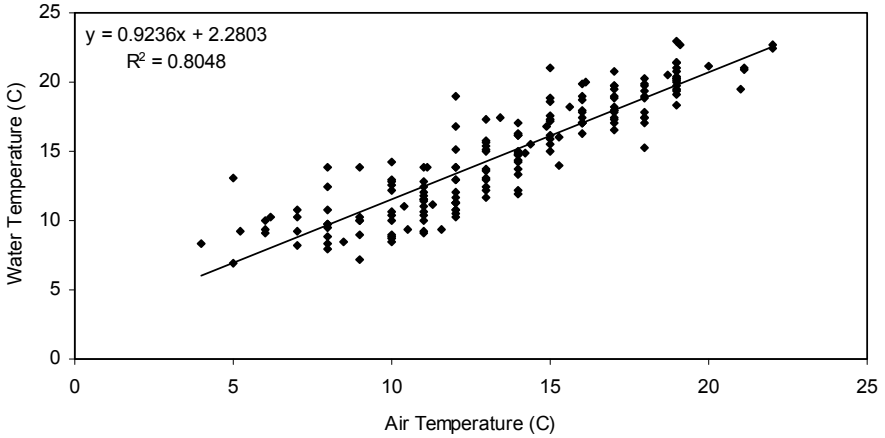

Figure 20. *Correlation of daily average Ohau Channel water temperature with daily average air temperature from Rotorua Airport.*

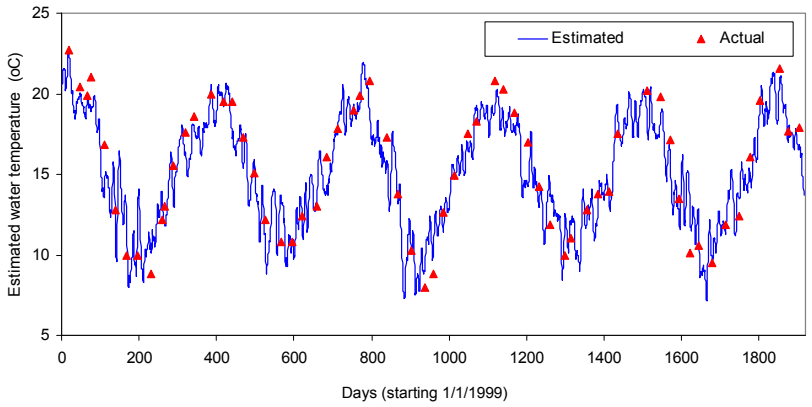

Figure 21. *Temperature measured in the Ohau Channel compared with estimated derived from correlations with air temperature with an adjustment of +1°C (refer to text).*

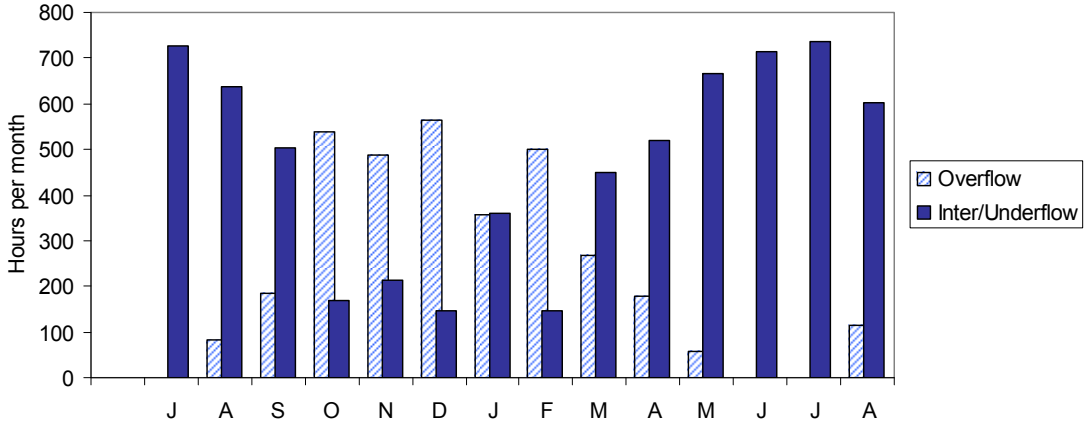

Figure 22. *Seasonal pattern for overflow and, inter/underflow events for the Ohau Channel entry to Lake Rotoiti in 1981-82 (Vincent et al 1986).*

Based on the results of Figure 22, the inflow data entered into the DYRESM-CAEDYM model was modified to compensate for the effect of short-circuiting of water to the

Kaituna River. For the overflow case, only 20% of the water entering from the Ohau Channel was used as input to the DYRESM-CAEDYM model. For the interflow or underflow case, 100% of the Ohau Channel water is estimated to reach the main lake basin. Based on these figures and the relative time of overflow or underflow/interflow each month (Figure 22), it was possible to estimate the percentage of Ohau Channel water that would reach the main basin and that should be included as input for The DYRESM-CAEDYM model (Figure 23). There will inevitably be some inter-annual variation in the frequency of overflow, underflow and interflow events represented in Figure 23, and any estimates will be complicated greatly by the interactions of a varying inflow temperature with the presence of internal waves in Lake Rotoiti. For example, Figure 24 shows how a varying water temperature and internal waves make the depth of insertion of the inflow highly variable, both within days and between days over a period of 2 weeks. It should also be noted that the insertion depth estimated in this way will overestimate the depth of insertion of the Ohau Channel water because it does not reflect entrainment of lake water that occurs for the interflow/underflow case.

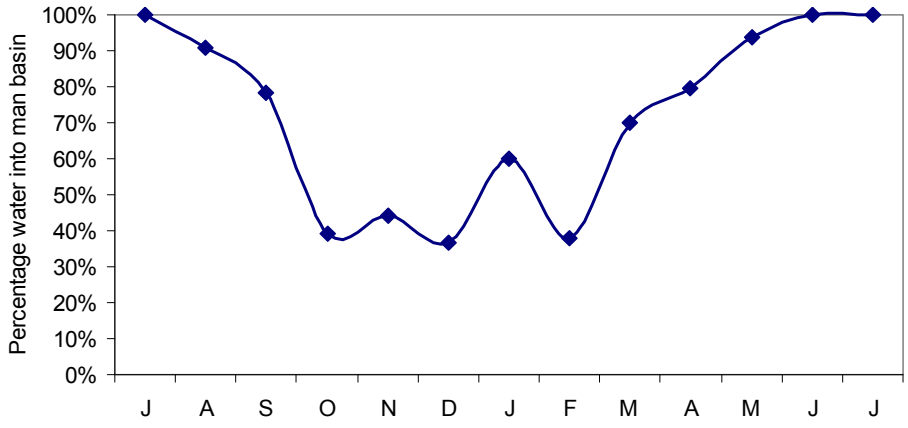

Figure 23. *Percentage of the Ohau Channel reaching the main basin of Lake Rotoiti.*

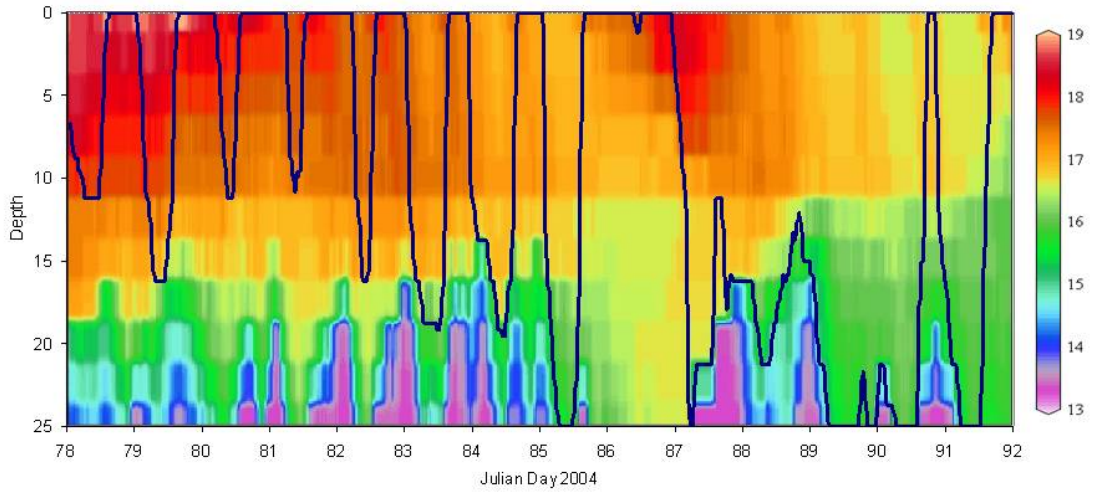

Figure 24. *Time-depth colour contour plot of water temperature (^{o}C) in Lake Rotoiti from 18 March to 1 April 2004. Thermal structure is based on thermistor chain data at the Narrows (25 m water depth). The continuous line shows the depth where the temperature of the Ohau channel matches the temperature of the lake water.*

The DYRESM-CAEDYM model is reliant on daily averaged input data related to inflow volume, temperature and composition, yet it is clear that the prescription of a single daily average temperature would not reflect the extent of variability of temperature and insertion depths for the Ohau Channel inflow. A more detailed analysis of temperature variations in the Ohau Channel was therefore carried out to examine the departure of instantaneous readings of temperature from the daily average value. These values are compared in Figure 25 with the corresponding values for surface water temperature in Lake Rotoiti, which were taken from the upper-most thermistor positioned at the Narrows. The pattern of variation in temperature in the Ohau Channel was translated into a histogram that represented the frequency of occurrence of different temperature differentials between the instantaneous and daily mean readings in the Ohau Channel (Figure 26). Based on this histogram, the Ohau Channel inflow used in the input to the DYRESM-CAEDYM model was partitioned into three separate components. Each component had identical composition, but one inflow was assigned 50% of the total Ohau Channel volume and a water temperature equal to the daily mean value, while the other

two inflows were each assigned 25% of the total inflow volume and a temperature either 1^0C higher (Ohau inflow 1) or 1^oC lower (Ohau inflow 2) than the daily mean value.

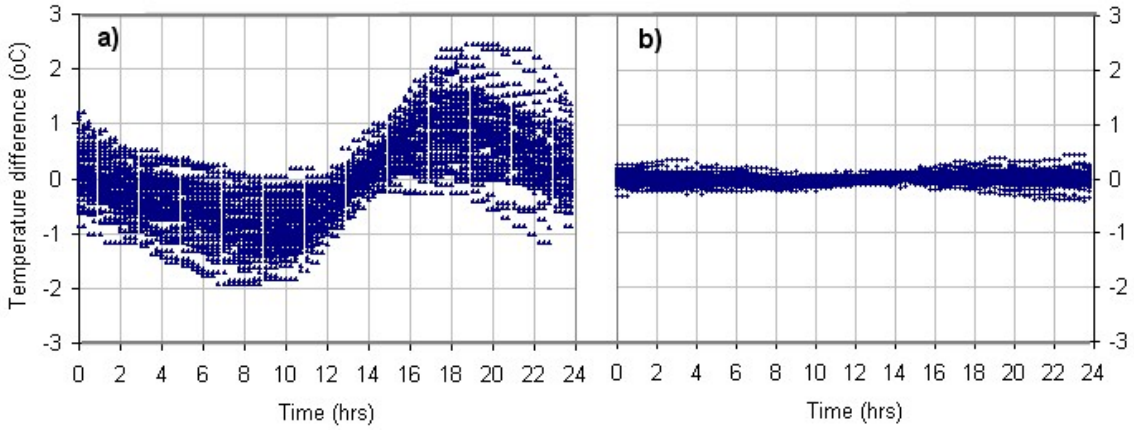

Figure 25. *Temperature difference between instantaneous measurements and daily averages for a) Ohau channel and b) surface water in Lake Rotoiti at the Narrows site. Negatives values imply that instantaneous temperature measurements are colder than daily average. Time represents time of day commencing at midnight.*

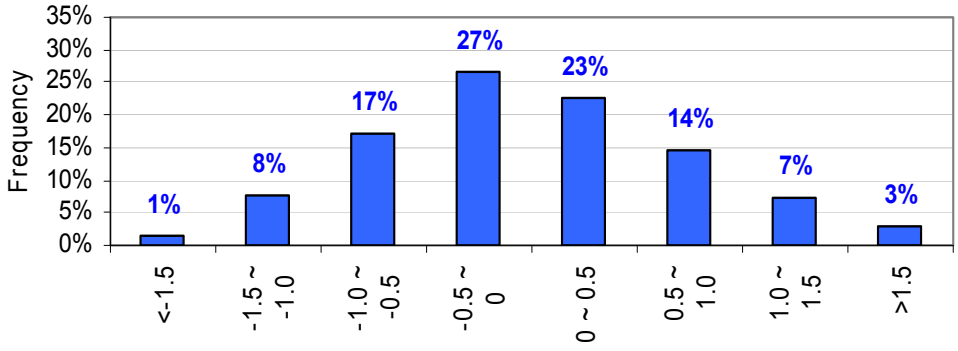

Figure 26. *Frequency of occurrence of departure of instantaneous water temperature in the Ohau Channel daily average values. Negatives ranges represent temperatures which are colder than the daily average. This plot was used to partition the Ohau Channel into three inflows for input to the DYRESM-CAEDYM model (see text).*

In order to accurately derive Ohau Channel insertion depths into Lake Rotoiti, a further detailed analysis of entrainment of lake water with the Ohau plume was carried out. This analysis not only provides more accurate estimates of the insertion depth, but also provides the properties of the underflow or interflow at the horizontal insertion point into the lake. For example, Gibbs (1992) estimated that the Ohau Channel underflow may be 4 to 5 times greater in volume than the initial inflow by the time it inserts horizontally into the lake. The 'drop off' near the Ohau Channel entrance to Lake Rotoiti (refer to Figure 15) also plays an important role in the entrainment, with the inflow initially proceeding as a jet of water for around 100m after the drop off, before, if becomes an underflow and re-establishes continuity with the bottom of the lake (Vincent et al., 1986). For this case the resulting dilution of the inflow may be modelled with the empirical equation of Jirka and Watanabe (1980) for a buoyant surface jet entering a quiescent pond:

$$D = \frac{Q_u}{Q_i} = \frac{Q_i + Q_r}{Q_i} = \frac{1.2 \cdot U_i}{\left(g \cdot \frac{\rho(T_i) - \rho(T_r)}{\rho(T_i)} \cdot \left(\frac{A_i}{2} \right)^{1/2} \right)^{1/2}} - 0.2$$

where D is the dilution factor, Q_u *and* T_u are the volume and temperature of the underflow, Q_i *and* T_i are the volume and temperature of the initial inflow, Q_r *and* T_r are the entrained flow and vertical averaged temperature of the lake water, and A_i *and* U_i are the area and velocity of the initial inflow. This case does not account for entrainment in the plunge zone of the inflow, however, because Jirka and Watanabe (1980) developed their model for a surface overflow only. The entrainment that occurs when the inflow cools and plunges or, in the case of Lake Rotoiti, when the jet of cool surface water loses momentum and plunges, may be reduced compared with an inflow plume which followed the sloping bottom of the lake.

The entrainment was examined for a period when the effect of internal waves on the stratification was relatively weak in Lake Rotoiti, and when the Ohau Channel would have been an underflow at the Narrows station. The thermistor reading at the bottom of

the Narrows close to the lake bed was compared to the thermistor reading in the Ohau Channel. Various offsets of time were used to reflect the lag between water in the Ohau Channel and its transport to the Narrows. A lag time of 10 hours was found to minimise the difference between the two readings (Figure. 27) and equates to the value estimated by Vincent et al. (1984, 1986) in their analysis of travel times of the Ohau Channel plume to a station also situated in the Narrows region. Using a 10-hour lag time, a mass balance approach for heat content associated with the initial inflow, the entrained surface water and the sum of the two represented by heat content at the Narrows, may then be used to assess the dilution factor for the Ohau Channel plume from its entrance at the lake until its arrival at the Narrows. This dilution was found to fit well with experimental simulations of the Ohau Channel by Leong (1988) and with a modified DYRESM inflow model (see Spigel et al., in press, for more information) that was developed specifically to reflect the enhanced entrance mixing of the inflow jet due to water being entrained from all directions, followed by the reduced entrainment as the inflow plunges rapidly to the lake bed.

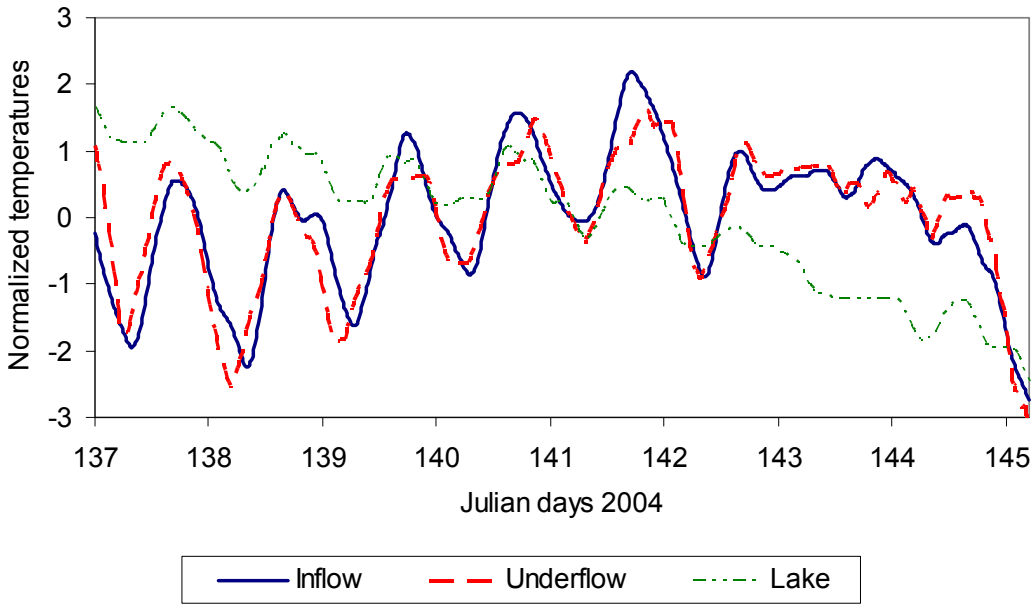

Figure 27. *Comparison of temperatures for the inflow Ohau Channel inflow, the underflow (measured at the Narrows) and in surface waters of Lake Rotoiti. A lag of 10 hours has been applied to the underflow values.*

2.5 Geothermal heating

It is well known that there is considerable geothermal heating of water in Lake Rotoiti. The geothermal heat flux enhances convective circulation in hypolimnetic waters and results in relatively small gradients in water composition within the hypolimnion (Gibbs 1992). The effect of geothermal heating is most evident when stratification is present and waters in the hypolimnion and largely uninfluenced by the comparatively large heat fluxes that occur at the water surface and act to obscure the geothermal flux. In Lake Rotoiti bottom temperatures increase by c. 2 to 3°C in most years during the stratified period and linear regression of temperature with time explains a relatively high percentage of the variation in temperature (Figure 28). A more in-depth examination of the regression slopes is given in Figure 29 in which there appears to be some continuity in the temperature increment in the hypolimnion between successive years. Without knowledge or parameterisation of the causes of these inter-annual fluctuations, the result will be deviations between measured temperatures in the hypolimnion and those simulated with the DYRESM model.

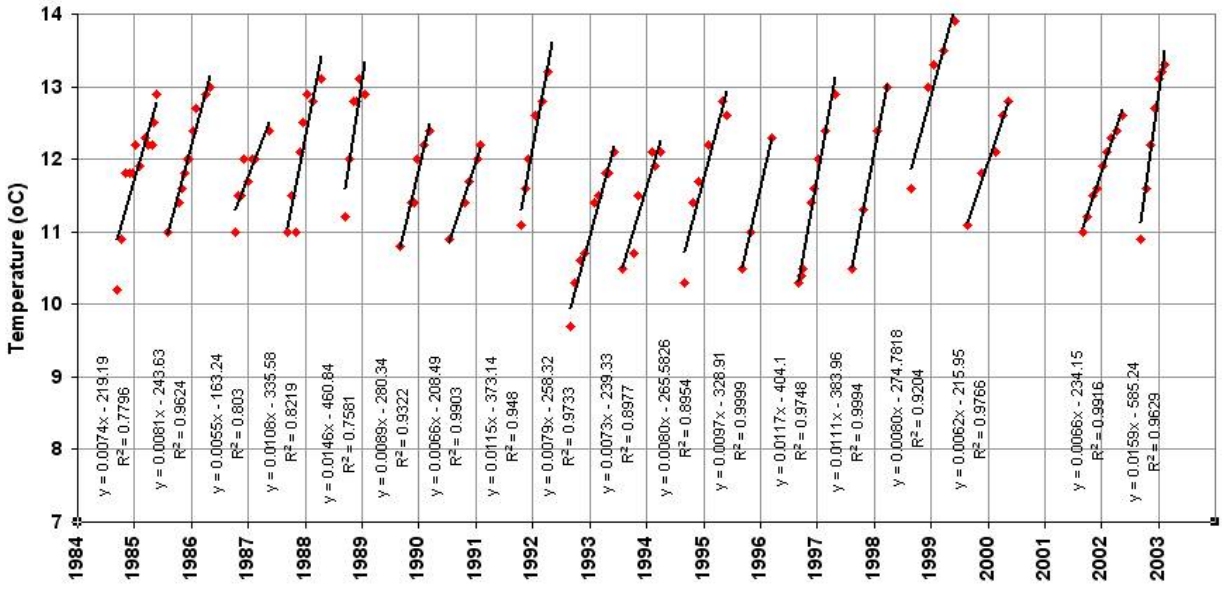

Figure 28. *Linear regressions of hypolimnetic (60-m depth) temperatures versus time in Lake Rotoiti from 1984 to 2003.*

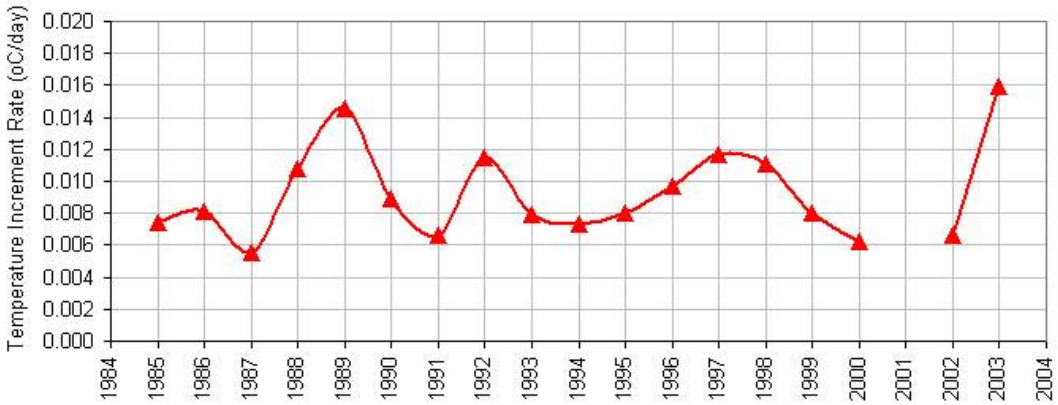

Figure 29. *Temperature increment in the hypolimnion of Lake Rotoiti based on regression slopes from Figure 28.*

Furthermore, the standard DYRESM code does not include a geothermal heating component and would therefore be likely to substantially underestimate temperature in the hypolimnion. A modified version of the code was therefore supplied by Dr Robert Spigel from NIWA in Christchurch. This code had initially been adapted to account for geothermal heat fluxes in Lake Taupo. For Lake Rotoiti a geothermal heat flux of 10 MW was supplied to bottom waters.

2.6 CAEDYM model inputs

Concentrations of dissolved oxygen, chlorophyll *a* divided into the buoyant (akin to cyanobacteria) and non-buoyant groups (akin to diatoms), nutrients (NO_3-N, NH_4-N, total nitrogen (TN), DRP and total phosphorus (TP)), biochemical oxygen demand specified in carbon equivalents using a stoichiometric conversion of 32/12 and suspended solids were specified for each inflow (i.e. three Ohau Channel inflows of different volume and temperature but identical water quality properties, and geothermal and non-geothermal inflows). There is no capacity to include nutrient inputs in rainfall in the standard version of DYRESM-CAEDYM, but this feature could be examined in future in order to refine simulation results. For brevity, only plots of the Ohau Channel composition are given below. Nutrient concentrations in the model input data for the Ohau Channel were taken from measurements, generally around monthly frequency, with these measurements

interpolated to provide a daily frequency of input required for the model. Similarly, measurements for the other inflows (e.g. coldwater streams: Tawhakarere, Ruato, Tapuaeharuru, Taupo Waiiti, Tumoana, Ruahine, Otuatura, and geothermal streams: Parengarenga, Hauparu and Te Turoa) were converted to loads by multiplying by the mean volume of each stream, then summing the loads separately for coldwater and geothermal stream inputs. These loads were then divided by the total coldwater or geothermal inflow volume and were used as the respective stream concentrations for DYRESM-CAEDYM input, together with the volume of each component, which for the coldwater stream was estimated to be 70% of the total residual (from the water balance) flow volume and 30% for the geothermal streams.

Figure 30 shows concentrations of nitrogen species in the Ohau Channel from 1 January 1999 to 28 February 2004. Dissolved and particulate organic fractions of nitrogen constitute the majority of the nitrogen. For phosphorus, the dissolved reactive component constitutes a larger fraction of total phosphorus (Figure 31) than the dissolved inorganic nitrogen contributions to the total nitrogen.

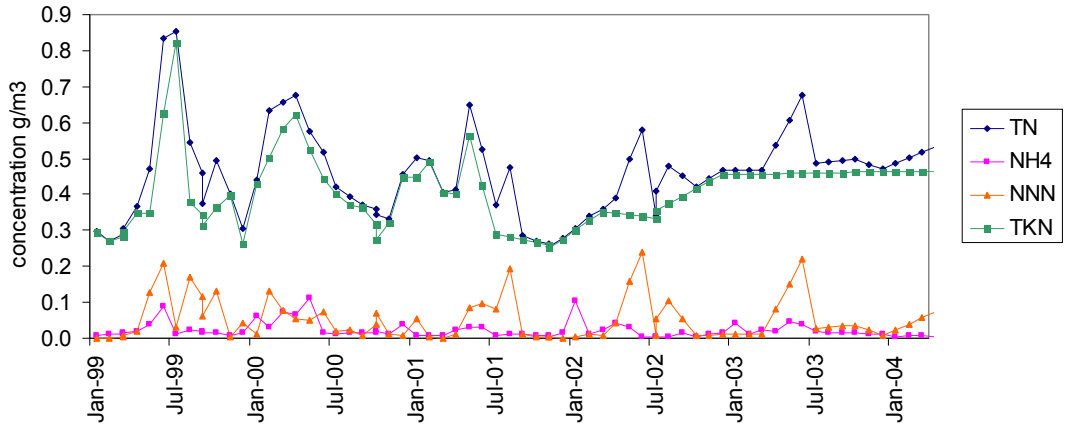

Figure 30. *Concentrations of nitrogen species in the Ohau Channel based on interpolation (lines) of measured values (points). NNN represents oxidised nitrogen species (NO_3-N + NO_2-N).*

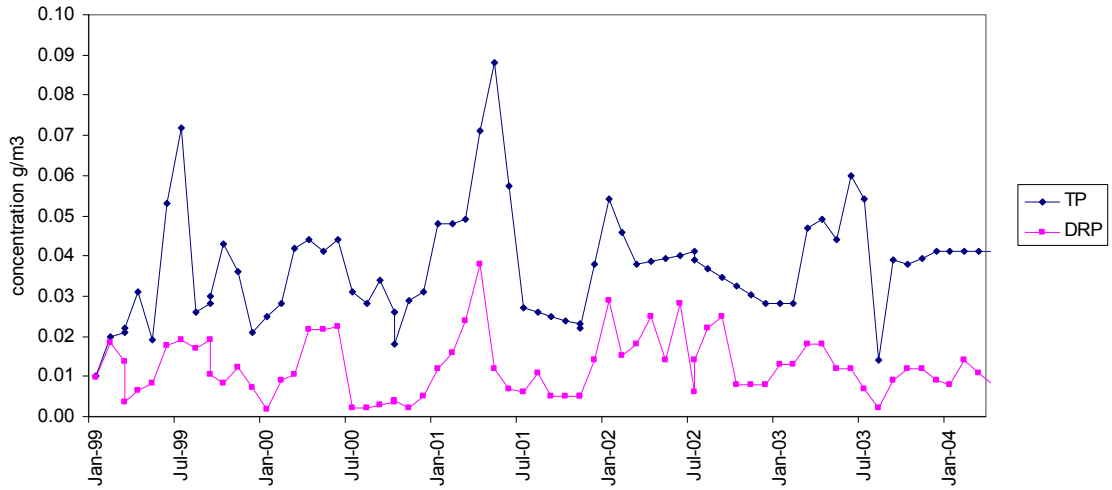

Figure 31. *Concentration of phosphorus species in the Ohau Channel based on interpolation (lines) of measured values (points).*

The Ohau Channel inflow file included concentrations of chlorophyll-*a*, which were approximated using phytoplankton and chlorophyll-*a* data collected from Lake Rotorua as part of the Environment BOP monitoring programme. Mean monthly phytoplankton cell counts for two sites (2 and 5) for the period September 1998 to September 2002 were divided into two groups (cyanobacteria and other phytoplankton (dominated by diatoms and green algae)). A 2-point running average was applied to smooth the highly variable data, and a proportion was allocated to each group. Values of chlorophyll-*a* concentration (0-8m tube sample) collected from the same sites and for the identical period were then multiplied by the cell count proportion, to derive an equivalent chlorophyll *a* concentration for each group (Figure 32). This method ignores variations in chlorophyll *a* content per cell between the two groups. There were no phytoplankton cell count data after September 2002 so mean proportions for the corresponding time in the previous years (1998-2002) were multiplied by the measured chlorophyll *a* concentrations for the period of interest, to extend the time series. After September 2003 it is assumed that the two groups represent 50% of the total cell count composition and

chlorophyll *a* concentrations were then allocated 50/50 to each group. Linear interpolation was than used to give a daily concentration for the entire period (Figure 32).

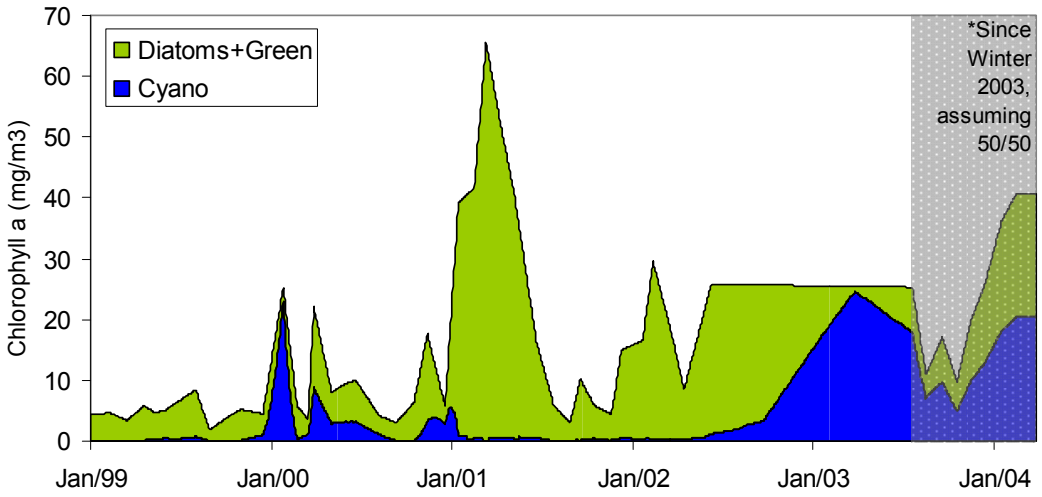

Figure 32. *Chlorophyll a concentrations for cyanobacteria (Cyano) and other phytoplankton (Diatoms + Green) for Lake Rotorua based on 0-8m depth integrated chlorophyll a and surface cell counts from sites 2 and 5.*

3.0 Model Results

Simulations commenced in July 2001 and extended until 30 June 2003, i.e., two-year runs. Sensitivity analyses were conducted on a small number of physical parameter inputs used in the DYRESM model, in order to develop a good understanding of the effect of these parameters on the model output, with care taken to ensure maintenance of realistic parameter bounds.

A comparison of measured and modelled temperature data is shown in Figures 33 and 34 (note extended period (2 years) in Figure 34). The abrupt nature of temporal transitions in temperature in the field measurements is a result of the frequency of measurement; approximately 2-weekly to monthly, whereas simulation output is at daily intervals. The

most obvious anomaly in the comparison is a slight excess of cooling in the simulations in the winter period of 2002. In the subsequent summer of 2002-3, temperature in the bottom waters is lower than observed values (Figure 34). This may also be a result of the very large apparent input of geothermal heat in the 2002-3 stratified period (see Figures 28 and 29) since the geothermal heat input to the model (10 MW, see above) was an average value based on the data presented in Figure 29.

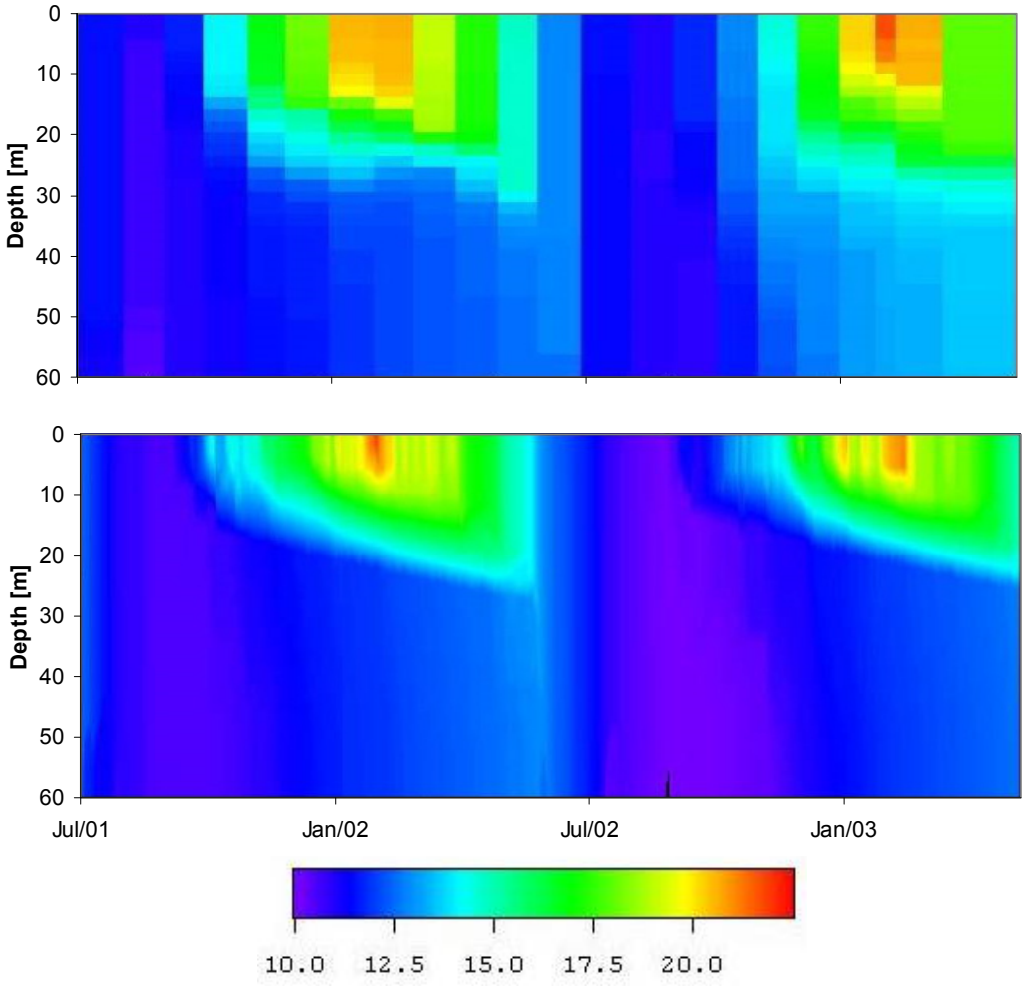

Figure 33. *Time-depth contour of temperature from 1 July 2001 to 12 May 2003 (680 days) based on field measurements (Narrows Station, upper panel) and simulations (lower panel). Only depths from 0 to 60m are shown. Colour temperature scale is in degrees Celsius.*

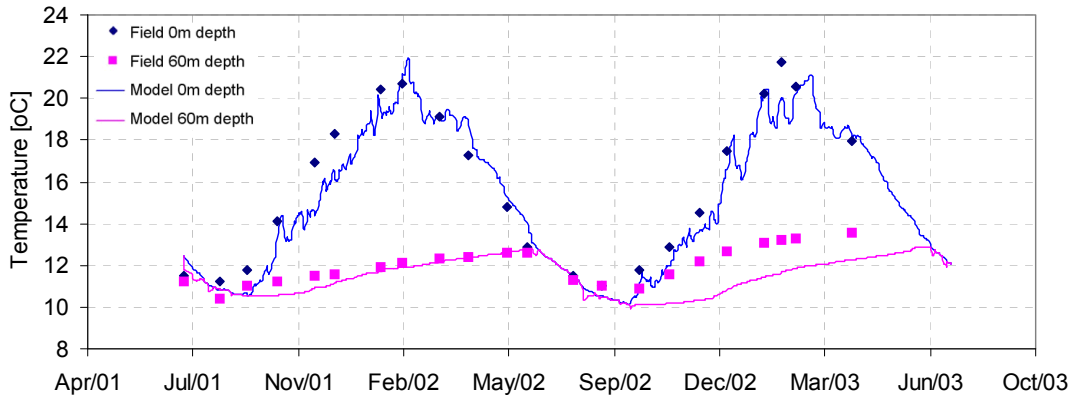

Figure 34. *Temperature from 1 July 2001 to 30 June 2003 (730 days) based on field measurements (Crater Station, 0 and 60m) and simulations for the corresponding depths.*

The depth of insertion of the inflows was examined using the DYRESM model simulations. The simulated inflow insertion depth used the modified version of DYRESM, which is described in part in Spigel et al. (2004) and accounts for spread of the Ohau Channel as a jet in the surface layer, followed by plunging to the lake bed in the case of an interflow or underflow. Figure 35 shows that the inflow inserts over the full range of water column depths over the course of the year. In winter it is predominantly an underflow, inserting mostly into the bottom-most layer of the DYRESM model, while during the course of summer it begins a transition from insertion near the water surface in spring and proceeding to the very base of the thermocline just before the end of summer. Keeping in mind the effects of internal waves and thermocline seiching, and despite considering the effect of variations in temperature in the Ohau Channel, it is likely that the inflow would in reality spread over an even greater range of depths than those represented in Figure 35.

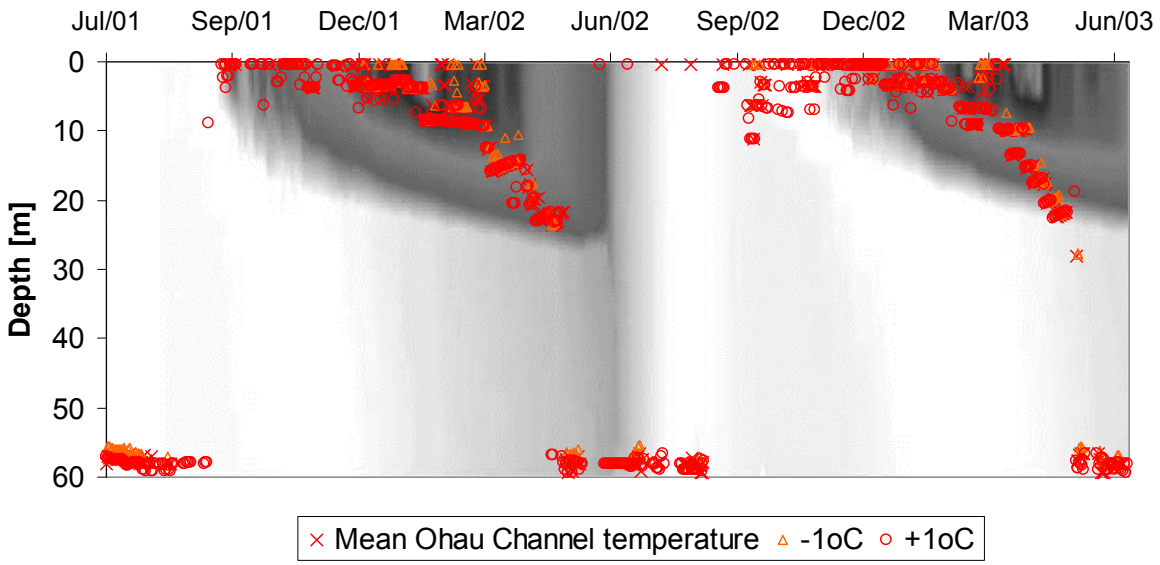

Figure 35. *Grey scale time-depth contour plot of temperature in Lake Rotoiti based on simulations from 1 July 2001 to 30 June 2003 (730 days). Superimposed on the simulation output is the insertion depth for the Ohau Channel inflow, predicted from the DYRESM model output, and separated into three components on the basis of temperature (see text).*

Comparisons of field measurements and simulation output of dissolved oxygen concentrations are shown in Figure 36. The simulations were obtained after extensive sensitivity analysis and calibration of parameters that influenced the dissolved oxygen concentration. There is a requirement for considerable time and effort to be spent in the calibration phase of CAEDYM simulations. This requirement relates to ecological parameters which have wide variations for several reasons, e.g., current state of knowledge of some processes is limited, different species have different physiological rates and the model tends to 'lump' species together, and temporal and spatial scales vary between field measurements and model output. For the case of dissolved oxygen, levels in the bottom waters were especially sensitive to the oxygen consumption rate of sediments prescribed in the model. The oxygen dynamics are mostly well reproduced though there is a tendency for the model simulations not to capture the gradual loss of

oxygen through the hypolimnion during each stratified period, suggesting that convective mixing may be over-emphasised in the model simulations or that there is a depth gradient of oxygen consumption in the water column or bottom sediments. A model versus field data comparison between surface and 60m depth dissolved oxygen (Figure 37) indicates that surface oxygen levels are slightly under-predicted in the model output, while at 60m levels decline slightly more rapidly than the field data in the early stages of stratification (October to December) but not in the latter stages. The simulation output was considered acceptable for making judgements about the effect of Ohau Channel diversions on dissolved oxygen in Lake Rotoiti.

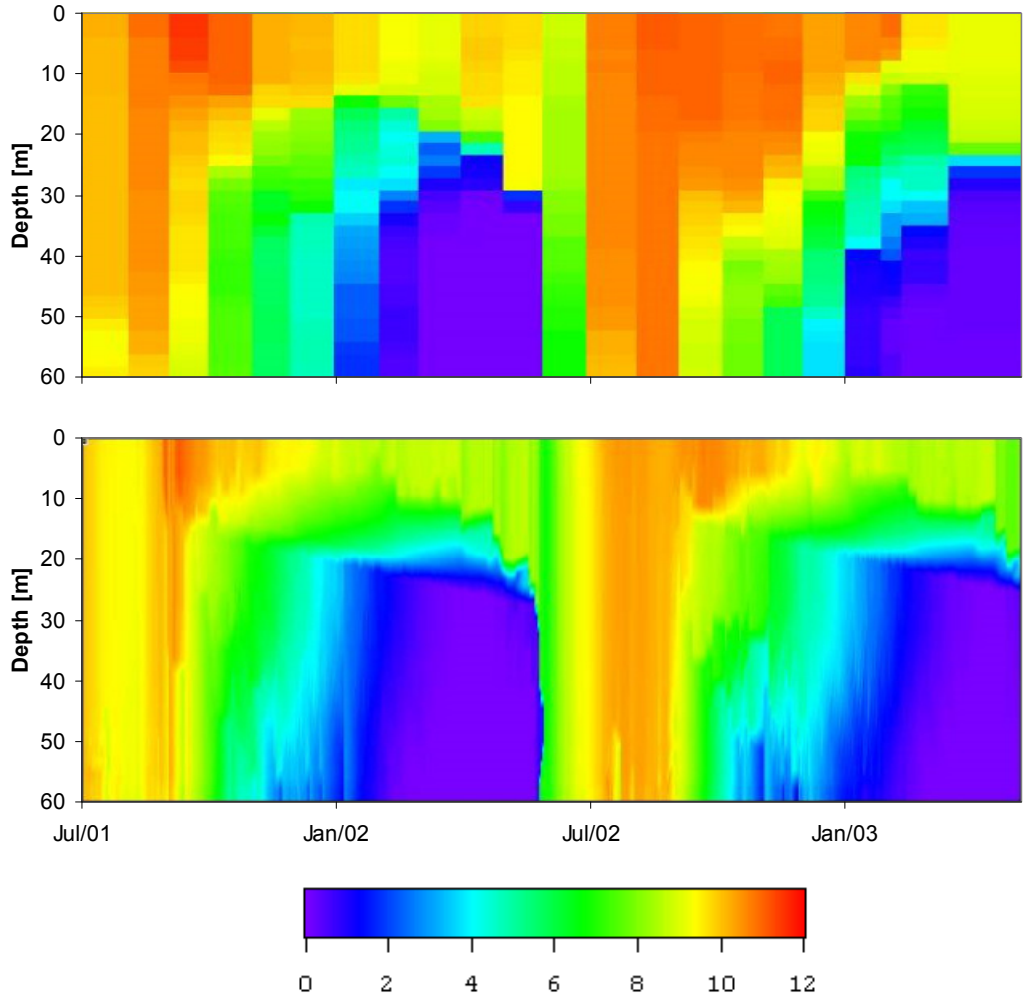

Figure 36. *Dissolved oxygen from 1 July 2001 to 12 May 2003 (680 days) based on field measurements (Crater Station, 0 and 60m) and simulations for the corresponding depths.*

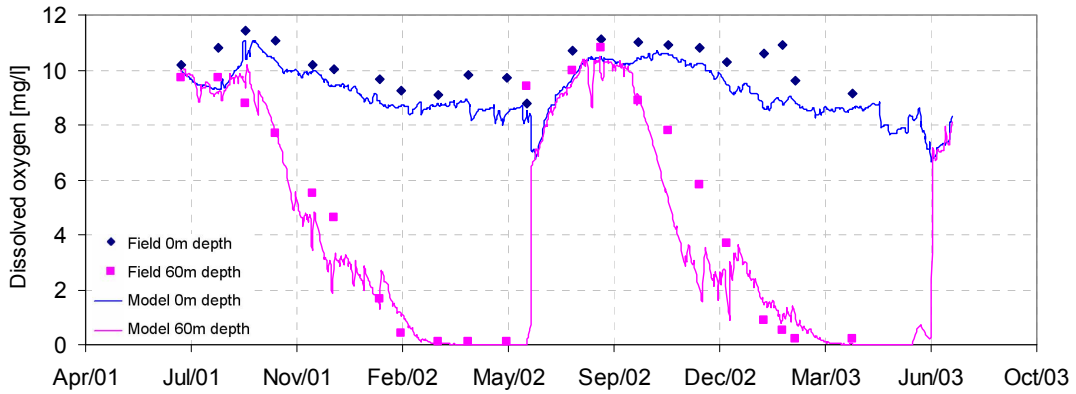

***Figure 37**. Dissolved oxygen from 1 July 2001 to 30 June 2003 (730 days) based on field measurements (Crater Station, 0 and 60m) and simulations for the corresponding depths.*

As expected, simulations of nutrient concentrations did not reproduce field measurements as accurately as was the case for temperature and dissolved oxygen, despite considerable time spent in the calibration phase. Some of the dynamics of nutrients in Lake Rotoiti are complex and not completely understood (see Priscu et al., 1986), and this adds to the difficulty of capturing and understanding all of the processes, and reproducing these in a model. The comparisons of model simulation output and field measurements are shown for depths of 0m (surface) and 60m, as these depths presented the best time series data. Figure 38 shows concentrations of ammonium at these two depths.

Field measurements of ammonium at 60m are characterised by two distinct peaks over the annual cycle (Figure 38). One peak occurs around December when bottom waters are still well oxygenated, after c. 2 months of stratification. This peak may be associated in part with the regeneration of ammonium from the winter diatom 'bloom' but may also be due to ongoing breakdown of organic matter in the 'closed' environment created by the existence of the hypolimnion. This peak was not well represented in the model simulations. The subsequent decline in NH_4-N is due to nitrification, while oxygen is still present in the hypolimnion for this oxidation process (Priscu et al., 1986; Hamilton et al., 2003). The other peak in NH_4-N occurs immediately prior to winter mixing, when

there is no oxygen in the hypolimnion to support nitrification, and NH_4-N continues to build up. This phase is captured in the model simulations, which appear to provide a reasonable extrapolation of the maximum levels of NH_4-N likely to be attained prior to winter mixing. Surface concentrations of ammonium are reasonably well represented in the model simulations, with elevated levels at winter turnover being reproduced by the simulations, followed by levels generally close to analytical detection limits for the remainder of the period.

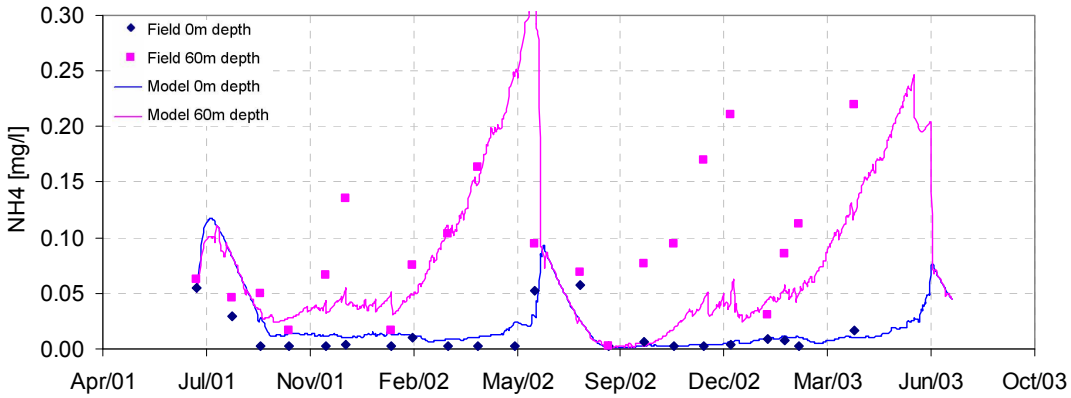

Figure 38. *Ammonium concentrations from 1 July 2001 to 30 June 2003 (730 days) based on field measurements (Crater Station, 0 and 60m) and simulations for the corresponding depths.*

In the absence of capturing one of the annual peaks of NH_4-N, specifically the one which leads to enhanced nitrification in the bottom waters, it is clear that there will be a discrepancy between model simulations and field measurements of NO_3-N in deeper (60m) waters. This is shown in Figure 39, where the build-up of NO_3-N at 60m around January to March does not show up at all in the model output, though the simulations capture the slightly elevated levels present in the winter mixing period, and the generally low levels of NO_3-N at the water surface.

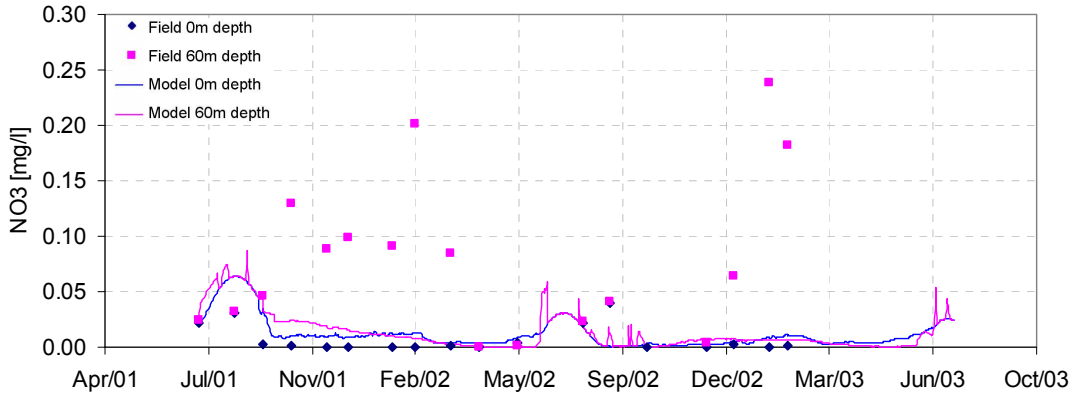

Figure 39. *Nitrate concentrations from 1 July 2001 to 30 June 2003 (730 days) based on field measurements (Crater Station, 0 and 60m) and simulations for the corresponding depths.*

A comparison of field measurements and model output of DRP for the surface and 60m depth is given in Figure 40. In this case the seasonal build-up of phosphorus in the hypoliminion is captured, but with a temporal offset between the field data and the simulation output. This lag may be due in part to an artificially large winter-spring diatom peak (see below) which depletes nutrients too rapidly prior to the establishment of stratification. To compensate for this the input of phosphorus from the bottom sediments is slightly artificially elevated in the model (i.e. the slope of the DRP build-up in the hypolimnion is higher; refer to Figure 40). This effect may result in a slight overestimation of the effect of the bottom sediments in the nutrient dynamics of Lake Rotoiti, but conversely, could be viewed as contributing a conservative prediction for the impacts of surface inflows on the nutrient dynamics of Lake Rotoiti (i.e. the effect on nutrient dynamics of diversions of the Ohau Channel are likely to be underestimated in the case of phosphorus). Simulated levels of DRP in surface waters at winter turnover are close to measured levels and also reflect a summertime decline, though again slightly too rapidly (see discussion on effects of winter diatom peak above). The pattern of simulated levels in late summer being close to analytical detection limits is encouraging and suggests that the uptake and regeneration rates of DRP may closely match reality.

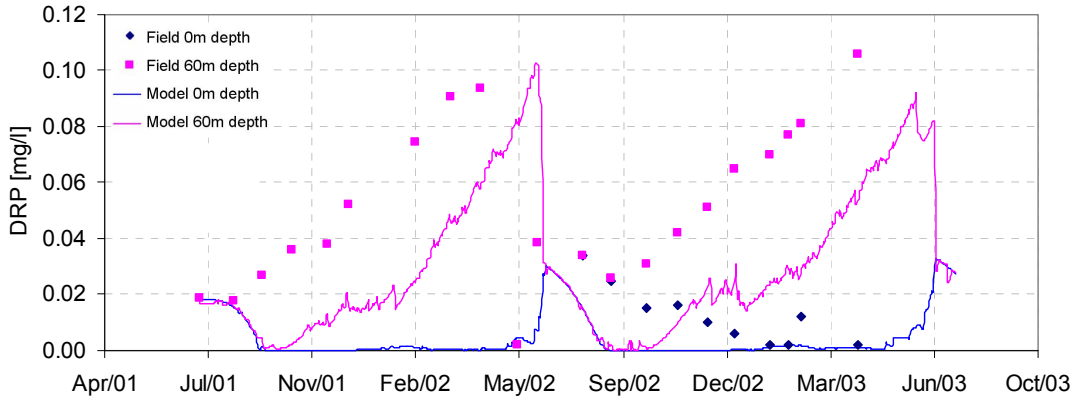

***Figure 40**. Dissolved reactive phosphorus concentrations from 1 July 2001 to 30 June 2003 (730 days) based on field measurements (Crater Station, 0 and 60m) and simulations for the corresponding depths.*

As part of the calibration process, concentrations of total nitrogen and total phosphorus were also examined. For reasons of brevity the results are not reproduced graphically here, but a brief discussion ensues. For the case of total phosphorus, the general patterns observed in DRP (Figure 40) occur, with the same lag in build-up of hypolimnetic TP in the simulation compared with the field data; at this time most of the TP in the hypolimnion is in the form of DRP. Total nitrogen concentrations in surface and bottom waters were mostly too low, partly related to the absence of the first ammonium peak in the model simulations. Nitrogen fixation by cyanobacteria was not simulated in the model and it is not known to what extent this process may have elevated total nitrogen concentrations in Lake Rotoiti. Measurements of nitrogen fixation in Lake Rotoiti in the 2002-3 summer, when there were very large populations of the cyanobacterium *Anabaena*, suggest that fixation may only have accounted for a few percent of the total nitrogen present in the lake.

Figure 41 shows concentrations of chlorophyll *a* for field measurements and simulations at the two depths (0 and 60m), with chlorophyll *a* separated into contributions from

cyanobacteria and other phytoplankton. The predicted diatom peak in winter-spring is perhaps too high while the cyanobacteria peak is perhaps too low, at least during the period of January and February 2003, when there was a lake-wide bloom of *Anabaena planktonica*. Generally, however, the seasonal succession of cyanobacteria and other phytoplankton (specifically diatoms) reported anecdotally and by Vincent et al. (1984), is reproduced in the model simulations. It is possible that the elevated diatoms levels predicted in the model simulation, particularly in winter-spring of 2002, may have depleted nutrients too severely (see Figures 38 to 40), leading to an inability to reproduce the very high biomass of cyanobacteria in January and February 2003.

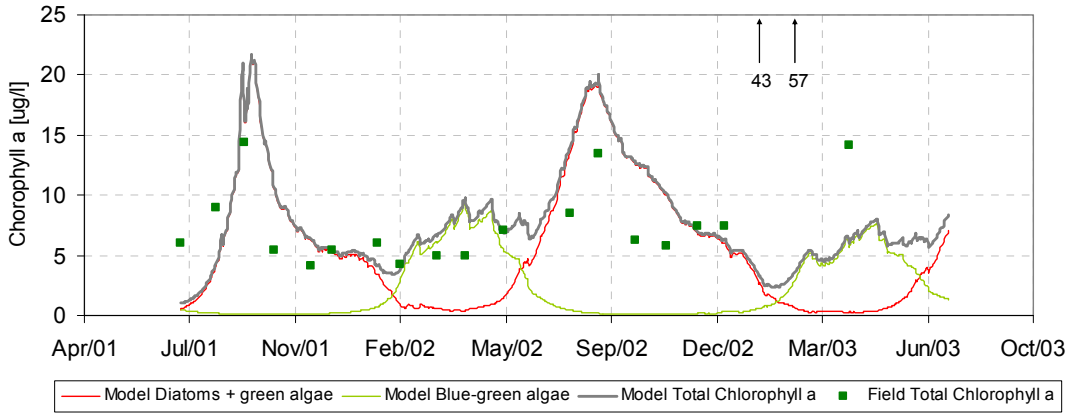

Figure 41. *Concentrations of chlorophyll* a *from 1 July 2001 to 30 June 2003 (730 days) based on field measurements (Crater Station, 0 and 60m) and simulations for the corresponding depths. Chlorophyll* a *is separated into contributions from cyanobacteria (blue-green algae), other phytoplankton (diatoms + green algae) and total chlorophyll* a.

A further examination of simulations of cyanobacteria and other phytoplankton is shown in Figures 42 and 43, respecitvely, which serves to illustrate the very different temporal and spatial distributions of these groups in Lake Rotoiti. Diatoms grow rapidly during the winter turnover period but decay rapidly once stratification sets up around September, though there is some persistence in the surface layer and apparently also as a weak deep

chlorophyll maximum which tracks the progressive deepening of thermocline through to the end of the year. Cyanobacteria have a very different pattern of distribution than diatoms and are dominant in late summer, being well adapted to the prolonged stratified conditions through buoyancy. The increase in cyanobacteria in the bottom waters in July-August 2003 reflects a deep insertion of water from the Ohau Channel (see insertion depths, Figure 35) which has moderate levels of cyanobacteria, and not a net growth of cyanobacteria at these depths. The simulations of phytoplankton biomass were considered adequate to make predictions about the behaviour of Lake Rotoiti under different conditions relating to Ohau Channel diversion. Ongoing research will address some of the issues that have been raised above in relation to the reasons for discrepancies between model simulations and observed data and may be the subject of more intensive studies designed specifically to elucidate certain processes and model parameters.

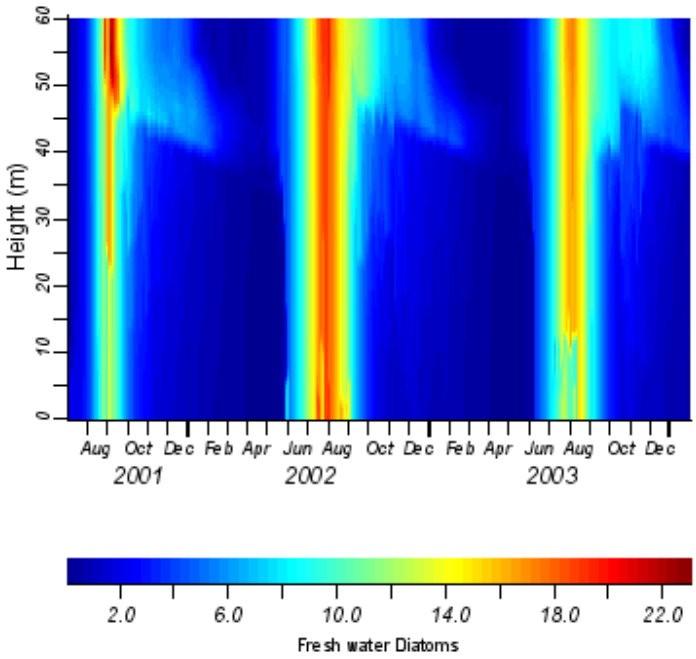

Figure 42. *Elevation (height)-time contours of simulations of chlorophyll a (mg L^{-1}) associated with diatoms and other phytoplankton from 1 July 2001 to 30 June 2003 (730 days).*

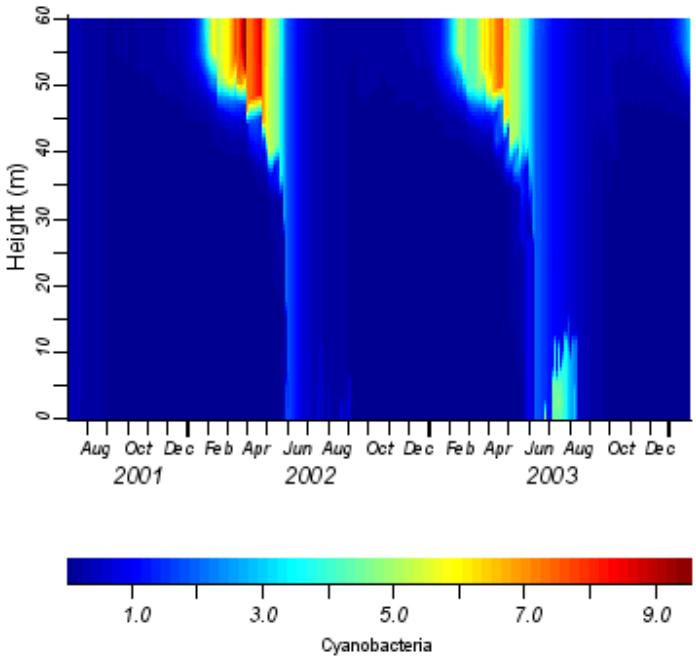

Figure 43. *Elevation (height)-time contours of simulations of chlorophyll a ($\mu g\ L^{-1}$) associated with cyanobacteria from 1 July 2001 to 30 June 2003 (730 days).*

4.0 Management Scenarios

For the present time, management scenarios have been run as relatively coarse diversions of the Ohau Channel; 0% and 50% maintained, and compared against the current case (100% maintained). More specific modifications of the amount of water diverted can be made if required. It should be noted that model simulations use a percentage diversion that reflects only the Ohau Channel water that enters the main body of the lake; the simulations do not reflect the water short-circuited to the Kaituna outlet, which is not included in the inflow data file for DYRESM-CAEDYM. Time series plots for 0m and 60m depth are again used to make direct comparisons between the different model runs (100, 50 and 0% of current Ohau Channel flows maintained), which are for a period of 943 days from 1 July 2001 to 31 January 2004. For most variables there is little purpose in carrying out quantitative comparisons between the different flow scenarios (e.g. temperature and dissolved oxygen in Figure 44), but where warranted (e.g. important

variables where differences are clearly evident in the simulations) a quantitative comparison has been carried out.

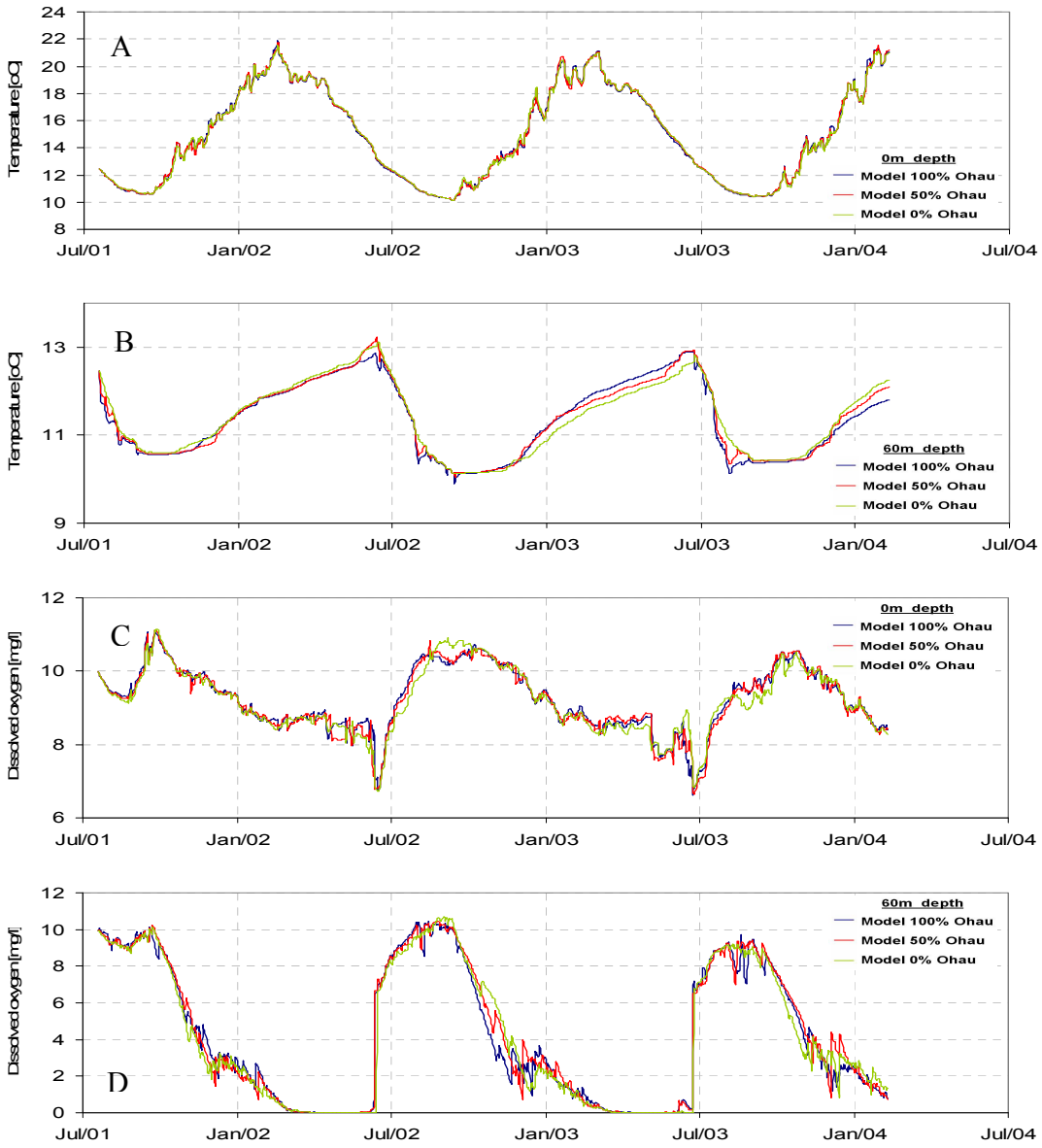

Figure 44. *Simulations of temperature at (a) surface (0m) and (b) 60m depth and dissolved oxygen concentrations at (c) 0m and (d) 60m for three different scenarios relating to % of Ohau Channel diversion.*

There were only very small changes in temperature (< 0.5°C) and dissolved oxygen (< 0.5 mg L^{-1}) under the different Ohau Channel flow scenarios (Figure 44). Given the inherent variability in measurements of these components and in the output from model simulations, no further discussion of the contributing sources of variability is entered into here. Similarly, levels of inorganic nutrients showed some variability between the different flow cases, but there was no clearly discernible pattern that could be related to flow (Figures 45 and 46), except perhaps that concentrations of NH_4-N and DRP may have been slightly lower in both surface and bottom waters with the progression from 50 to 0% of Ohau Channel inflow maintained.

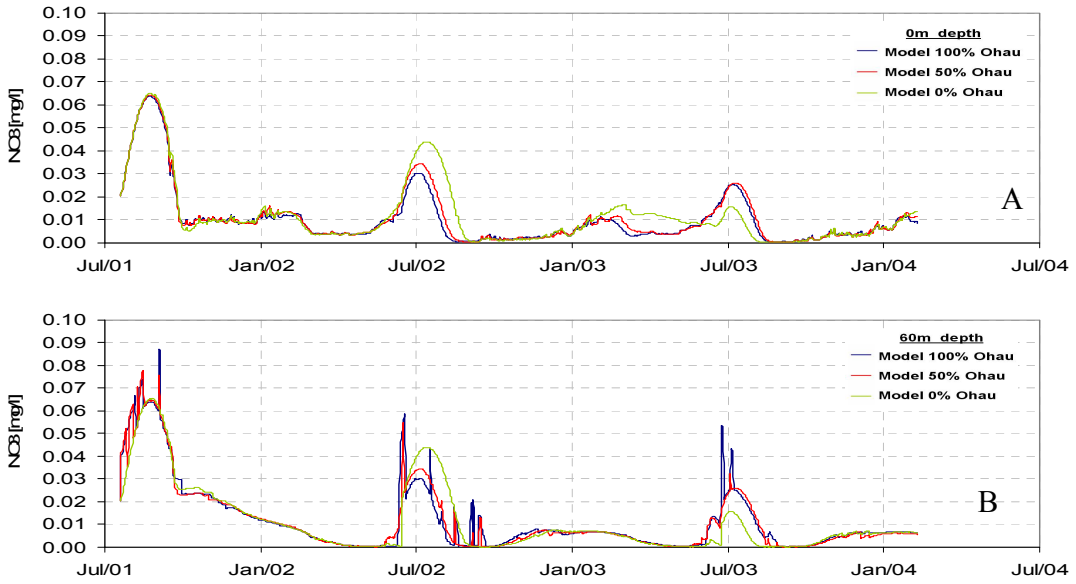

Figure 45. *Simulations of concentrations of nitrate for (a) surface (0m) and (b) 60m for three different scenarios relating to % of Ohau Channel diversion*.

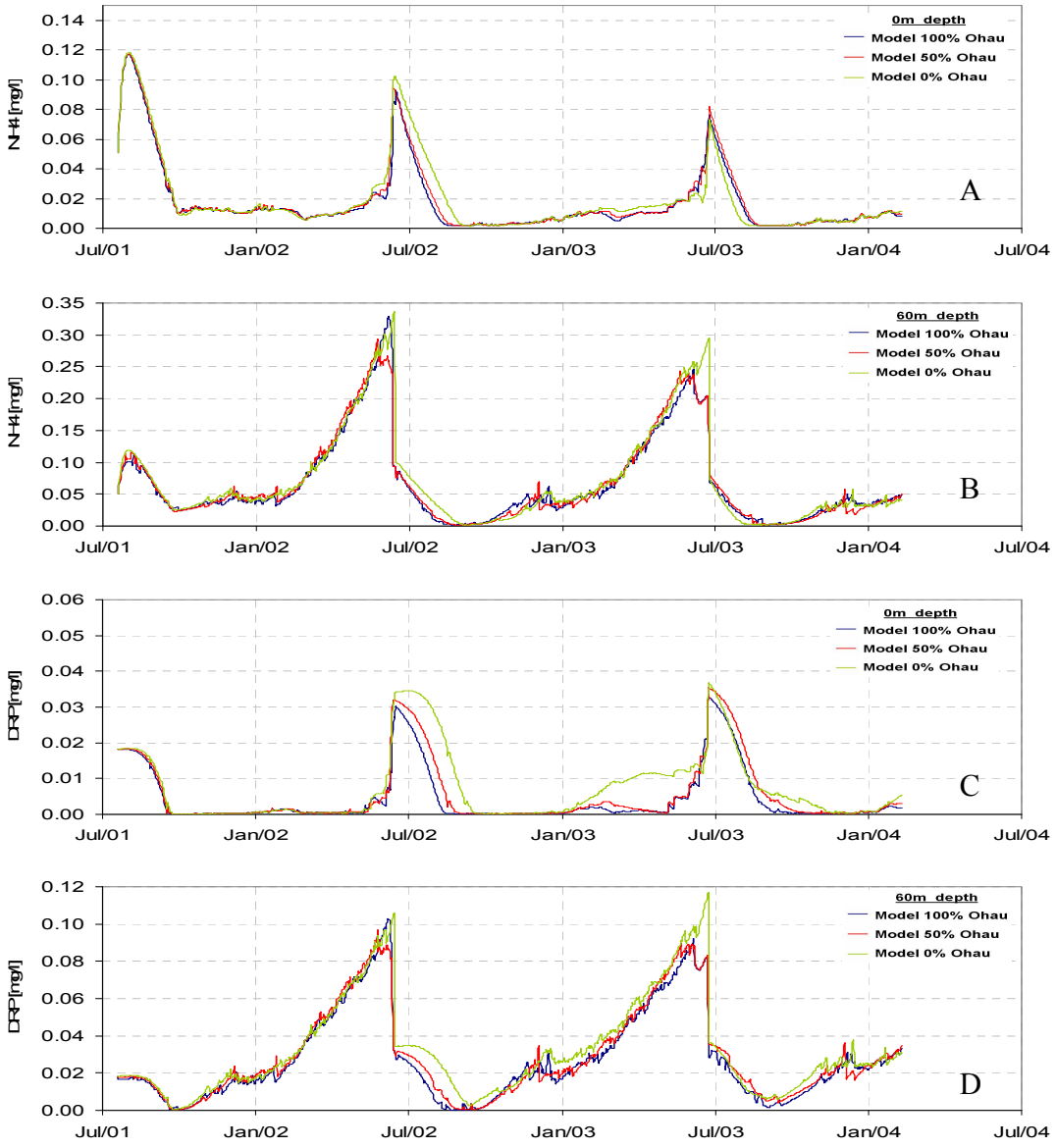

Figure 46. *Simulations of concentrations of ammonium at (a) surface (0m) and (b) 60m depth and dissolved reactive phosphorus at (c) 0m and (d) 60m for three different scenarios relating to % of Ohau Channel diversion.*

Chlorophyll *a* concentrations differed most under the different flow regimes. In the case of diatoms, there appeared to be a subtle shift in the phase of the peak but no consistency in the direction of the shift: in the 0% case it occurred a few days earlier in 2002, but a few days latter in 2003, but there was very little change in the size of the peak.

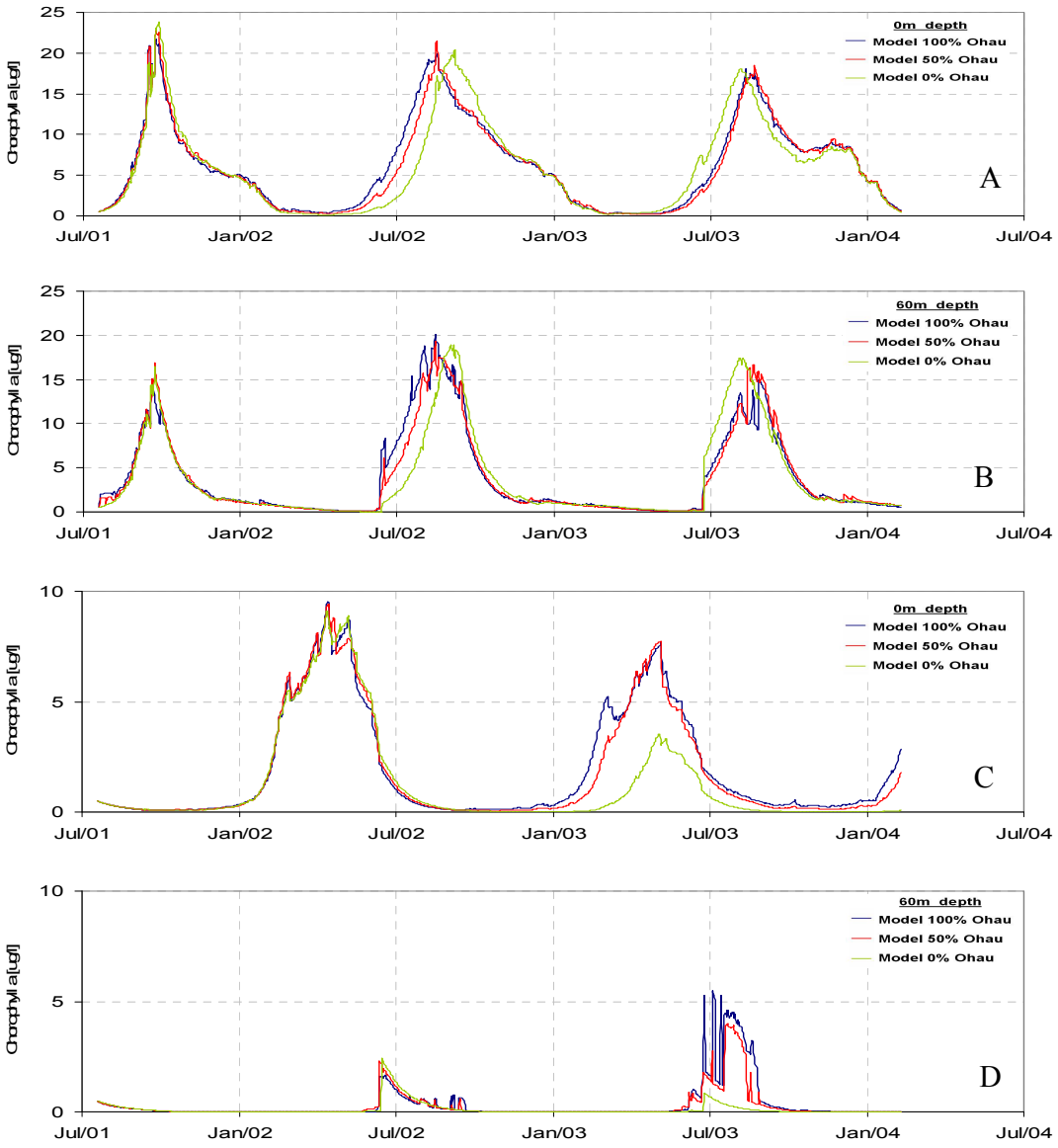

Figure 47*. Simulations of concentrations of chlorophyll* a *related to diatoms and other phytoplankton at (a) surface (0m) and (b) 60m depth and for cyanobacteria at (c) 0m and (d) 60m for three different scenarios relating to % of Ohau Channel diversion.*

For the case of cyanobacteria, there was quite a marked change in the magnitude of the summer peak at the surface, but only in the second (2002-3) summer. Concentrations of cyanobacterial chlorophyll *a* in the bottom waters (60m) were also only noticeably different in the second summer of the simulations. For this case it is relatively easy to distinguish the effects of mixing and dispersion of the biomass into the bottom waters at the time of winter mixing from what is brought into the bottom waters from the Ohau Channel. In other words there is a marked difference between cyanobacterial chlorophyll *a* between the three cases in July-August 2003 that reflects the different levels brought in with in deep insertion from the Ohau Channel.

In view of the differences in the simulations of cyanobacterial chlorophyll *a* for the various flow cases, additional simulations were used to extend the length of the run, by repeating the 2002 and 2003 meteorological, inflow and outflow data for the years 2004 and 2005. This hypothetical simulation effectively allowed a comparison of biomass over four summers, to test whether the decrease in cyanobacterial chlorophyll *a* in the second year of the simulation was a 'one-off' or indicative of a consistent summer decline. Figure 48 shows that the decline of cyanobacterial chlorophyll *a* was consistent for the 0% Ohau flow case. Diatom chlorophyll *a* (not shown) showed almost no change between the two cases. Table 2 compares the peak cyanobacterial chlorophyll *a* levels in the surface waters for each summer of the simulation. Overall, cyanobacterial chlorophyll *a* decreased from 1.9 to 0.9 μg L^{-1}.

Table 2. *Peak cyanobacterial chlorophyll a levels (C,* μg L^{-1}*) in the surface waters for each summer of the simulation.*

Year	C (μg L^{-1}), 100% of Ohau flow	**C** (μg L^{-1}), 0% of Ohau flow
2002	9.5	**9.1**
2003	7.6	**3.5**
2004	7.8	**3.4**
2005	**6.0**	**1.9**

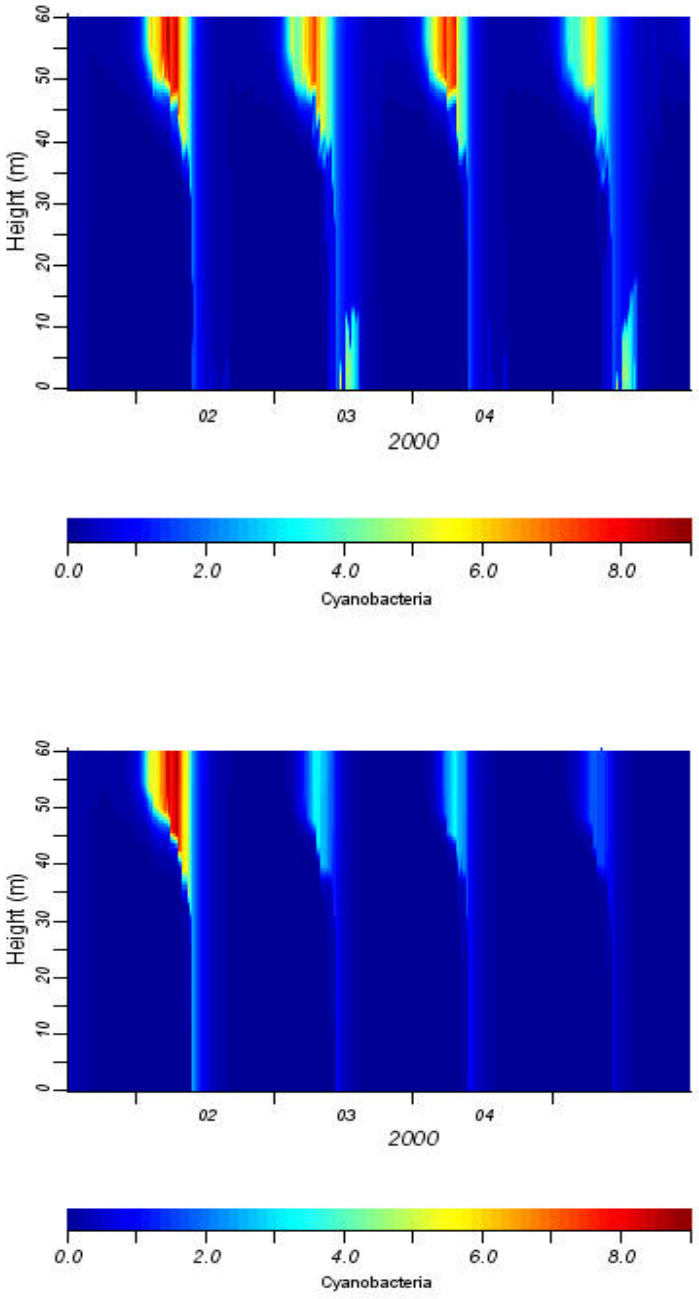

Figure 48. *Elevation (height)-time contours of simulations of chlorophyll a ($\mu g\ L^{-1}$) associated with cyanobacteria from 1 July 2001 to 31 December 2005.*

It should be emphasised that the simulation results for cyanobacteria appear to be quite sensitive to the concentrations assigned for the Ohau Channel. The results suggest that every effort should be made to provide intensive measurements of chlorophyll *a* for the Channel, including differentiation of the species composition. The results from this monitoring could readily be adapted into the model, to further refine predictions.

5.0 References

Burns N. M.; Deely J.; Hall J.; Safi, K. 1997: Comparing past and present trophic states of seven Central Volcanic Plateau lakes, New Zealand. *New Zealand Journal of Marine and Freshwater Research*. 31: 71-87.

Ellery, G. 2004: Lake level and volume summary of the Rotorua lakes. Environment Bay of Plenty Internal Report 2004/08. November 2004.

Gibbs, M. M. 1992: Influence of hypolimnetic stirring and underflow on the limnology of Lake Rotoiti. *New Zealand Journal of Marine and Freshwater Research*. 26:453-463.

Gibbs, M. M.; Hawes, I.; Stephens, S. 2003: Lake Rotoiti-Ohau Channel: Assessment of effects of engineering options of water quality. NIWA Client Report 2003: 142.

Hamilton, D. P.; Hawes, I; Gibbs, M. M. *in press*. Climatic shifts and water quality response in North Island lakes, New Zealand. *Verh. Internat. Verein. Limnol*.

Hamilton, D. P.; Alexander, W.; Burger, D. 2003: Nutrient budget for lakes Rotorua and Rotoiti. Part 1: Internal nutrients. Centre for Biodiversity and Ecology Report, University of Waikato – Report to the Lakes' Water Quality Society.

Jirka, G. H.; Watanabe, M. 1980: Thermal structure of cooling ponds. *Journal of the Hydraulics Division ASCE*. 106: 701-715.

Leong, D. C. K. 1988: Mixing of dense river inflows to lakes. *Research Report 88/6*, Department of Civil Engineering, University of Canterbury, Christchurch, 81 p. (Report submitted in partial fulfilment of the requirements for the degree of Master of Engineering).

Priscu, J. C.; Spigel, R. H.; Gibbs, M. M.; Downes, M. T. 1986: A numerical analysis of hypolimnetic nitrogen and phosphorus transformations in Lake Rotoiti, New Zealand: A geothermally influenced lake. *Limnology and Oceanography*. 31: 812-831.

Rutherford, J. C.; Dumnov S. M.; Ross A. H. 1996: Predictions of phosphorus in Lake Rotorua following load reductions. *New Zealand Journal of Marine and Freshwater Research.* 30: 383-396.

Spigel, R.; Howard-Williams, C.; Gibbs, M.; Stephens, S.; Waugh, B. *in press*. Field Calibration of a Formula for Entrance Mixing of River Inflows to Lakes: Lake Taupo, North Island, New Zealand. *New Zealand Journal of Marine and Freshwater Research*.

Vincent, W. F.; Gibbs, M. M.; Dryden, S. J. 1984: Accelerated eutrophication in a New Zealand lake: Lake Rotoiti, central North Island. *New Zealand Journal of Marine and Freshwater Research*. 18: 431-440.

Vincent, W. F.; Gibbs, M. M.; Spigel, R. H. 1991: Eutrophication processes regulated by a plunging inflow. *Hydrobiologia.* 226(1): 51-63.

Vincent, W F.; Spigel, R. H.; Gibbs, M. M.; Payne, G. W.; Dryden, S. J., May, L. M.; Woods, P.; Pickmere, S.; Davies, J.; Shakespeare, B. 1986: The impact of the Ohau Channel outflow from Lake Rotorua on Lake Rotoiti. DSIR. Taupo Research Laboratory, unpublished report 92. 46 pp.

Appendix 1

Survey Report

Lake Rotorua and Rotoiti Surveys

Survey – 16 February to 12 May 2004

Report Prepared by Brad Scarfe and Dirk Immenga for

THE UNIVERSITY OF WAIKATO
Te Whare Wānanga o Waikato

1 June 2004

Background

This report outlines details of a hydrographic survey of Lake Rotorua and Lake Rotoiti undertaken by the University of Waikato for NIWA (Scott Stephens, Hamilton Office). The survey objective was to collect soundings for creation of hydrodynamic numerical grids. The numerical modelling is part of a larger scale project by Environment Bay of Plenty to improve the health of Lake Rotoiti.

The hydrographic survey was undertaken during three field trips beginning on 16 February and concluding 12 May 2004. The fieldwork consisted of two main components:

1. Creation of a model between the WGS84 ellipsoid and the earth geoid to precisely measure lake levels during surveying (*Geodetic Survey*).
2. Collecting soundings over the two lakes (*Hydrographic Survey*).

The most recent bathymetric surveys of lakes Rotorua and Rotoiti were in 1966 and 1976 respectively. Updated bathymetric data was required to improve hydrodynamic model grid for the lakes, and also for any engineering works that are undertaken in Lake Rotorua (e.g. groynes) or Lake Rotoiti (e.g. temporary or permanent diversion of the Ohau Channel). An updated bathymetric survey in digital form might also provide useful data for other research such as government and private organizations (e.g. IGNS, DOC, RDC, LINZ etc.).

Methodology

Geodetic Survey

The water levels over a lake surface vary as water flows from one region to another. Correction for the water level at the exact location of a sounding removes any possible error caused by measuring the water level from a remote location. RTK GPS (Scarfe, 2002; Saunders, 2003) is considered the best methodology to ensure that water level undulations are correctly compensated for. However, using GPS to measure height over large areas introduces an additional error that needs to be modelled, namely the separation between the WGS84 ellipsoid and the earths geoid.

GPS receivers measure horizontal and vertical heights relative to the WGS84 ellipsoid, which is a global approximation of the shape of the earth. Water levels for hydrographic surveys need to be measured relative to the earth's geoid, which is in simplistic terms, mean sea level over the earth. Over small areas (< 15 km), the difference can be represented by an incline model as the two surfaces appear as two converging or diverging planes. To calculate this model, control marks over the survey area with heights relative to the WGS84 ellipsoid and an orthometric datum are required. A number of these marks created by LINZ (www.linz.govt.nz) exist around the Rotorua Township, but extra control surveying was required around Lake Rotoiti to calculate the WGS84 height of LINZ orthometric marks. The extra surveying involved an adjusted network of

fast static and kinematic GPS observations. The network adjustment report is attached in Appendix 2.

Figure 49 shows the control marks used in this project to create the geoid-ellipsoid incline plane model with associated residual error for each point. The errors are expected to be caused by undulations in the earth's geoid over the error rather than by measurement error. There have been suggestions that the land is very mobile around Rotorua and some movement has occurred to the LINZ marks although this was not investigated. Future surveys of these lakes are suggested to use the same model to ensure agreement unless further survey work improves the model. The model was generated using Trimble Geomatics office and the parameters are seen in Table 1.

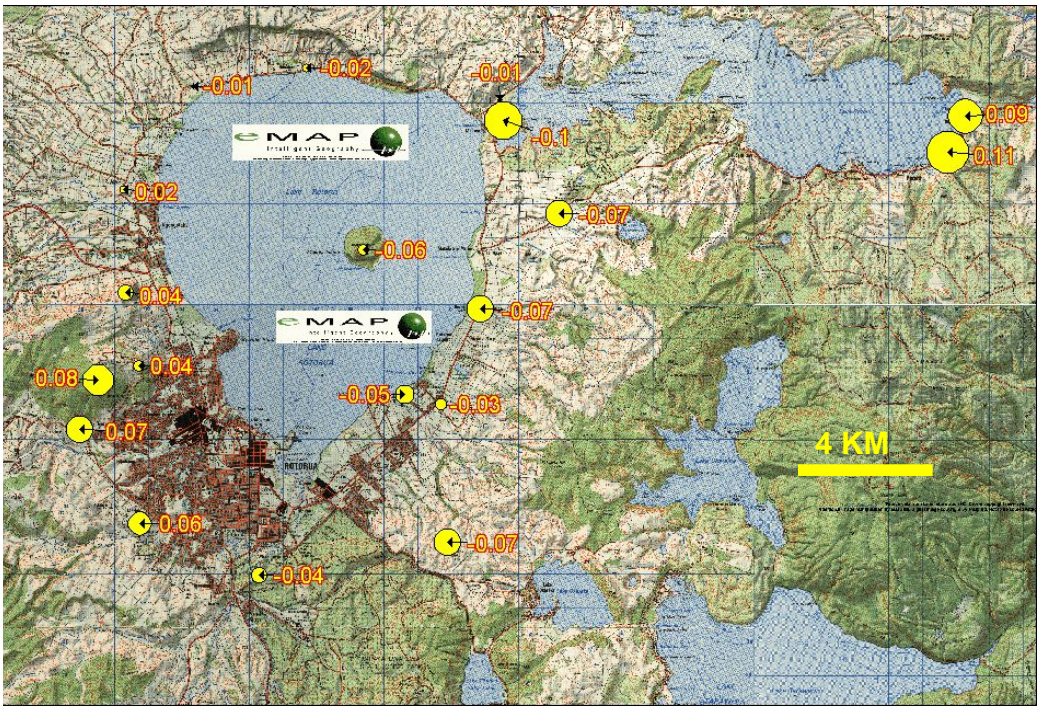

Figure 49. Residual vertical error between geoid-ellipsoid incline plane model and measured heights.

Table 1. Parameters of geoid-ellipsoid incline plane model

Datum	Name	NZGD2000
	Method	Molodensky
Geoid Model	Method	Geoid Grid Model
	Model	EGM96 (Global)
	File	Ww15mgh.ggf
Horizontal Adjustments	None	
Lat/Long/Height Adjustments	None	
Vertical Adjustment	Origin North (m)	769154.272671578
	Origin East (m)	401917.072397806
	Constant Adjustment (m)	-1.3856378963595
	Slope north	-0.00000377718487
	Slope East	-0.000013204598324

Coordinates

- Northings and Eastings are relative to BOP NZGD2000
- Latitudes and Longitudes are relative to BOP NZGD2000 which can be assumed to be WGS84 values for the purposes of this project
- Elevations are relative to are relative to Moturiki Vertical Datum 1953
- Errors are in meters
- Some of the elevation values are derived from the incline plane geoid-ellipsoid model and are only accurate to 0.01-0.05 m.
- Future use of these coordinates should include comparisons with most recent LINZ values as well as values in the network adjustment report in the appendix of this report

Point Name	Northing	Latitude	N error	Easting	Longitude	E error	WGS84 Height	h error	Elevation	Northing	Easting
AGYT	769095.085	38°02'22.08851"S	0.000	388088.174	176°19'49.50667"E	0.000	311.241	0.000	282.0124	769095.085	388088.174
PAPAROA	770545.861	38°01'35.18946"S	0.028	391986.115	176°22'29.41592"E	0.028	333.4	0.013	N/A	N/A	N/A
AGY4	768486.133	38°02'41.84405"S	0.035	388201.33	176°19'54.11099"E	0.035	309.53	0.018	280.3584	768486.12	388201.19
OKAWA	767759.87	38°03'05.42542"S	0.042	388778.233	176°20'17.73002"E	0.042	308.736	0.021	279.5570	N/A	N/A
AGUA	68056.886	38°02'56.03841"S	0.043	401438.96	176°28'57.01803"E	0.043	314.995	0.015	286.2855	768056.89	401438.71
AGUB	69154.264	38°02'20.44375"S	0.035	401917.06	176°29'16.61644"E	0.034	309.433	0.012	280.6585	769154.4	401916.4
BE48	767667.768	38°03'08.65976"S	0.000	398753.005	176°27'06.85285"E	0.000	309.395	0.000	281.2000	767667.768	398753.005
CAMP	770949.04	38°01'22.03684"S	0.039	389871.069	176°21'02.71576"E	0.039	308.916	0.019		N/A	N/A
LODGE	768388.896	38°02'44.96207"S	0.039	387463.376	176°19'23.83986"E	0.039	309.822	0.02	280.61	N/A	N/A
CANAL	768474.138	38°02'42.20235"S	0.05	387563.027	176°19'27.93216"E	0.05	309.456	0.025	280.2460	N/A	N/A

Hydrographic Survey

The hydrographic survey was undertaken by Brad Scarfe (surveyor and hydrographic operator) and Dirk Immenga (field work planning and vessel operator) during three trips to the Lake. The equipment used was:

- KNUDSEN MP320 dual frequency Hydrographic echo-sounder
- TRIMBLE MS 750 RTK GPS
- AML sound velocity profiler
- ORCA 6 meter purpose built alloy pontoon craft

The survey accuracy specification were within 20 cm in the vertical and about 10 cm in the horizontal.

Coordinate System and Survey Datum

Since positions were calculated with GPS (using the WGS84 ellipsoid), it was considered best to use the Bay of Plenty local circuit (New Zealand Geodetic Datum 2000) during all data collection and processing. This system has the smallest variations with the WGS84 ellipsoid and the positions were converted to New Zealand Map Grid (NZMG) at a later stage.

The datum for the survey was Moturiki Vertical Datum 1953. Trimble's Hydropro Navigation software converts the RTK GPS heights to Moturiki Vertical Datum 1953 using the incline plane geoid-ellipsoid model. The shoreline was digitised from high-resolution geo-referenced aerial photographs supplied by Environment BOP. The Rotorua shoreline around the Ohau Channel was assigned a value of 279.80 m and the entire Rotoiti shoreline was assigned a value of 279.20 m. These values are approximately 0.10 m above the generally observed water levels during the time of surveying. No information was supplied to show the maximum water levels that occur on these two lakes.

Results

Effect of Lake Weed on Soundings

Echo soundings are returned off the first reflective surface below the transducer. In much of the shallow region of western Lake Rotoiti, the reflective surface is the dense lake weed. In some areas, 3-4 bad soundings off weed were returned for every one good soundings. Figure 50 shows the true lake floor as well as the erroneous soundings. The erroneous soundings increased the processing time significantly. When not bad soundings are present processing time can be trivial. When many bad soundings exist such as in the Okere Arm and Okawa Bay, processing times were close to 50 % of the survey time. Note that only every 10 soundings were logged and that the processing time would have been significantly greater if the sounding were not filtered in this way. A paper output was required as a check on the correct bottom depth where the lake weed made bottom determination difficult.

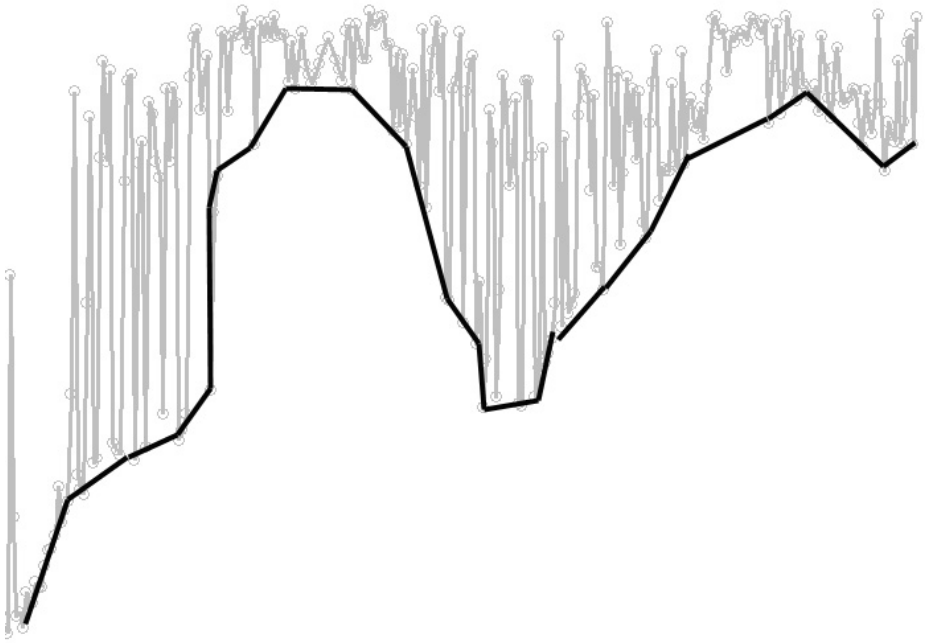

Figure 50. Effect of lake weed on soundings. The black line shows the true lake floor and the grey circles and lines show the bad soundings caused by reflection of the weed.

Checks on Survey Data

Everyday, or when the base station was changed during the day, checks were made to ensure there were no gross errors present in the data. This included:

- checking the RTK GPS Tide against reliable tide boards
- placing the RTK GPS antenna on known marks such as the Okawa Bay tide board and a coordinated nail on a jetty in the Ohau Channel
- running lines over previous survey coverage and comparing the depths.

An indication of the final precision of the survey can be made by comparing overlapping survey data from crosslines as well as from the check lines over previous survey coverage. 17 different survey files that used different base station setups or were collected on different days were compared. There was a total of 264 depths compared over a range of depths and locations. The average difference between the depths was 0.00m, with a standard deviation of 0.12 m (therefore 95 % confidence interval of 0.24 m). It is concluded that the final survey data is within the required specifications for the survey.

Planned versus Actual Survey Coverage

Two specifications for survey coverage were made for this project. Initially the two lakes were divided into regions (Figure 51), with each region representing one days surveying. However, later specifications required 10 m x 10 m runlines around both sides of the Ohau channel, stepping out to 30 m x 30 m lines and then 100 m x 100 m lines. This requirement caused the survey time to increase significantly without addition survey day being allocated. Also, the processing time was significantly increased due to the presence of the lake weed. Consequently, the majority of Lake Rotorua has not been surveyed. The survey data that was collected did fulfil the requirements for NIWA to create their numerical model grids. The final survey coverage can be seen in Figure 52 and Figure 53.

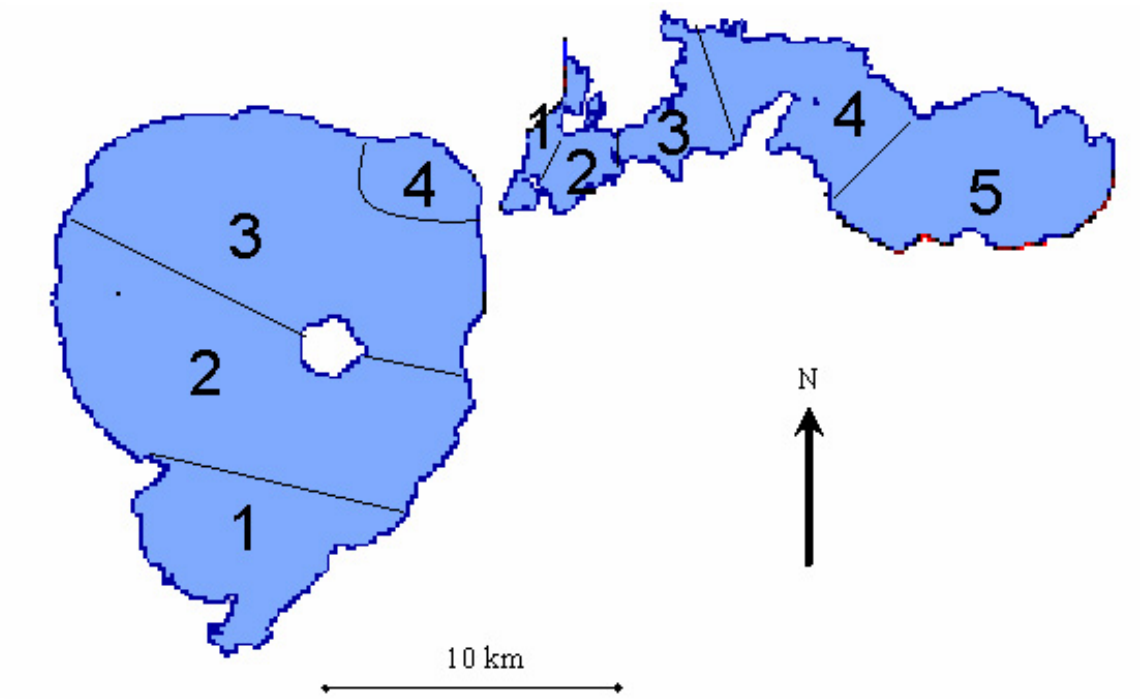

Figure 51. Initial plan of survey regions. Each region represented one days surveying

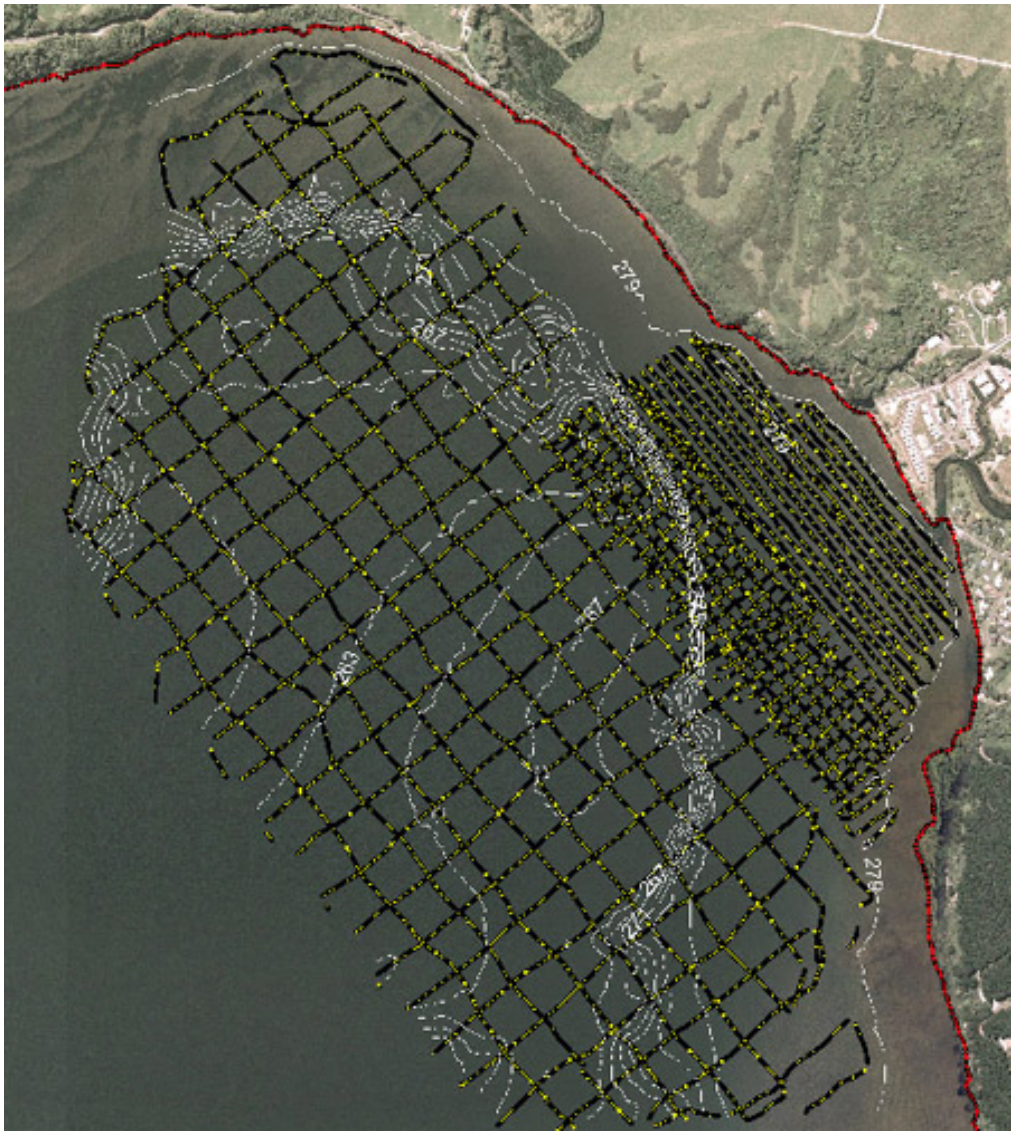

Figure 52. Survey coverage for Lake Rotorua around Ohau channel

Figure 53. Survey Coverage for Lake Rotoiti

Conclusion and Recommendations

The main objective of this survey was to provide bathymetry data for Scott Stephens of NIWA (Hamilton) to create hydrodynamic numerical model grids of the Lakes. This objective was stated as achieved by Scott in an email dated 19 May 2004 (See Appendix 2). The accuracy of the survey has been shown to be within acceptable limits.

However there are still unresolved issues regarding the survey coverage over Lake Rotorua that are being discussed between the concerned parties. It is believed that the proposed, unsurveyed 300 m spacing lines over Lake Rotorua will not improve greatly on the existing bathymetry chart because of the spacing of runlines. It is recommended that any more effort put in to survey Lake Rotorua is undertaken in a systematic way that identifies key regions of interest, collects multibeam soundings over deep features and measures dense single beam depths in shallows in areas important to safe boat navigation.

Interest in surveying other Lakes in the Rotorua District, including Lake Tarawera, has been shown by various parties. Ideally each of the lakes would have complete survey coverage, but this cannot be done at once and needs to be worked towards over time. The stages of each lake survey could involve:

1. Single beam reconnaissance survey to identify general features
2. Multibeam reconnaissance survey to further identify general features
3. Spot surveys with multibeam over areas of interest (depth > 5 m) identified from reconnaissance survey
4. Spot surveys with single beam over areas of interest (depth < 5 m) identified from reconnaissance survey
5. Complete coverage of lake bathymetry

This is the current state of the survey data for each of the lakes:

Lake Rotorua

The 1966 survey has achieved Stage 1 and the major features can be seen from the existing chart. Stage 2 would involve regular spaced multibeam lines over the complete lake to further identify areas of interest. An alternative methodology would be to undertake Stage 3 with complete coverage over small areas of interest before Stage 2. This would provide more immediately impressive images that could be used for publicity, tourism etc and may help raise more funding to undertake Stage 2 at a later date. Possible features could be the deep southern features or the steep northern banks. Stage 4 is an important step for navigational safety in shallow waters.

Lake Rotoiti

Stage 1 has been achieved through the recent survey. Stage 2 is considered unnecessary because most of the features have been identified in Stage 1. This differs to Lake Rotorua where there are still areas that require reconnaissance with multibeam lines to show the complexity of different areas. The next step for Lake Rotoiti would be Stage 3 spot surveys with multibeam. Stage 4 has been achieved for

the Okere Arm, Okawa Bay and around the Ohau channel. Stage 4 is required in the rest of the shallow areas of the lake, mainly for navigational safety objectives.

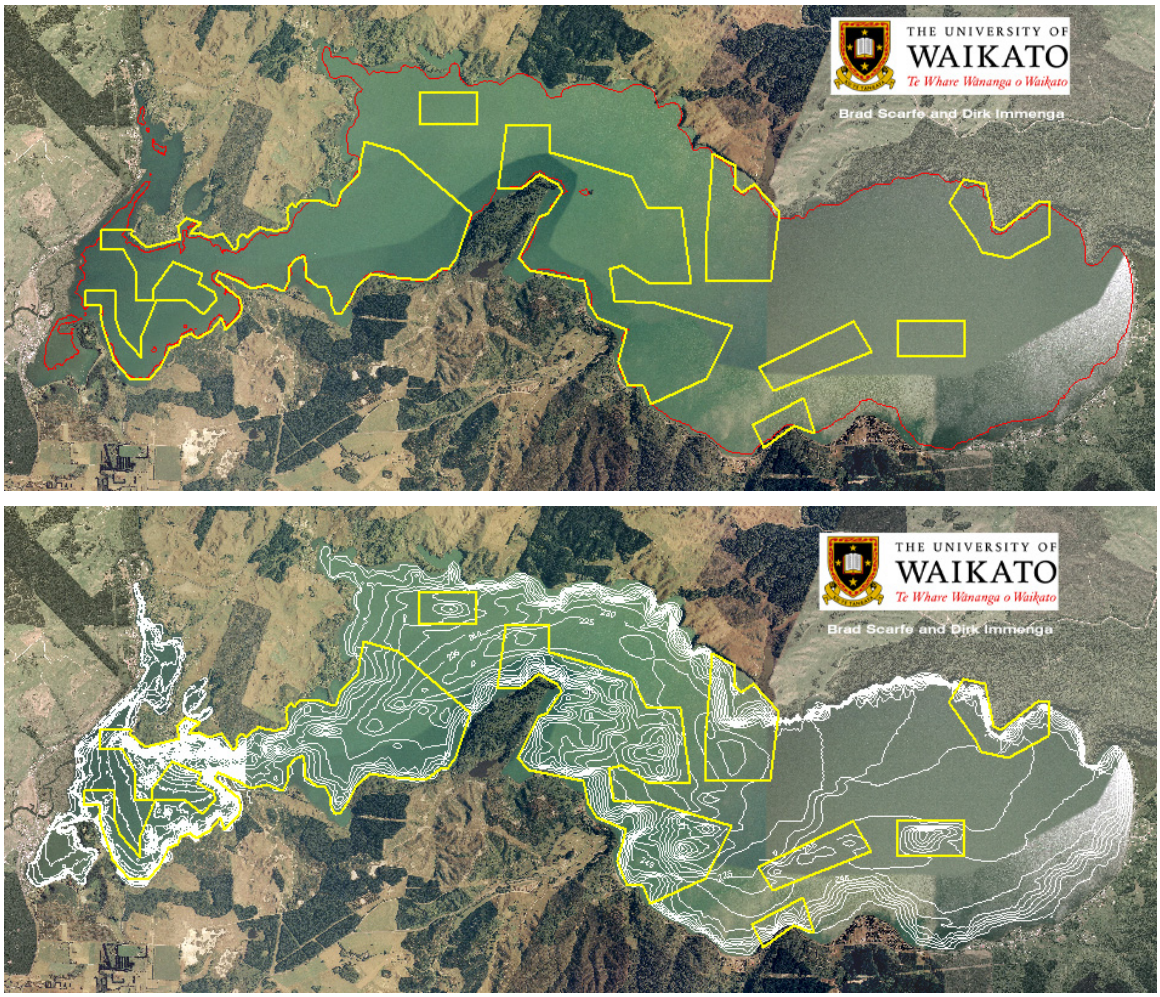

Figure 54. Proposed areas for multibeam survey of Lake Rotoiti shown as yellow areas. The top line has a red line showing the 5 m depth contour which is the recommended cutoff for multibeam surveying. The bottom image has 1 m contours in the western Lake and 5 m contours for the eastern Lake.

Lake Tarawera

The existing chart of the lake achieves Stage 1. The survey for this lake should be approached in a similar way to Lake Rotorua with particular interest in areas of volcanic activity. The first step can either involve the entire lake can be surveyed with a regular spaced multibeam grid reconnaissance survey or certain areas surveyed with 100 % survey coverage.

References

Scarfe, B. E., 2002. Water Level Corrections (WLC) Using RTK GPS. *The Hydrographic Journal*, April vol. 104.

Saunders, P., 2003. RTK Tide Basics. *Hydro International,* December 2003, Vol. 7 Number 10. p 26-29.

Appendix 1 - Network Adjustment Report

Project : Copy of TGO Rotorua Lakes

User name	Brad	**Date & Time**	1:19:41 p.m. 10/03/2004
Coordinate System	New Zealand GD2000	**Zone**	Bay of Plenty 2000
Project Datum	New Zealand Geodetic 2000		
Vertical Datum		**Geoid Model**	EGM96 (Global)
Coordinate Units	Meters		
Distance Units	Meters		
Height Units	Meters		

Adjustment Style Settings - 95% Confidence Limits

Residual Tolerances

To End Iterations : 0.000010m
Final Convergence Cutoff : 0.005000m

Covariance Display

Horizontal
Propogated Linear Error [E] : U.S.
Constant Term [C] : 0.00000000m
Scale on Linear Error [S] : 1.96

Three-Dimensional
Propogated Linear Error [E] : U.S.
Constant Term [C] : 0.00000000m
Scale on Linear Error [S] : 1.96

Elevation Errors were used in the calculations.

Adjustment Controls

Compute Correlations for Geoid : False

Horizontal and Vertical adjustment performed

Set-up Errors

GPS
Error in Height of Antenna : 0.010m

Centering Error : 0.020m

Back to top

Statistical Summary

Successful Adjustment in 1 iteration(s)

Network Reference Factor : 0.97
Chi Square Test (α=95%) : PASS
Degrees of Freedom : 88.00

GPS Observation Statistics

Reference Factor : 0.97
Redundancy Number (r) : 88.00

Variance Group Statistics

Group Name	Reference Factor	Redundancy Number
Day1 Kinematic	0.88	11.55
Day1 Kinematic Long Sess	0.62	1.93
Day1 Static	0.97	8.58
Day4 Kinematic	1.09	30.34
Day3 Kinematic	0.61	7.24
Day2 Kinematic	0.48	15.72
Day 5 static	1.18	3.70
Day 5 Kinematic	1.38	8.93

Individual GPS Observation Statistics

Observation ID	Reference Factor	Redundancy Number
B1	0.51	2.37
B2	0.53	2.39
B7	0.60	1.82
B8	0.59	2.33
B9	0.26	2.33
B10	0.39	2.34
B20	0.52	2.30
B21	0.51	2.29
B22	0.42	2.31
B23	1.23	2.17
B24	0.27	2.23

B27	0.62	1.93
B28	0.70	1.85
B38	1.25	2.19
B39	0.50	2.23
B40	1.72	2.33
B42	0.46	2.37
B44	0.43	2.41
B45	0.44	2.43
B46	0.86	2.40
B48	0.59	2.48
B49	0.75	2.47
B50	0.20	2.50
B51	1.89	2.49
B52	1.56	2.52
B53	1.27	2.55
B54	0.49	2.52
B55	1.50	2.51
B60	0.69	2.57
B61	0.91	2.58
B62	1.10	2.58
B63	0.79	2.58
B79	0.54	1.87
B80	0.41	1.90
B81	1.63	2.58
B82	1.90	2.58
B87	1.05	2.00
B89	1.31	1.71

Weighting Strategies

GPS Observations

Alternative Scalar Applied to Variance Groups

Day1 Kinematic : 0.82
Day1 Kinematic Long Sess : 0.61
Day1 Static : 0.95
Day4 Kinematic : 1.10
Day3 Kinematic : 0.61
Day2 Kinematic : 0.46
Day 5 static : 1.20
Day 5 Kinematic : 1.40

Back to top

Adjusted Coordinates

Adjustment performed in New Zealand Geodetic 2000

Number of Points : 10
Number of Constrained Points : 2
Horizontal and Height Only : 2

Adjusted Grid Coordinates

Errors are reported using 1.96σ.

Point Name	Northing	N error	Easting	E error	Elevation	e error	Fix
AGYT	769095.085m	0.000m	388088.174m	0.000m	N/A	N/A	N E h
AGUB	769154.263m	0.032m	401917.060m	0.032m	N/A	N/A	
BE48	767667.769m	0.000m	398753.005m	0.000m	N/A	N/A	N E h
AGUA	768056.887m	0.039m	401438.959m	0.039m	N/A	N/A	
PAPAROA	770545.861m	0.026m	391986.115m	0.026m	N/A	N/A	
AGY4	768486.133m	0.032m	388201.330m	0.032m	N/A	N/A	
OKAWA	767759.870m	0.038m	388778.233m	0.038m	N/A	N/A	
CAMP	770949.040m	0.036m	389871.069m	0.036m	N/A	N/A	
LODGE	768388.896m	0.036m	387463.376m	0.036m	N/A	N/A	
CANAL	768474.138m	0.046m	387563.027m	0.046m	N/A	N/A	

Adjusted Geodetic Coordinates

Errors are reported using 1.96σ.

Point Name	Latitude	N error	Longitude	E error	Height	h error	Fix
AGYT	38°02'22.08851"S	0.000m	176°19'49.50667"E	0.000m	311.241m	0.000m	Lat Long h
AGUB	38°02'20.44376"S	0.032m	176°29'16.61645"E	0.032m	309.433m	0.012m	
BE48	38°03'08.65976"S	0.000m	176°27'06.85285"E	0.000m	309.395m	0.000m	Lat Long h
AGUA	38°02'56.03839"S	0.039m	176°28'57.01801"E	0.039m	315.001m	0.016m	
PAPAROA	38°01'35.18945"S	0.026m	176°22'29.41592"E	0.026m	333.401m	0.013m	
AGY4	38°02'41.84405"S	0.032m	176°19'54.11098"E	0.032m	309.530m	0.018m	
OKAWA	38°03'05.42543"S	0.038m	176°20'17.73002"E	0.038m	308.738m	0.021m	
CAMP	38°01'22.03685"S	0.036m	176°21'02.71576"E	0.036m	308.917m	0.019m	
LODGE	38°02'44.96208"S	0.036m	176°19'23.83986"E	0.036m	309.823m	0.020m	

CANAL	38°02'42.20234"S	0.046m	176°19'27.93215"E	0.046m	309.460m	0.026m	

Coordinate Deltas

Point Name	ΔNorthing	ΔEasting	ΔElevation	ΔHeight	ΔGeoid Separation
AGYT	0.000m	0.000m	N/A	0.000m	N/A
AGUB	0.000m	0.000m	N/A	0.000m	N/A
BE48	0.000m	0.000m	N/A	0.000m	N/A
AGUA	0.000m	0.000m	N/A	-0.002m	N/A
PAPAROA	0.000m	0.000m	N/A	0.000m	N/A
AGY4	0.000m	0.000m	N/A	0.000m	N/A
OKAWA	0.000m	0.000m	N/A	0.001m	N/A
CAMP	0.000m	0.000m	N/A	0.001m	N/A
LODGE	0.000m	0.000m	N/A	0.000m	N/A
CANAL	0.000m	0.000m	N/A	0.001m	N/A

Back to top

Control Coordinate Comparisons

Values shown are control coord minus adjusted coord.

Point Name	ΔNorthing	ΔEasting	ΔElevation	ΔHeight
AGYT	N/A	N/A	N/A	N/A
BE48	N/A	N/A	N/A	N/A

Back to top

Adjusted Observations

Adjustment performed in New Zealand Geodetic 2000

GPS Observations

GPS Transformation Group: <GPS Default>

Azimuth Rotation : -0°00'00.4636" **(1.96σ)** : 0°00'00.5549"
Network Scale : 1.00000173 **(1.96σ)** : 0.00000268
Number of Observations : 38
Number of Outliers : 0

Observation Adjustment (Critical Tau = 3.42). Any outliers are in red.

Obs. ID	From Pt.	To Pt.		Observation	A-posteriori Error (1.96σ)	Residual	Stand. Residual
B51	CAMP	OKAWA	**Az.**	198°59'09.7742"	0°00'01.3628"	0°00'00.4816"	0.32
			ΔHt.	-0.180m	0.012m	0.045m	3.34
			Dist.	3371.217m	0.022m	0.011m	0.45
B82	CAMP	LODGE	**Az.**	223°18'47.6190"	0°00'01.1728"	0°00'01.6314"	1.09
			ΔHt.	0.905m	0.011m	-0.041m	-3.03
			Dist.	3514.445m	0.020m	-0.027m	-1.06
B40	AGYT	AGUA	**Az.**	94°31'48.1325"	0°00'00.4333"	-0°00'00.1322"	-0.35
			ΔHt.	3.759m	0.016m	0.054m	2.79
			Dist.	13391.108m	0.028m	0.020m	0.84
B52	CAMP	AGY4	**Az.**	214°12'23.1864"	0°00'01.4833"	-0°00'00.6559"	-0.38
			ΔHt.	0.613m	0.012m	-0.036m	-2.77
			Dist.	2975.557m	0.021m	0.007m	0.28
B81	CAMP	LODGE	**Az.**	223°18'47.6190"	0°00'01.1728"	0°00'01.1754"	0.79
			ΔHt.	0.905m	0.011m	-0.037m	-2.71
			Dist.	3514.445m	0.020m	-0.019m	-0.73
B55	CAMP	AGY4	**Az.**	214°12'23.1864"	0°00'01.4833"	-0°00'00.0082"	0.00
			ΔHt.	0.613m	0.012m	0.035m	2.67
			Dist.	2975.557m	0.021m	-0.010m	-0.39
B53	CAMP	AGY4	**Az.**	214°12'23.1864"	0°00'01.4833"	0°00'00.3899"	0.22
			ΔHt.	0.613m	0.012m	-0.033m	-2.25
			Dist.	2975.557m	0.021m	0.001m	0.05
B38	AGYT	AGUA	**Az.**	94°31'48.1325"	0°00'00.4333"	0°00'00.0564"	0.16
			ΔHt.	3.759m	0.016m	-0.030m	-2.24
			Dist.	13391.108m	0.028m	0.001m	0.02
B23	AGYT	PAPAROA	**Az.**	69°40'07.3075"	0°00'01.4713"	0°00'00.5174"	0.46
			ΔHt.	22.159m	0.013m	0.000m	0.03
			Dist.	4159.172m	0.030m	-0.050m	-2.21
B62	CAMP	LODGE	**Az.**	223°18'47.6190"	0°00'01.1728"	-0°00'00.2485"	-0.17
			ΔHt.	0.905m	0.011m	0.026m	1.97
			Dist.	3514.445m	0.020m	0.003m	0.11
B89	LODGE	AGYT	**Az.**	41°35'18.7404"	0°00'07.9246"	-0°00'06.5689"	-1.46
			ΔHt.	1.418m	0.020m	-0.007m	-0.53

			Dist.	942.908m	0.036m	0.037m	1.78
B61	CAMP	LODGE	**Az.**	223°18'47.6190"	0°00'01.1728"	-0°00'00.1004"	-0.07
			ΔHt.	0.905m	0.011m	0.022m	1.57
			Dist.	3514.445m	0.020m	-0.012m	-0.47
B46	AGY4	OKAWA	**Az.**	141°37'15.7538"	0°00'05.2619"	-0°00'00.8096"	-0.15
			ΔHt.	-0.793m	0.013m	-0.018m	-1.44
			Dist.	927.511m	0.024m	-0.014m	-0.56
B63	CAMP	LODGE	**Az.**	223°18'47.6190"	0°00'01.1728"	0°00'00.0362"	0.02
			ΔHt.	0.905m	0.011m	0.019m	1.38
			Dist.	3514.445m	0.020m	0.007m	0.28
B49	CAMP	OKAWA	**Az.**	198°59'09.7742"	0°00'01.3628"	-0°00'00.4511"	-0.30
			ΔHt.	-0.180m	0.012m	-0.016m	-1.30
			Dist.	3371.217m	0.022m	0.006m	0.23
B87	LODGE	CANAL	**Az.**	49°32'38.0166"	0°00'53.6536"	-0°00'35.6711"	-1.02
			ΔHt.	-0.363m	0.020m	0.020m	1.08
			Dist.	131.136m	0.034m	0.026m	1.19
B28	AGYT	AGY4	**Az.**	169°33'24.4507"	0°00'10.7766"	-0°00'00.0809"	-0.01
			ΔHt.	-1.711m	0.018m	-0.007m	-0.62
			Dist.	619.376m	0.032m	-0.023m	-1.08
B60	CAMP	LODGE	**Az.**	223°18'47.6190"	0°00'01.1728"	0°00'00.3287"	0.22
			ΔHt.	0.905m	0.011m	0.014m	1.07
			Dist.	3514.445m	0.020m	-0.015m	-0.59
B27	AGYT	AGY4	**Az.**	169°33'24.4507"	0°00'10.7766"	-0°00'03.2392"	-0.45
			ΔHt.	-1.711m	0.018m	0.001m	0.10
			Dist.	619.376m	0.032m	-0.022m	-1.02
B1	AGYT	AGUB	**Az.**	89°50'17.8736"	0°00'00.3924"	-0°00'00.0194"	-0.05
			ΔHt.	-1.809m	0.012m	-0.012m	-0.88
			Dist.	13829.030m	0.026m	0.003m	0.11
B54	CAMP	AGY4	**Az.**	214°12'23.1864"	0°00'01.4833"	0°00'00.1408"	0.08
			ΔHt.	0.613m	0.012m	0.012m	0.87
			Dist.	2975.557m	0.021m	0.001m	0.04
B7	BE48	AGUA	**Az.**	81°45'55.6119"	0°00'02.6359"	0°00'00.8684"	0.55
			ΔHt.	5.605m	0.016m	-0.005m	-0.47
			Dist.	2713.998m	0.035m	-0.017m	-0.82

B8	BE48	AGUB	**Az.**	64°50'39.0072"	0°00'01.5492"	-0°00'00.1349"	-0.10
			ΔHt.	0.037m	0.012m	0.009m	0.70
			Dist.	3495.848m	0.026m	-0.019m	-0.79
B48	CAMP	OKAWA	**Az.**	198°59'09.7742"	0°00'01.3628"	-0°00'01.0324"	-0.68
			ΔHt.	-0.180m	0.012m	-0.003m	-0.19
			Dist.	3371.217m	0.022m	0.020m	0.79
B2	AGYT	AGUB	**Az.**	89°50'17.8736"	0°00'00.3924"	0°00'00.1106"	0.31
			ΔHt.	-1.809m	0.012m	-0.007m	-0.45
			Dist.	13829.030m	0.026m	0.019m	0.79
B20	BE48	PAPAROA	**Az.**	293°02'58.6657"	0°00'00.7481"	0°00'00.1863"	0.28
			ΔHt.	24.005m	0.013m	0.006m	0.48
			Dist.	7353.528m	0.027m	-0.018m	-0.75
B79	CAMP	CANAL	**Az.**	223°04'22.4825"	0°00'01.9485"	-0°00'00.5838"	-0.43
			ΔHt.	0.543m	0.018m	-0.005m	-0.49
			Dist.	3384.109m	0.032m	0.016m	0.72
B21	BE48	PAPAROA	**Az.**	293°02'58.6657"	0°00'00.7481"	0°00'00.4777"	0.72
			ΔHt.	24.005m	0.013m	-0.004m	-0.33
			Dist.	7353.528m	0.027m	-0.011m	-0.48
B44	AGY4	OKAWA	**Az.**	141°37'15.7538"	0°00'05.2619"	-0°00'03.7397"	-0.68
			ΔHt.	-0.793m	0.013m	0.002m	0.16
			Dist.	927.511m	0.024m	-0.008m	-0.33
B10	BE48	AGUB	**Az.**	64°50'39.0072"	0°00'01.5492"	-0°00'00.1037"	-0.07
			ΔHt.	0.037m	0.012m	0.008m	0.65
			Dist.	3495.848m	0.026m	-0.005m	-0.21
B39	AGYT	AGUA	**Az.**	94°31'48.1325"	0°00'00.4333"	-0°00'00.2163"	-0.59
			ΔHt.	3.759m	0.016m	0.008m	0.50
			Dist.	13391.108m	0.028m	-0.011m	-0.48
B22	BE48	PAPAROA	**Az.**	293°02'58.6657"	0°00'00.7481"	0°00'00.3646"	0.54
			ΔHt.	24.005m	0.013m	-0.006m	-0.43
			Dist.	7353.528m	0.027m	-0.007m	-0.31
B80	CAMP	CANAL	**Az.**	223°04'22.4825"	0°00'01.9485"	-0°00'00.5257"	-0.39
			ΔHt.	0.543m	0.018m	-0.004m	-0.35
			Dist.	3384.109m	0.032m	0.012m	0.53

B42	AGYT	AGUB	**Az.**	89°50'17.8736"	0°00'00.3924"	-0°00'00.1793"	-0.50
			ΔHt.	-1.809m	0.012m	-0.007m	-0.52
			Dist.	13829.030m	0.026m	0.009m	0.38
B45	AGY4	OKAWA	**Az.**	141°37'15.7538"	0°00'05.2619"	-0°00'02.4004"	-0.44
			ΔHt.	-0.793m	0.013m	-0.006m	-0.47
			Dist.	927.511m	0.024m	-0.011m	-0.47
B24	AGYT	PAPAROA	**Az.**	69°40'07.3075"	0°00'01.4713"	-0°00'00.4555"	-0.40
			ΔHt.	22.159m	0.013m	0.004m	0.25
			Dist.	4159.172m	0.030m	-0.001m	-0.06
B9	BE48	AGUB	**Az.**	64°50'39.0072"	0°00'01.5492"	-0°00'00.2087"	-0.15
			ΔHt.	0.037m	0.012m	0.005m	0.36
			Dist.	3495.848m	0.026m	-0.006m	-0.25
B50	CAMP	OKAWA	**Az.**	198°59'09.7742"	0°00'01.3628"	0°00'00.3058"	0.20
			ΔHt.	-0.180m	0.012m	0.000m	0.01
			Dist.	3371.217m	0.022m	0.008m	0.31

Back to top

Histograms of Standardized Residuals

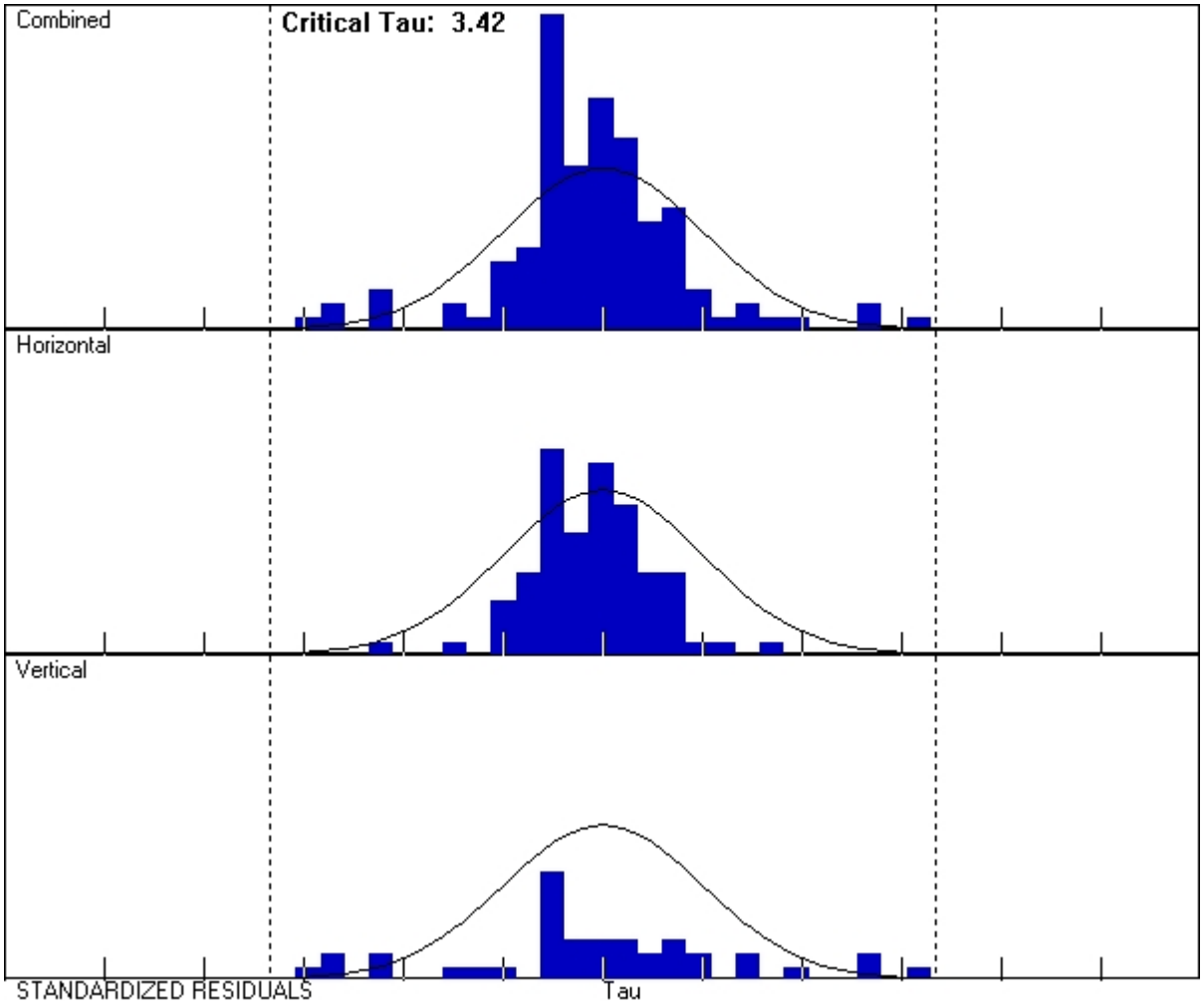

Back to top

Point Error Ellipses

AGUB	AGUA	PAPAROA
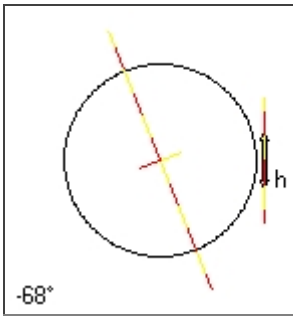	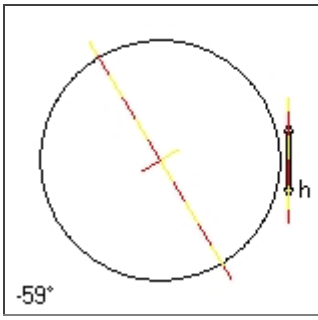	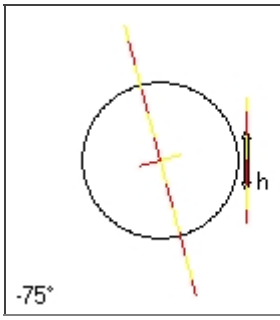
Tick Size: 0.0100m Horizontal Bivariate Scalar: 2.45σ Vertical Univariate Scalar: 1.96σ		
AGY4	OKAWA	CAMP

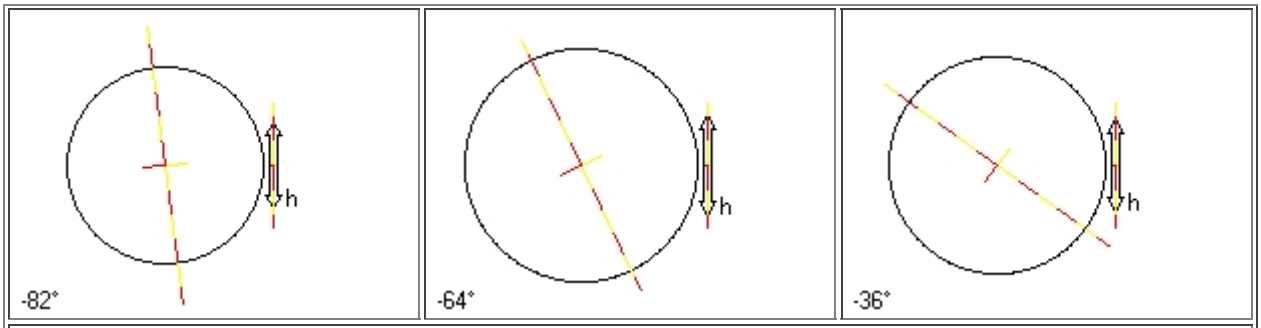

Tick Size: 0.0100m Horizontal Bivariate Scalar: 2.45σ Vertical Univariate Scalar: 1.96σ

LODGE	CANAL	

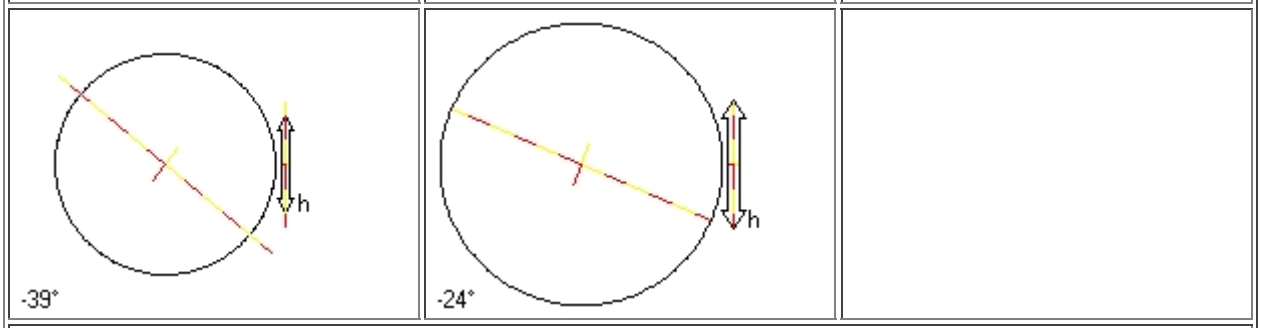

Tick Size: 0.0100m Horizontal Bivariate Scalar: 2.45σ Vertical Univariate Scalar: 1.96σ

Back to top

Covariant Terms

Adjustment performed in New Zealand Geodetic 2000

From Point	To Point		Components	A-posteriori Error (1.96σ)	Horiz. Precision (Ratio)	3D Precision (Ratio)
AGYT	AGUB	**Az.**	89°50'18.3372"	0°00'00.4730"	1:436618	1:436618
		ΔHt.	-1.808m	0.012m		
		ΔElev.	?	?		
		Dist.	13829.006m	0.032m		
AGYT	AGUA	**Az.**	94°31'48.5961"	0°00'00.6077"	1:339847	1:339847
		ΔHt.	3.760m	0.016m		
		ΔElev.	?	?		
		Dist.	13391.084m	0.039m		
AGYT	PAPAROA	**Az.**	69°40'07.7711"	0°00'01.2761"	1:161971	1:161971
		ΔHt.	22.160m	0.013m		
		ΔElev.	?	?		
		Dist.	4159.165m	0.026m		
AGYT	AGY4	**Az.**	169°33'24.9143"	0°00'10.7909"	1:19105	1:19105
		ΔHt.	-1.711m	0.018m		

		ΔElev.	?	?		
		Dist.	619.375m	0.032m		
AGYT	LODGE	**Az.**	221°35'03.3868"	0°00'07.9434"	1:25975	1:25975
		ΔHt.	-1.418m	0.020m		
		ΔElev.	?	?		
		Dist.	942.906m	0.036m		
AGUB	BE48	**Az.**	244°49'19.4988"	0°00'01.8711"	1:110398	1:110398
		ΔHt.	-0.038m	0.012m		
		ΔElev.	?	?		
		Dist.	3495.842m	0.032m		
BE48	AGUA	**Az.**	81°45'56.0755"	0°00'03.0006"	1:68928	1:68928
		ΔHt.	5.606m	0.016m		
		ΔElev.	?	?		
		Dist.	2713.994m	0.039m		
BE48	PAPAROA	**Az.**	293°02'59.1293"	0°00'00.7212"	1:286145	1:286145
		ΔHt.	24.006m	0.013m		
		ΔElev.	?	?		
		Dist.	7353.515m	0.026m		
AGY4	OKAWA	**Az.**	141°37'16.2174"	0°00'05.2910"	1:38919	1:38919
		ΔHt.	-0.793m	0.013m		
		ΔElev.	?	?		
		Dist.	927.509m	0.024m		
AGY4	CAMP	**Az.**	34°13'05.9193"	0°00'01.5842"	1:130494	1:130494
		ΔHt.	-0.613m	0.012m		
		ΔElev.	?	?		
		Dist.	2975.552m	0.023m		
OKAWA	CAMP	**Az.**	18°59'37.9568"	0°00'01.4720"	1:140268	1:140268
		ΔHt.	0.179m	0.012m		
		ΔElev.	?	?		
		Dist.	3371.211m	0.024m		
CAMP	LODGE	**Az.**	223°18'48.0826"	0°00'01.2974"	1:159161	1:159161
		ΔHt.	0.906m	0.011m		
		ΔElev.	?	?		
		Dist.	3514.439m	0.022m		
CAMP	CANAL	**Az.**	223°04'22.9461"	0°00'02.0259"	1:101995	1:101995
		ΔHt.	0.544m	0.018m		
		ΔElev.	?	?		
		Dist.	3384.103m	0.033m		

LODGE	CANAL	**Az.**	49°32'38.4802"	0°00'53.6565"	1:3851	1:3851
		ΔHt.	-0.362m	0.020m		
		ΔElev.	?	?		
		Dist.	131.136m	0.034m		

Back to top

Appendix 2 – Confirmation of Job Completion

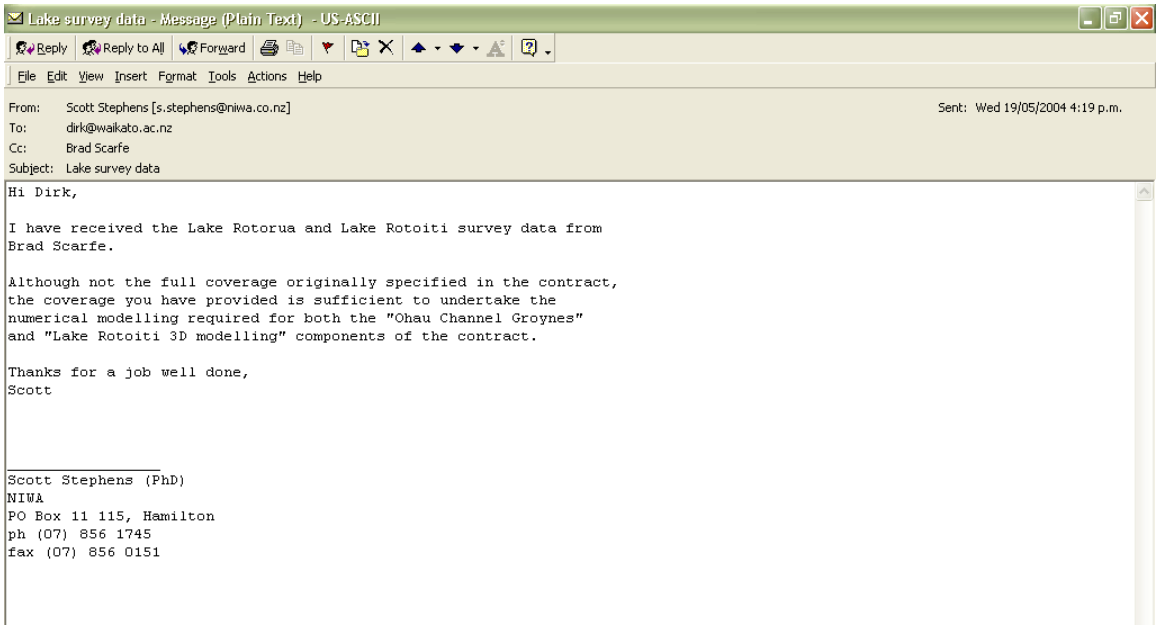

Lake survey data - Message (Plain Text) - US-ASCII

Reply | Reply to All | Forward

File Edit View Insert Format Tools Actions Help

From: Scott Stephens [s.stephens@niwa.co.nz] Sent: Wed 19/05/2004 4:19 p.m.
To: dirk@waikato.ac.nz
Cc: Brad Scarfe
Subject: Lake survey data

Hi Dirk,

I have received the Lake Rotorua and Lake Rotoiti survey data from
Brad Scarfe.

Although not the full coverage originally specified in the contract,
the coverage you have provided is sufficient to undertake the
numerical modelling required for both the "Ohau Channel Groynes"
and "Lake Rotoiti 3D modelling" components of the contract.

Thanks for a job well done,
Scott

_____
Scott Stephens (PhD)
NIWA
PO Box 11 115, Hamilton
ph (07) 856 1745
fax (07) 856 0151

Appendix 3 - Daily Logs

16 Febuary 2004

The survey team (Brad Scarfe and Dirk Immenga meet at University to pack and download geodetic info about the area from the LINZ website.
On arrival in Rotorua we met with people from ORCA to get info about the accommodation. We also had a meeting with the Harbourmaster Andrew Lang to discuss the project and the procedures on and around the Lakes.
In the afternoon we drove around Lake Rotoiti to survey LINZ benchmarks and establish new base station locations. The data processing in the evening did cause some problems.

17 Febuary 2004

In the morning heavy rain prevented us from conducting any land surveying until 0900. In the meantime B. Scarfe did some pre survey processing while D. Immenga drove around the perimeter on Lake Rotoiti. Late morning more GPS measurements were carried out to calculate the geoid separation. Staff at EBoP were contacted to solve the issu of different datums around the area.In the afternoon Scarfe processed the collected data while Immenga conducted some sound velocity checks around the western part of the Lake.

18 Febuary 2004

Due to issues with the geoid separation we contacted TRIMBLE in the US and in Christchurch. Having resolved most of them the boat was taken to Okawa Bay for level checks on the existing tide staff at the jetty. After calibrating the gear and sounder the survey was started at 1200 and carried on out 1800.Most of the 10 m grid was completed. In the evening more datum data was processed.

19 Febuary 2004

In the morning the Okawa Bay 30 m lines were completed and in the afternoon D. Immenga carried on with the Okere Arm 30 lines until joining with the Ohau Channel area. The battery for powering the basestation was stolen, luckily not while surveying was underway. Back in Hamilton at 1900.

24 Febuary 2004

Arrival at lake Rotoiti around 1300.Due to the battery theft another base station location was chosen. In the afternoon B.Scarfe processed some more data while D. Immenga prepared the boat for surveying. The Okere Arm 30 m lines were surveyed up to the weir, ended surveying at 1930.

25 Febuary 2004

On the water before 0800 to work on 30 m lines. No significant change in bathy in the Okere Arm raised the question of the necessity to carry on there. A call to Scott Stephens at NIWA clarified the issue and the survey area was moved to the 100 m grid south of Te Akau Point until the wind got to strong around lunchtime. B. Scarfe processed some data while D. Immenga drove to Rotorua to organize the days ahead. Back on the water late afternoon until 1830. Later some more base stations were established near Lake Rotorua at the Marama Resort.

26 Febuary 2004

In the morning a journalist from the Rotorua Daily Post joined the team for an interview and a photosession. The survey of the 10 m grid on Lake Rotorua was then started. These and the 30 m grid was finished before lunchtime. In the afternoon B. Scarfe stayed back to process more data while D. Immenga carried on with the 30 m X lines and the 100 m longshore lines. Off the water at 1830.

27 Febuary 2004

On the water before 0800, D. Immenga surveyed all remaining 100 m lines on Lake Rotorua. Finished by 1315. Back in Hamilton by 1700.

10 May 2004

Back in Lake Rotoiti and on the water by 1300. Surveying the 300 lines until darkness around 1730.

11 May 2004

On the water by 0630, all remaining 300 m lines done by 1430. In the afternoon work was continued on the 100 m lines until darkness.

12 May 2004

Atrocious weather on the Lake. We still went out and managed to finish the outlined work in the morning. After a meeting with the harbourmaster the team was back in Hamilton late afternoon.